An Analysis of the Relationships Between Soil Moisture, Rainfall, and Boundary Layer Conditions, Based on Direct Observations from Illinois

by

Kirsten L. Findell

B.S.E., Princeton University (1992)

Submitted to the Department of Civil and Environmental Engineering in partial fulfillment of the requirements for the degree of

Master of Science in Civil and Environmental Engineering

at the

MASSACHUSETTS INSTITUTE OF TECHNOLOGY

June 1997

Signature of Author: .....
Department of Civil and Environmental Engineering
May 23, 1997

Certified by: .....
Elfatih A. B. Eltahir
Assistant Professor
Thesis Supervisor

Accepted by: .....
Joseph M. Sussman
Chair, Departmental Committee on Graduate Studies

An Analysis of the Relationships Between Soil Moisture, Rainfall, and Boundary Layer Conditions, Based on Direct Observations from Illinois

by

Kirsten L. Findell

B.S.E., Princeton University (1992)

Submitted to the Department of Civil and Environmental Engineering
on May 23, 1997 in partial fulfillment of the
requirements for the degree of
Master of Science in Civil and Environmental Engineering

Abstract

This study of the soil moisture—rainfall feedback uses a dataset beginning in 1981 of bi-weekly neutron probe measurements of soil moisture at up to 19 stations in Illinois to show that soil moisture can play a significant role in maintaining drought or flood conditions during the summer. Results of a linear correlation analysis between initial soil saturation and rainfall in the subsequent three weeks showed that a positive correlation between these two variables is present from early June through mid-August. This correlation is more significant than the serial correlation within precipitation time series, suggesting the likelihood of a physical mechanism linking soil moisture to subsequent rainfall.

This result prompted further investigation into the nature of such a physical pathway linking soil moisture to subsequent rainfall. Near-surface hourly observations of pressure, P, temperature, T, wet-bulb temperature, T_w, and relative humidity, f, from 13 stations in and close to Illinois were used in these analyses. From each hourly set of direct observations of P, T, T_w, and f, wet-bulb depression, T_{dpr}, temperature of the lifting condensation level (LCL), T_{LCL}, pressure depth to the LCL, P_{LCL}-P_s, mixing ratio, w, potential temperature, θ, virtual potential temperature, θ_v, wet-bulb potential temperature, θ_w, and equivalent potential temperature, θ_E were computed. Time series of the spatial average of each of these quantities were then calculated by averaging data from the 13 stations at each hour.

An analysis of the connections between an average soil saturation time series for the whole state of Illinois with these state-wide average boundary layer conditions did not yield the anticipated positive correlation between soil moisture and moist static energy, as quantified by T_w, θ_w, or θ_E. It is not clear if this is due to limitations of the data or of the theory. There was evidence, however, that moisture availability (or lack thereof) at the surface has a very strong impact on the wet-bulb depression of near-surface air, particularly from mid-May through the end of August, showing good correspondence to the period of significant soil moisture–rainfall association.

The final set of analyses performed included an investigation of hourly boundary layer and rainfall data. Data from the 82 hourly rainfall stations were averaged to compare state-wide hourly rainfall to state-wide hourly boundary layer conditions. A link between high MSE and high rainfall was noted for much of the range of MSE during the summer months, and a link between low T_{dpr} and high rainfall was evident for all of the months analyzed (April through September). These analyses, then, suggest that the significant but weak correlation between soil moisture and rainfall during Illinois summers is due not to soil moisture controls on the boundary layer entropy, but rather to soil moisture controls on the wet-bulb depression of near-surface air.

Thesis Supervisor: Elfatih A. B. Eltahir
Title: Assistant Professor of Civil and Environmental Engineering

Acknowledgments

There are many individuals who have contributed in countless ways to my academic and personal growth since I've been at MIT. Thanks are due to my advisor, Elfatih Eltahir, both for his guidance and feedback on this work, and for his willingness to welcome me into his research group. I am forever grateful to Dennis McLaughlin for his enormous patience with me when I was blindly searching for the research discipline that was right for me. His advice, support and understanding are still appreciated more than he can know.

Many people at the Parsons Lab have helped to make this place a warm and welcoming second home, but a few people deserve special recognition for their companionship and laughter. Jeremy Pal, for all the soil moisture conversations, for his insights and theories on human nature, and, of course, for his computer expertise. Sanjay Pahuja for the plants, the stories, the yoga, the bibliography, and for his ability to find the beauty in everything. Pat Dixon for her warmth and caring, and for sharing a bit of herself with me. Sheila Frankel for taking care of the lab and for getting computers in our offices. Cynthia Stewart for making sure that sanity comes before deadlines. Lynn Reid for her tough big-sisterly love. Tom Ravens, David Senn, Julie Kiang, John MacFarland, Ida Primus, and Guiling Wang for making me smile every time I see them. And, of course, Freddi-Jo Eisenberg for being my biographer and soul-mate.

Thanks also go to John Hansman for the runs, swims, and conversations: he has helped diffuse many headaches and frustrations; to Laura and Hans Indigo for their friendship and support, and for helping to give me a life outside of MIT; to Miriam Bowling for laughing with me and helping me keep things in perspective; to my amazing sister Leanne for always believing in me and knowing just when to tell me so; to my brother Kent and my mother Carol for the open doors whenever I need an escape from the city; to my father George for his belief that I can do anything I want to do; to my house mates Becky Frank and Susan Kaplan for helping to make our house a home; and especially to my yoga teachers extraordinaire, Gurucharan Singh Khalsa and Hari Kaur Frank for helping me take care of myself and always encouraging me to keep up!

Steven Hollinger, Randy Peppler, Tami Creech, and Jim Angel of the Illinois State Water Survey were kind enough to contribute their soil moisture and precipitation data to this study. Special thanks go to Jim Angel for responding to my last-minute request for digital information on the Illinois state line.

Much appreciation also goes to the National Science Foundation for supporting me with a Graduate Student Fellowship.

Table of Contents

List of Figures

Chapter 1: Introduction

It has long been recognized that soil moisture plays an important role in regional climate systems through its effect on the partitioning between sensible and latent heat fluxes and on the albedo of the surface. Early work by Namias (1952, 1960, 1962) showed that spring precipitation and soil moisture can impact summer precipitation in the interiors of continents. More recently, many researchers have noted the negative correlation between soil moisture states and mean and maximum temperatures (Karl, 1986; Georgakakos et al., 1995; Huang et al., 1996), and stressed the potential increase in surface heating and decrease in local evaporative contributions to atmospheric humidity that anomalously low soil moisture states can affect (Rind, 1982; Trenberth, 1988; Oglesby, 1991). Recent work by Williams and Renno (1993) and Eltahir and Pal (1996) suggests a link between rainfall and surface wet bulb temperature during convective rainfall storms in the tropics. Wet bulb temperature is an indicator of surface conditions, including, among other variables, soil moisture. Afternoon storms during the summer months in the Midwestern United States are thought to be of a similar convective nature as tropical storms. As stated in early work by Carlson and Ludlam (1966), during the summer "the tropical cumulonimbus convection and its own nearly-neutral stratification tend to advance into higher latitudes."

Many recent studies involving General Circulation Models (GCMs) have offered support to Namias' hypothesis, showing that changes in the soil moisture regime at the end of

spring/beginning of summer can significantly impact summer precipitation over continental land masses (Shukla and Mintz, 1982; Rowntree and Bolton, 1983; Rind, 1982; Yeh et al., 1984; Oglesby and Erickson, 1989; Oglesby, 1991; Fennessy and Shukla, 1996). These GCMs, however, have all been rather broad-brush, making global or continental-scale soil moisture changes. Regional climate studies (Pan et al., 1995; Georgakakos et al., 1995; Huang et al., 1996; Pal and Eltahir, 1997, for example) have also been used to test this hypothesis regarding the feedback from soil moisture to the atmosphere. The FIFE experiment in Kansas provided some short-term real data with which to test the soil moisture–rainfall feedback. Both Betts et al. (1996) and Eltahir (1997) find a positive feedback relationship between soil moisture and boundary layer conditions. However, due to a lack of adequate long-term data on soil moisture, no models have been tested against any directly observed, long-term soil moisture data sets.

This study attempts to fill this gap by analyzing the relationship between precipitation and soil moisture using the Illinois Climate Network (ICN) data set: a record of soil moisture values measured bi-weekly at 19 stations across the state of Illinois since 1981 (Hollinger and Isard, 1994). Though this data set is somewhat limited in both temporal and spatial extent, it is the largest available data set of its kind and its analysis should prove worthwhile. If, as many GCM and regional studies results suggest, spring soil moisture does indeed affect summer precipitation, the data should support this hypothesis.

To make this data analysis comparable to modeling studies, the framework for the analysis is posed as an initial value problem. We are interested in how precipitation responds to an initial soil moisture condition. In contrast to a computer model, it is difficult to isolate these two variables when dealing with real data. Nevertheless, the 14 years of data (1981-1994) are more

than has previously been available for this kind of analysis, and could provide some insight into the coupled land-atmosphere system. Furthermore, this analysis, based on actual observations, should provide a testing framework for future numerical experiments involving soil water and precipitation.

After a more detailed discussion of the literature on these processes and on previous data analyses and modeling experiments, this hypothesis will be tested in Chapter 3 by analyzing 14 years of data on soil moisture and subsequent rainfall in Illinois. As predicted by the theory herein, a positive but weak correlation was found during the summer months. This correlation prompted the investigation of the correlations between soil moisture and subsequent boundary layer conditions in Chapter 4, where we expected to see evidence of increased soil moisture being followed by increase BLE. This expectation was not met. It is not clear if this is due to limitations of the data or of the theory. Though this soil moisture–BLE link was not observed, there was evidence that high soil moisture is likely to be followed by low wet-bulb depression, T_{dpr}, particularly during the summer.

The next phase of analyses, presented in Chapter 5, focused on the link between boundary layer conditions and rainfall using hourly data. Indeed, a link between high MSE and high rainfall was noted for much of the range of MSE during the summer months, and a link between low T_{dpr} and high rainfall was evident for all of the months analyzed (April through September). These analyses, then, suggest that the significant but weak correlation between soil moisture and rainfall during Illinois summers is due not to soil moisture controls on the boundary layer entropy, but rather to soil moisture controls on the wet-bulb depression of near-surface air.

Chapter 2: The Role of Soil Moisture in the Climate System

A. Background and Theory

Atmospheric dynamics over oceans are quite different from those over land. Water has a much larger heat capacity than soil, and the oceans act as a reservoir for heat and energy. As a result, the diurnal temperature fluctuations that can be enormous over dry land masses like deserts are reduced to just a few degrees over oceans. Similarly, seasonal shifts in mean temperature are much reduced over oceans as compared to lands.

Evaporative processes at the surface of oceans are also quite different from those over land. Evaporation occurs when three things are available: 1) moisture, 2) energy to convert liquid water to water vapor, and 3) a transport mechanism to carry saturated air away from the moisture source. Over open water, moisture is never in short supply, while over land it can often be the limitation on evaporation. When evaporation is limited, regardless of the controlling mechanism, incoming energy is dissipated by the less efficient mechanism of sensible heat flux, which leads to a rise in air temperature. Indeed, it is this difference between the oceanic and land surface ratios of sensible to latent (evaporative) heat flux which is responsible for the larger temperature fluctuations over land. Parched ground has no moisture available for evaporation, so all of the available energy goes to sensible heating of the air, and the air temperature quickly rises. Over a body of water, on the other extreme, evaporation, E, occurs at the potential rate (a function of the

other two limiting factors, energy and transport mechanisms), and much less energy is available for sensible heat transfer.

The amount of moisture in the soil controls where the energy balance of the surface lies in relation to these desert and ocean extremes. This is quantified by the Bowen ratio, β, which is defined as the ratio of sensible heat flux, H, to latent heat flux, λE, where λ is the latent heat of vaporization. Both terms have units of energy flux (W/m^2 in S.I. units). Typical values of β are on the order of 0.07 over open oceans, where the sea surface temperature responds little to the diurnal cycle of solar forcing (Betts et al., 1996), to many hundreds over dry land surfaces, where all of the energy transfer occurs as sensible heating (e.g. dry lake bed example in Wallace and Hobbs, 1977, p. 345). During the night over land, both H and λE are very small because the land responds quite quickly to the disappearance of solar forcing. The sensible heat flux is often directed downward at night when a temperature inversion is present, so the Bowen ratio may be negative in sign.

The comparison of land surface and oceanic controls on atmospheric dynamics is an extreme example of the potential role that soil moisture could play in effecting local weather and climate. An increase in soil moisture increases the heat capacity and thermal conductivity of the land surface, thereby increasing its thermal stability (McCorcle, 1988). Furthermore, if water availability is the limitation on evaporative exchange, then an increase in soil moisture would allow for an increase in the production of latent heat and a decrease in the production of sensible heat. This mechanism is important in dry to normal conditions, but above some threshold of moisture availability, energy input or transport of saturated air away from the moisture source become the controlling factors on evaporation. Increasing soil moisture beyond this point will not

affect the Bowen ratio. Since this threshold moisture level is variable due to the variability of winds (the transport mechanism) and incoming solar radiation (the energy source), it generally appears in data only as decreased sensitivity, rather than a clear cut-off level, of the Bowen ratio to moisture availability at high moisture contents.

Another important aspect of the influence of soil moisture on land-atmosphere interactions are the time scales of the many components of the land-atmosphere system. Because the thermal mass of water is so large, oceans respond slowly–with lags on the order of a season–to changes in radiative or other forcing, and they only respond to the low frequency variability. Similarly, soil moisture acts like a reservoir of water which damps out high frequency fluctuations and increases the memory of the land surface system (Entekhabi et al., 1996). This memory bank is an important aspect of the feedback loop between the land surface and the atmosphere.

Theories abound on the role that soil moisture plays in the moisture and energy budgets of the boundary layer (e.g., Betts et al., 1996; Entekhabi et al., 1996; Eltahir, 1997). They all agree that soil moisture is an important component of the system, but there is disagreement on the relative strengths of the many different ways which soil moisture can effect the boundary layer. These differences will be discussed in the next section. In this section, we will simply sketch the broad outline of the soil moisture–rainfall feedback.

When a stove-top pot is heated from below, energy is added to the lowest levels of the fluid. This begins to generate turbulence and turbulent heat flux away from the heat source, and to create an instability where relatively cold, dense, low energy fluids are overlying relatively warm, less dense, high energy fluids. Turbulence acts to mix these fluids and create uniform profiles of temperature and energy throughout the range of the turbulent activity. As more heat is

added to the system, the strength of the turbulence grows and the depth of the mixed layer grows until the whole pot is boiling and well mixed.

Since the atmosphere is largely transparent to solar radiation, the main heat source for tropospheric air is the land surface. The system acts much like a pot on a stove, with the added complication of the heat associated with phase changes of water (heat is consumed by evaporation and released by condensation). During the day, the temperature of the land surface increases in response to solar forcing, and the corresponding flux of terrestrial radiation increases (this flux is proportional to the fourth power of ground temperature). Net radiation at the surface, R_{net}, is the sum of incoming short wave solar radiation, outgoing long wave terrestrial radiation (negative in sign), and incoming long wave radiation returned to the surface by backscattering off of molecules in the atmosphere, particularly condensed water in clouds. Some of this net radiation is consumed as heat flux into the ground, G, (usually on the order of 15% or less, [Betts et al., 1996]). The remainder, and typically the greater percentage, of R_{net} is transferred to the air, partly as sensible heat, and partly as latent heat: $R_{net} - G = H + \lambda E$. Both the turbulent sensible and latent heat fluxes increase the moist static energy (MSE) of the boundary layer (Betts et al., 1996; Carlson and Ludlam, 1966), and mix the lower levels of troposphere so that quantities like mixing ratio and potential temperature are nearly constant throughout this mixed layer. MSE is very closely related to the entropy variable equivalent potential temperature, θ_E (Emanuel, 1994), and the terms moist static energy and boundary layer entropy (BLE) are used almost interchangeably. Temperature, T, is not constant in the mixed layer because the pressure, P, decreases nearly hydrostatically with increasing height. Potential temperature, θ, accounts for the P dependence of T: it is defined as the temperature a parcel of air would acquire if it were taken dry adiabatically to 1000 mb. Convection begins when turbulence is strong enough to bring parcels of air from low

levels up past their level of free convection (LFC), where they are neutrally buoyant with respect to environmental air. Above the LFC, a parcel is positively buoyant and will rise freely until it reaches the level of neutral buoyancy (LNB), cooling and, after reaching saturation, condensing out water vapor as it goes. Initial saturation occurs at the lifting condensation level (LCL), which is often below the LFC. The LCL is usually the cloud base level, while the LNB is approximately the cloud top. If convection is strong enough, and if enough vapor condenses out, precipitation occurs. Since the primary energy source for the boundary layer growth described here is surface fluxes, which are forced by incoming solar radiation, the convective boundary layer is only present during daylight hours (Wallace and Hobbs, 1977).

Soil moisture plays a role in this process by its effect on the Bowen ratio: i.e., by its effect on the partitioning of sensible and latent heat fluxes. Sensible heat flux is largely responsible for the turbulent mixing of near-surface air, so when sensible heat flux increases the boundary layer grows more rapidly. Since the increase of the moist static energy (MSE) in this mixed layer is proportional to the *sum* of the latent and sensible heat fluxes, the contribution of MSE from the land surface is not dependent on the Bowen ratio. For a given amount of available energy, R_{net} - G, a larger Bowen ratio means more sensible heating of the air, a deeper boundary layer, and therefore, less MSE per unit depth. Wet soils should lead to a smaller Bowen ratio and, by the same reasoning, more MSE per unit depth.

An additional level of complexity in this soil moisture–moist static energy relationship is suggested by Eltahir (1997). Since soil moisture affects the albedo, α, of the surface, for a given level of incoming solar radiation, wet soils will decrease the surface albedo, thereby increasing the solar radiation at the surface ($R_{net,\ solar} = (1-\alpha)R_{incoming\ solar}$). By decreasing the air temperature,

wet soils decrease the outgoing terrestrial radiation. In addition, wet soils should lead to increased water vapor content of the air, so more of this terrestrial radiation should be scattered back towards the surface (greenhouse effect). Each of these three factors, increased $R_{net,\ solar}$, decreased $R_{outgoing\ terrestrial}$, and increased $R_{incoming\ terrestrial}$, leads to an increase in net radiation: $R_{net} = R_{net,\ solar} - R_{outgoing\ terrestrial} + R_{incoming\ terrestrial}$. Wet soils, then, should not only increase the moist static energy per unit depth of boundary layer by their impact on the boundary layer depth, they should also increase the contribution of moist static energy from the surface fluxes of sensible and latent heat by increasing net radiation at the surface.

This basic sketch of the processes leading to convective rainfall suggests that increased soil moisture should lead to increased moist static energy in the mixed layer, which should then lead to increased precipitation. However, the style of convection outlined here is not the only mechanism of rainfall production, particularly in the mid-latitudes. In much of the tropics, local convection is responsible for the majority of rainfall throughout the year. In mid-latitudes, on the other hand, synoptic systems play a highly significant part in rainfall production, particularly during the winter. The convective rainfall discussed here is expected to be important in mid-latitude regimes, such as the state of Illinois, only during the summer months. Even in the mid-latitude summers, the impact of soil moisture anomalies is reduced when synoptic winds are strong (Carlson and Ludlam, 1966; Entekhabi et al., 1996).

B. Previous Data Analyses

The works of Eltahir (1997), Entekhabi et al. (1996), Betts et al. (1996), Betts and Ball (1995), Williams and Renno (1993), and Carlson and Ludlam (1966), among others, have

contributed greatly to the theoretical understanding of the soil moisture–rainfall feedback. Some of the details of these studies will be discussed here.

As discussed above, the partitioning of available surface energy has many effects on the mixed layer. Dry soil leads to increased sensible heating, which leads to increased air temperatures and greater parcel buoyancy. This increases the depth of the boundary layer, and parcels must rise higher before reaching saturation at their Lifting Condensation Level (LCL). In addition, the turbulent energy associated with the parcel is increased, so there is more entrainment of air from above the mixed layer. This overlying air tends to have lower entropy, so, as pointed out by Betts et al. (1996), greater turbulence leads to reduction of the rate of entropy increase of the mixed layer. Carlson and Ludlam (1966) highlight the difference the depth of the mixed layer has on the wet-bulb potential temperature, θ_w, of the layer. The θ_w increases during the normal course of the morning and afternoon through both the increased air temperature from sensible heating and the increased water vapor content from evaporation of water from the land surface. When the ground is dry, the available surface energy, $R_{net} - G$, goes into warming and humidifying a deeper boundary layer. The increase of θ_w, then, is reduced over dry areas as compared to wet areas. Over moist areas, θ_w in a convective layer about 150 mb deep rises by about 2.5 °C per day; over arid regions, the convective layer is usually on the order of 400 to 500 mb deep, and the average daily rise in θ_w is on the order of only 0.5 °C per day (Carlson and Ludlam, 1966).

The wet-bulb potential temperature is an important measure which is closely related to convection and precipitation: it is conserved in pseudo-adiabatic transformations, and it defines the path of a parcel lifted from the surface after it reaches saturation. The wet-bulb potential temperature, θ_w, is defined as the temperature of a parcel taken moist adiabatically from its wet-

bulb temperature, T_w, to a reference pressure of 1000 mb. T_w and θ_w are very closely related and are, by definition, on the same pseudo-adiabat. Eltahir and Pal (1996) describe the role of wet-bulb temperature in triggering moist convection. The work of Williams and Renno (1993) shows a linear relationship between wet-bulb potential temperature and the convective available potential energy (CAPE) of surface air parcels, using surface and upper air data from many tropical locations. They found a zero-CAPE intercept at approximately 22-23 °C. The results of Eltahir and Pal (1996) show a similar linear relationship between wet-bulb temperature and the probability of afternoon rain in the Amazon, with a zero-probability of rainfall intercept at 22 °C. Ludlam (1980) showed that a θ_w of at least 20 °C is required for the buildup of substantial CAPE in western Europe. Dessens (1995) used daily minimum temperature, which generally occurs in the early morning, as an approximation of the θ_w in following afternoon. He states that there is a strong correlation between these two variables, and shows that θ_w is a good predictor of damage from severe hail storms in France. Zawadzki and Ro (1978) and Zawadzki et al. (1981) used vertical soundings from the Toronto area in summer to show that the mean and maximum precipitation rate are well correlated with parcel convective energy.

Betts et al. (1996) performed much of their analyses in terms of the equivalent potential temperature, θ_E, of the boundary layer. This variable is related to the entropy of the layer through the equation $(c_{pd} + r_t c_l) \ln \theta_E \equiv s + R_d \ln p_0$, where c_{pd} is the heat capacity of dry air at constant pressure, c_l is the heat capacity of liquid water, r_t is the total water mixing ratio, R_d is the gas constant of dry air, p_0 is a reference pressure of 1000 mb, and s is the specific entropy, or moist entropy (Emanuel, 1994, p. 120). Both s and θ_E are conserved in reversible moist adiabatic processes. During daylight hours, θ_E increases due to the surface flux of both sensible heat and

latent heat. Betts et al. (1996) stress that "this surface flux of θ_E is proportional to the *sum* of the [sensible heat flux + latent heat flux], and it is not affected by the Bowen ratio" (p. 7214). The contribution of low θ_E from above the boundary layer, however, tends to reduce θ_E in the layer. The degree to which this entrainment occurs is closely linked to the sensible heat flux from the surface and the associated deepening of the boundary layer: "if the surface [Bowen ratio] is large, although the surface θ_E flux may be unchanged, the large [sensible heat] flux drives more entrainment, produces a deeper [boundary layer], and the diurnal rise of θ_E is reduced" (p. 7214).

Using data from the FIFE site in Kansas, Betts et al. (1996) showed that, on days during July and August 1987 which were not substantially affected by precipitation or advection of cold air, higher soil moisture content was associated with higher mixing ratio, q, throughout the day, lower mean temperature, lower maximum temperature, and higher maximum θ_E. They state that "some of this shift of θ_E is associated with the sift of the entire diurnal path to higher q with higher soil moisture, but about half is the result of reduced entrainment of dry low θ_E into the boundary layer" (p. 7215).

Earlier work by Betts and Ball (1995) focused on subsets of the FIFE data, determined by rainfall and net radiation. Two of their many analyses are particularly relevant to this study. The first compared all days from June to September, 1987 to "wet" days and to "dry" days. "Wet" days were defined to be those with "significant rainfall during the daytime" (p. 25,682), and constituted 29 days. "Dry" days were "days for which the daytime diurnal cycle was not disturbed by rain or heavy overcast." (p. 25,682) They defined "overcast" as days with a 3-hour average near-noontime net radiation below a threshold: 450 W/m2 for June, July, and August, and 400 W/m^2 for September. There were 94 "dry" days in the data set. With these classifications,

they found that increased wetness led to higher maximum θ_E, higher maximum q, smaller diurnal range in T, and, as expected from their definition of the classifications, lower R_{net}. These classifications, however, are not determined from the soil moisture observations, and are therefore quite different from the wet, normal, and dry classifications used in this study.

A subsequent analysis in the Betts and Ball work did partition the data by soil moisture, but they only used the 94 days in the "dry" category described above. This is a critical difference between their study and this work. Within subcategories of the dry data, they found that the Bowen ratio and the pressure depth to the Lifting Condensation Level (LCL) were highly dependent on soil moisture: larger pressure depths and larger Bowen ratios were associated with drier soils. This was especially true between the two driest categories.

Eltahir (1997) stresses the importance of the control that soil saturation has on the albedo of the surface, in addition to the aforementioned Bowen ratio controls. Since water absorbs more solar radiation than dry soil, the albedo of a land surface is negatively correlated with soil saturation, particularly in the top 10 cm. This effect then propagates into the surface radiation budget: increased soil moisture should decrease the albedo, which then increases the net solar radiation at the surface. Eltahir showed that increased soil saturation should also increase the net terrestrial radiation by increasing the water content of the atmosphere, which will cause more longwave radiation to be directed back towards the surface, and by decreasing the surface temperature, which will result in a decreased radiation away from the surface. All else remaining equal, then, increased soil moisture should lead to an increase in available energy at the surface. This effect, like that discussed above in connection with the work of Betts et al. (1996), should lead to a positive relationship between soil saturation and the entropy of the boundary layer, by

increasing the surface flux of the sum of latent and sensible heats. Eltahir (1997) showed that FIFE data exhibits a positive relationship between soil saturation and wet-bulb temperature.

C. GCM Results

In addition to theoretical work and small-scale analyses of observations, much insight into the soil moisture—rainfall feedback has been gained from Global Climate Modeling studies. Shukla and Mintz (1982), tested two global scenarios: a wet-soil case, where evapotranspiration is at all times equal to the potential evapotranspiration, and a dry-soil case, where there is no evapotranspiration. Over almost the entire globe, precipitation in the dry-soil case was much less than precipitation in the wet-soil case; while surface temperatures in the dry-soil case were much higher than in the wet-soil case. They concluded that "surface evapotranspiration, which requires moisture in the soil, is a necessary (though not sufficient) condition for extratropical summer precipitation" (p. 1500).

The importance of the timing of soil moisture anomalies in their affect on other climatic variables is stressed by Oglesby's 1991 study of North American droughts. Reduced soil moisture profiles are introduced into two model runs, one beginning on March 1, and one beginning on May 1. In the May 1 run, most of the initial soil moisture anomaly is maintained throughout the summer, except along the east coast of the continent, showing that "through positive feedbacks, reduced soil moisture can be a self-perpetuating condition" (p. 893). The March 1 run, however, shows that the anomalous condition can, in fact, correct itself. The anomaly is apparent at 20 days only over the central United States, and at 50 days, virtually all of North America is at a normal, moist state. He explains these different behaviors by noting that during winter or early spring, when the March 1 anomaly is introduced, solar insolation is generally less than in late

spring and summer. The two primary direct effects of reduced soil moisture content–reduced local evaporation and increased surface heating–are, thus, expected to be less important in this earlier season, and the anomalous condition can be corrected prior to the onset of the new climatic regime.

Rind (1982) finds similar results in his GCM study of North America. By comparing runs which have initially reduced soil moisture levels across the entire United States to control runs, which have normal soil moisture levels on June 1, Rind found significant temperature increases and precipitation decreases across most of the U.S. The effects were most noticeable in June and least noticeable in August, and most consistent in the interior of the continent, where the oceans had the least influence.

Yeh et. al. (1984) conducted a series of numerical experiments which tested, among other things, the importance of the latitude of soil moisture anomalies. In each of the three latitudinal bands studied, namely 30°N-60°N, 0-30°N, and 15°S-15°N, initial saturation of the soil caused both an increase in local precipitation and cooling of the surface due to increased evaporation. Each of the simulations was run during the driest period for the latitudinal band: 1 July to 30 November for the northernmost region, and 1 January to 31 May for the other two.

The studies of Rowntree and Bolton (1983) and Fennessy and Shukla (1996) both found a positive feedback between soil moisture and precipitation. They determined that the strength of the impact is dependent on the size of the soil moisture anomaly region. Other important factors include the solar forcing and the strength of the background winds and regional circulation. Rowntree and Bolton work in terms of a vertically integrated relative humidity, defined as Q/Q_{sat}, where Q is the vertically integrated atmospheric water vapor (in g/cm^2), and Q_{sat} is the

corresponding saturation vapor content. This quantity is increased by an increase in Q, which can occur when evapotranspiration exceeds precipitation, and it is decreased by a rise in temperature, which leads to an increase in Q_{sat}. They found that an initial soil moisture anomaly over Central Europe affected the partitioning of turbulent heat fluxes at the ground, which in turn affected the modeled temperature, humidity and rainfall during the following 50 days. The atmospheric humidity was found to be much higher in wet soil cases than in dry soil cases, and "the likelihood of precipitation [was] much increased by the wet surface" (p. 503). Model runs with increased winds and circulation strength showed less response to the soil moisture anomaly.

Several studies have focused on the causes of the 1988 U.S. summer drought, studying both sea surface temperatures (SSTs) and soil moisture states. Trenberth et al. (1988) found that large-scale circulation patterns caused by SSTs in the Pacific were the likely primary cause, but that the low soil moisture conditions at the beginning of and throughout the season probably contributed to the severity and persistence of the drought. Atlas et al. (1993), on the other hand, found that tropical SST anomalies reduced the precipitation in the Great Plains, but did not significantly increase the surface temperatures. Simulations with reduced soil moisture levels, however, both increased surface temperatures and decreased precipitation, accurately approximating the actual 1988 scenario. Oglesby and Erickson (1989) used the NCAR CCM1 general circulation model to demonstrate that reduced spring soil moisture, like that of 1988, can "amplify or prolong summertime drought over North America" (p. 1375).

D. Results of Regional Climate Studies

Perhaps of more relevance to this analysis of data from Illinois are results from regional scale climate and/or hydrologic models. Pan et al. (1995) focused their study on the flood of

1993 as well as the drought of 1988. They tested the hypothesis that surface moisture availability provides an additional feedback mechanism, helping to maintain extreme wet or dry conditions. Models of a portion of the Midwestern U.S. showed that when all other climatic variables were simulated as observed in each of the two years of interest, extreme changes in the surface moisture conditions (i.e., 99% of saturation simulated with the temperature, wind, and other boundary conditions observed in 1988; 1% of saturation with the boundary conditions of 1993) significantly altered the total summer precipitation.

However, the study of Giorgi et al. (1996) led to the opposite conclusion. They found that local recycling effects were not important in the development of extreme climatic regimes, and, contrary to the aforementioned studies, that a dry soil initial condition provides for increased sensible heat flux, which contributes greater buoyancy to the air, enhancing convective systems and producing more precipitation. This cycle, then, supports a negative feedback mechanism between initial soil condition and precipitation.

In their regional modeling study of the 1988 and 1993 events over the Midwestern US, Pal and Eltahir (1997) found that the sensitivity of the model to soil moisture initialization was extremely dependent on the convection scheme used in the model. One convection scheme led to results which were highly dependent on the initial local soil moisture conditions, while a different scheme led to quick equilibration of soil moisture anomalies and showed little precipitation difference between wet and dry model runs.

Similar to the Giorgi et al. (1996) study, Georgakakos et al. (1996) found no evidence of soil water feedback to local precipitation in their study of two 2000 km^2 basins in Iowa and Oklahoma. Using daily precipitation and potential evapotranspiration as input, they were able to

accurately simulate observed daily discharge over a 40 year period in each of the basins. One of the primary forcings to the river discharge was an estimated soil moisture time series: the accuracy of their streamflow series (correlation with observations better than 0.8) suggests that their soil moisture series is good. Though soil moisture was not shown to affect precipitation, there were significant cross-correlations between upper soil water leading daily maximum temperature, especially during periods of extreme (high or low) soil water content.

Huang et al. (1996) created a 62 year (1931-1993) time series of monthly soil moisture data for the entire US using a one-layer soil moisture model. They found that soil moisture is a better predictor of future monthly temperature than is antecedent precipitation, particularly in the interior of the continent during summer.

On the smaller end of the spatial and temporal scales, Chang and Wetzel (1991) were able to model the effects of the spatial variability of vegetation and soil moisture on the development of individual storm events. Given the absence of real soil data, they estimated soil moisture from an antecedent precipitation index. The Illinois data set is not of high enough spatial or temporal resolution to be adequately compared to the results of Chang and Wetzel.

Each of the works mentioned above help to establish and/or substantiate the theory of why we expect to see a positive feedback between soil saturation and rainfall. The studies mentioned in Sections C and D highlight many attempts to discern the impact of soil water conditions on future climate through the use of numerical models. Analyses of small-scale sites such as FIFE have provided some real-world applications of these theories. In the following three chapters, we will test the theories presented here by looking at directly observed soil moisture, near-surface air,

and rainfall data from the state of Illinois, and see what these data can tell us about the soil moisture-rainfall feedback. We begin by analyzing soil moisture and rainfall data in Chapter 3. Chapters 4 and 5 will include analyses of the relationships between soil moisture and boundary layer conditions, and boundary layer conditions and rainfall, respectively.

Chapter 3: The Relationships Between Soil Saturation and Subsequent Rainfall

A. Soil Moisture Data

Though each of the studies described in the previous chapter provides analyses of the links between summer rainfall and spring soil moisture, all of them used indirect means to quantify soil moisture. Since 1981, scientists from the Illinois State Water Survey have been taking direct soil moisture measurements with a neutron probe at 8 grass-covered sites around their state (Hollinger and Isard, 1994). Seven additional sites were added in 1982, two more were on-line by 1986, and by 1992, the total was up to 19. Station locations are shown in Figure 3.1. Bi-weekly measurements were taken in the top 10 cm, in 20 cm intervals between 10 and 190 cm (10-30 cm, 30-50 cm, etc.), and in the 10 cm interval between 1.9 and 2 meters below the surface.

Many researchers (Owe and Chang, 1988; Shukla and Mintz, 1982) have noted the difficulty in obtaining a parameter that represents the soil moisture condition over a whole, large area. Though this data set is a very extensive collection, both temporally and spatially, we must consider the relevance of the parameter measured to this study. According to the hypothesis presented here, the initial soil water condition can provide some positive feedback to the convective regime during the summer months in Illinois. The parameter of interest, then, is the amount of soil water available for evapotranspiration. The rate at which soil water can be removed is a property of the unsaturated hydraulic conductivity of the soil. Eagleson (1978)

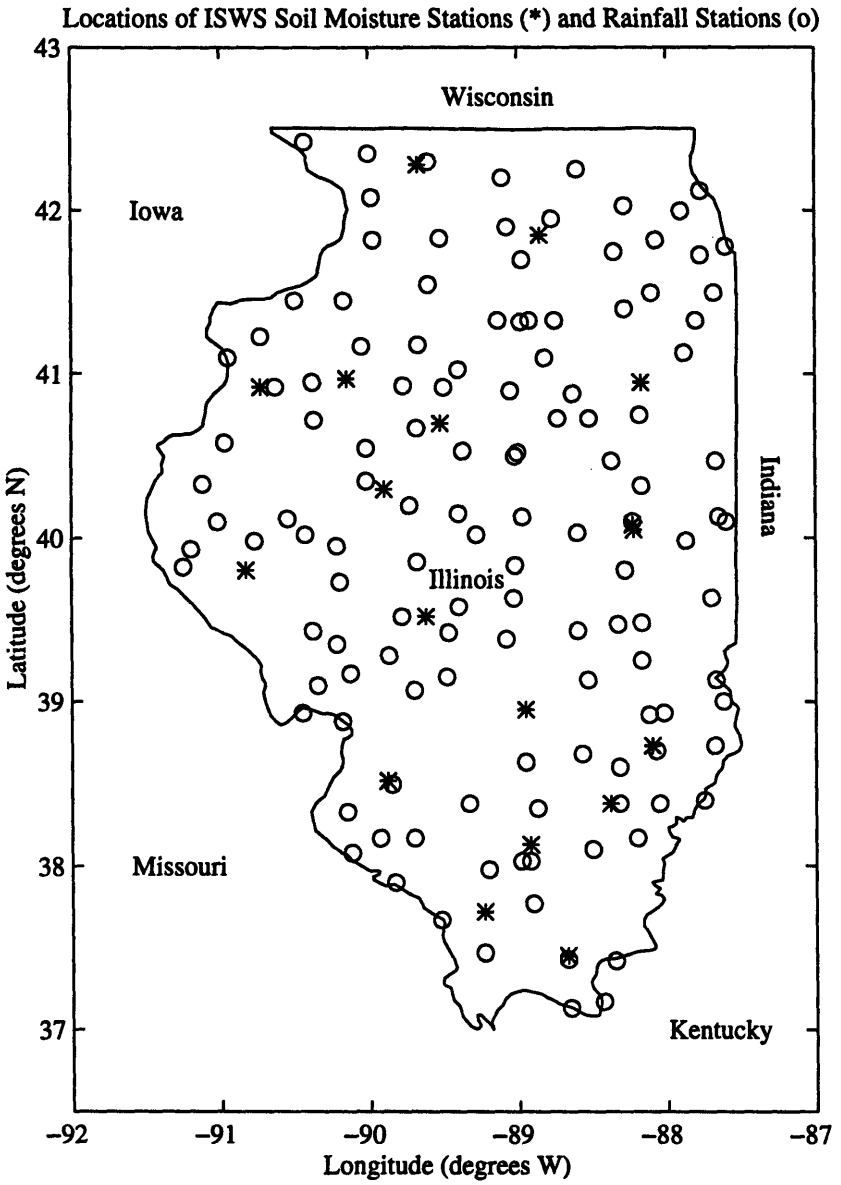

Figure 3.1: Locations of Illinois State Water Survey (ISWS) soil moisture stations and rainfall stations. Solid line is the Illinois state boundary.

stresses that in exfiltration processes (interstorm drying of the soil as well as extraction by plant roots) it is not the moisture content, q, but rather the soil saturation, q/n, where n is porosity, that is the controlling parameter. Therefore, soil saturation is used as an indicator of the overall soil water condition at each site. Note that this is used as a qualitative indicator of the soil condition, not as an exact measure of the mass of water in the soil: the data are by no means complete

enough to offer that level of detail. The soil moisture data, then, were first converted to soil saturations by dividing by the porosity (measurements were made at each of the 19 sites).

Though the sampling frequency (approximately every two weeks) is much greater than for most soil moisture field studies, 14 days is significantly longer than a normal wetting and drying cycle during a Midwestern summer. However, in this study we are not interested in the ability to predict a storm event or exactly describe the soil water condition at every moment in time. Rather, we are concerned with the mean climatic behavior over monthly or seasonal time scales rather than the predictability of erratic weather systems. It is also important to note that the sampling schedule was not set in response to particular storm or drought events (Hollinger, personal communication, 1996). The samples obtained, then, are like random realizations of the ensemble of soil moisture condition at all times throughout the entire state. The assumption implicit in this analysis is that there are enough observations distributed in time and space to give an adequate representation of the trends of the mean soil water condition in the state. An ideal data set for this analysis would have soil moisture sampled multiple times per day at many sites all over the state. Though this data set is not, by this standard, ideal, it is far more complete than any other data set known to date, and much useful information can be gleaned from it.

Simple linear interpolation was used to develop a daily time series of soil saturation for each depth interval at each site. Though each of the site-specific time series may miss important events, given no better knowledge of the soil conditions between observations, linear interpolation makes the most of the directly observed information that is available. Furthermore, since it is the large-scale soil saturation that is of interest--the soil moisture that can contribute to atmospheric humidity within the region--the state-wide average soil saturation was determined by averaging all

the station-specific values for each day within this 14 year time series. Relative to other data sets of soil moisture, 19 is a large number of stations.

An important consideration in any study related to soil moisture is the relevant depth of soil to analyze. The root zone depth is dependent on vegetation type and health, and can be extremely variable. Estimates for root zone depth usually are in the range of 10 cm to a few meters. Because the depth of soil from which moisture is available for evaporation is not constant, the analysis was initially performed for average saturations in all of the available surface soil layers: 0-10 cm, 0-30 cm, 0-50 cm, 0-70 cm, 0-90 cm, 0-110 cm, 0-130 cm, 0-150 cm, 0-170 cm, 0-190 cm, and the top 2 meters. The average saturation for the layer of interest was calculated by an appropriately weighted average of saturation within each 10 or 20 cm sample interval. Figures 3.2a-f show the average soil saturation for each of the 14 years for the top six surface layers, each highlighting 1988, a substantial drought year, and 1993, a substantial flood year. Figures 3.3a-d show seasonal average profiles of soil saturation, also highlighting 1988 and 1993. The summertime average (JJA) shows that during both of these extreme conditions, in the top meter of the profile 1988 is the driest of all the years and 1993 is the wettest of all the years. The effect of even the well-known drought of 1988 did not reach below this top meter of the soil: the soil between one and two meters was wetter than average during 1988. This is an indication that, in Illinois, effects of atmospheric phenomena do not reach below the top meter of the soil. This is consistent with the fact that most of the state is covered with crops, which tend to have a rooting depth of close to one meter.

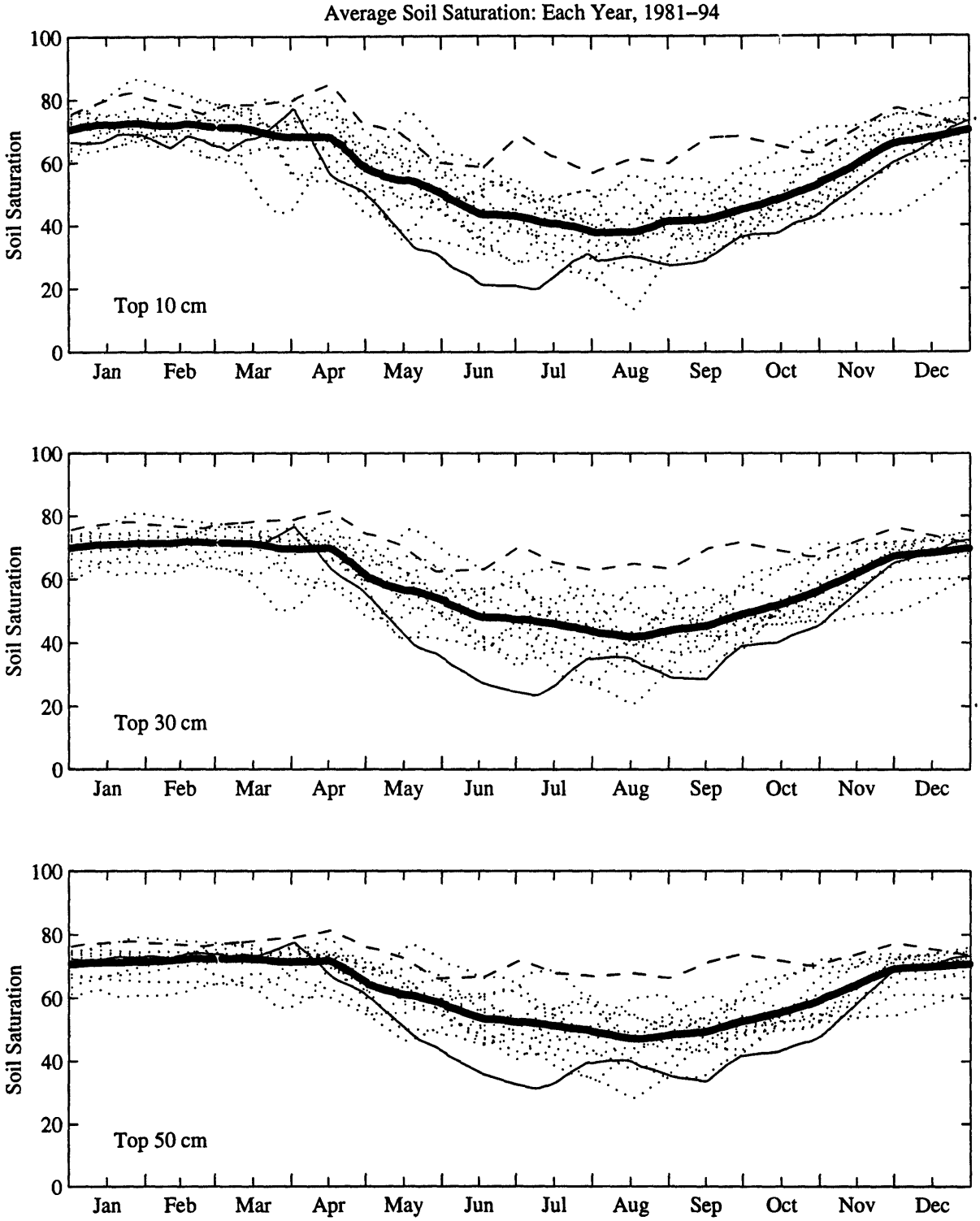

Figure 3.2: Annual average of soil saturation cycles for each year, 1981-1994. Dashed line is 1988 (extreme drought); solid line is 1993 (extreme flood); all other years are drawn with dotted lines; thick dotted line is average of all 14 years; a) top 10 cm, b) top 30 cm, c) top 50 cm.

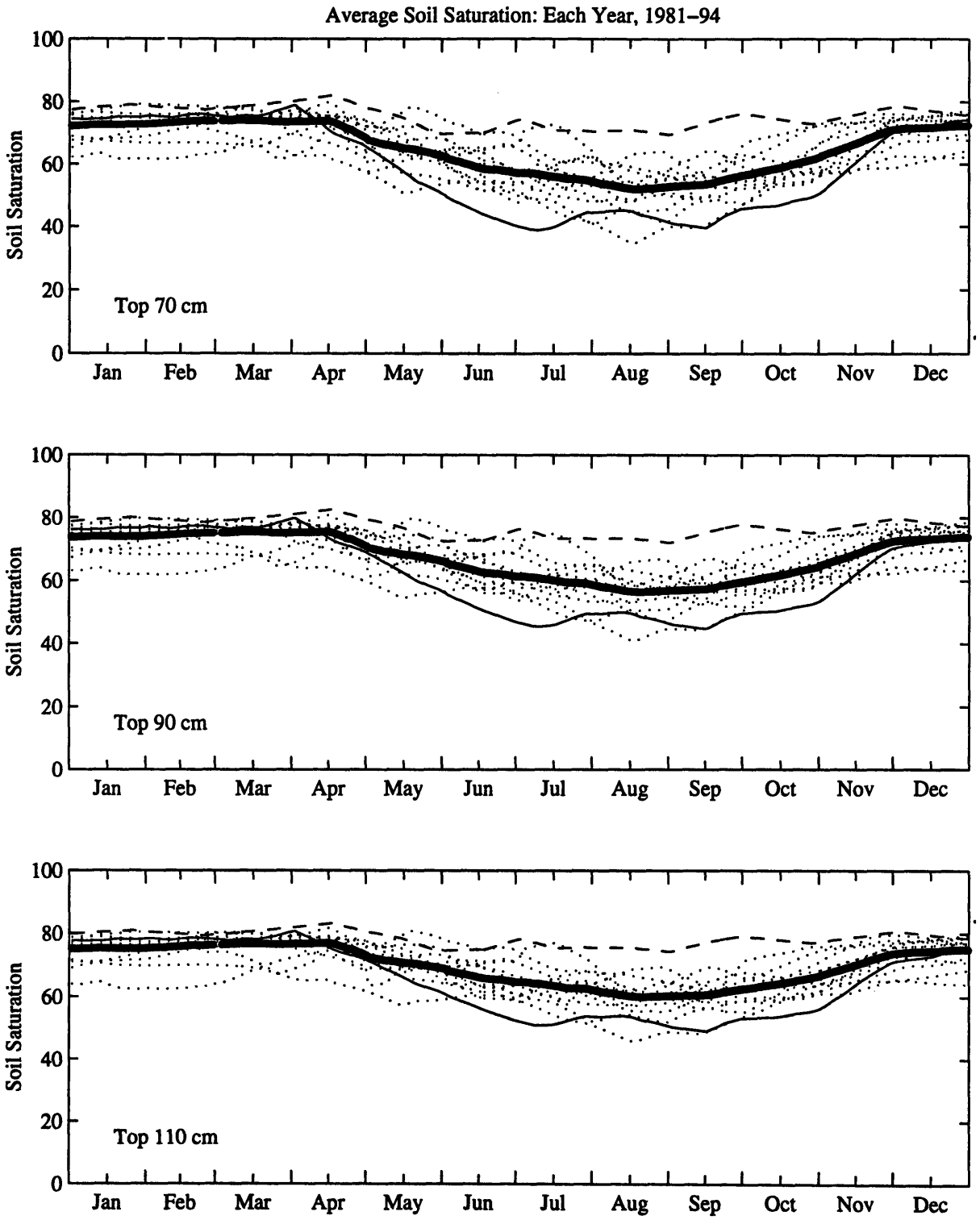

Figure 3.2 (cont.): d) top 70 cm, e) top 90 cm, f) top 1.1 m.

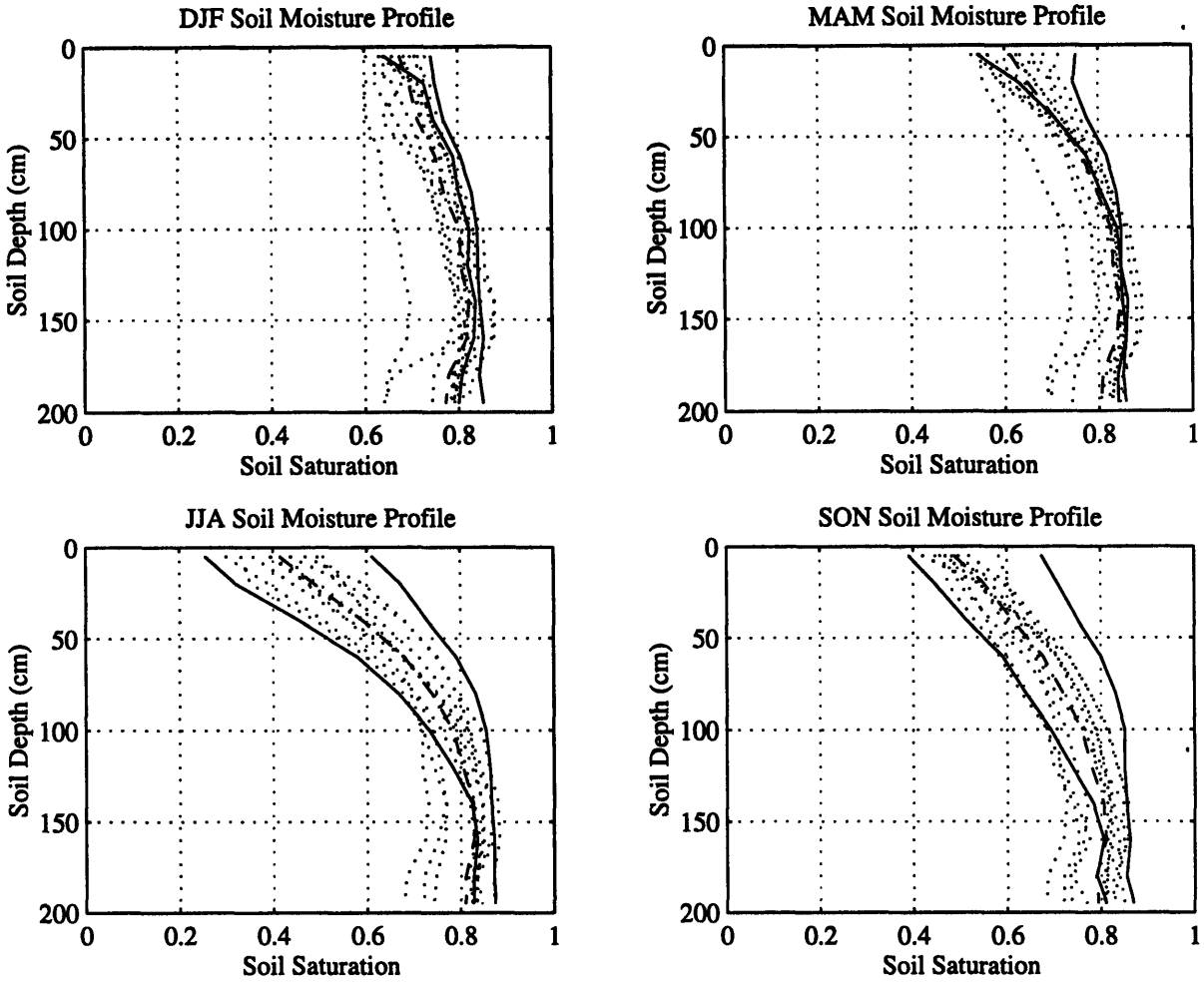

Figure 3.3: Seasonal average soil saturation profiles: a) December-February (DJF), b) March-May (MAM), c) June-August (JJA), d) September-November (SON). Left-most solid line is 1988 (extreme drought); right-most solid line is 1993 (extreme flood); all other years are drawn with dotted lines; dashed line is average of all 14 years.

B. Daily Precipitation Data

Measures of daily precipitation were available from the Illinois State Water Survey at 129 stations within the state. Their locations are shown in Figure 3.1. In Kunkel et al. (1990), data from these stations were bulked into 9 crop reporting zones: here, however, we have determined the state-wide average daily precipitation by averaging daily values at all 129 stations. This time series of the state-wide average daily rainfall was used in all the analyses discussed below. Figure

3.4 shows the average total monthly rainfall during the 14 years for which we have soil moisture observations (1981-1994).

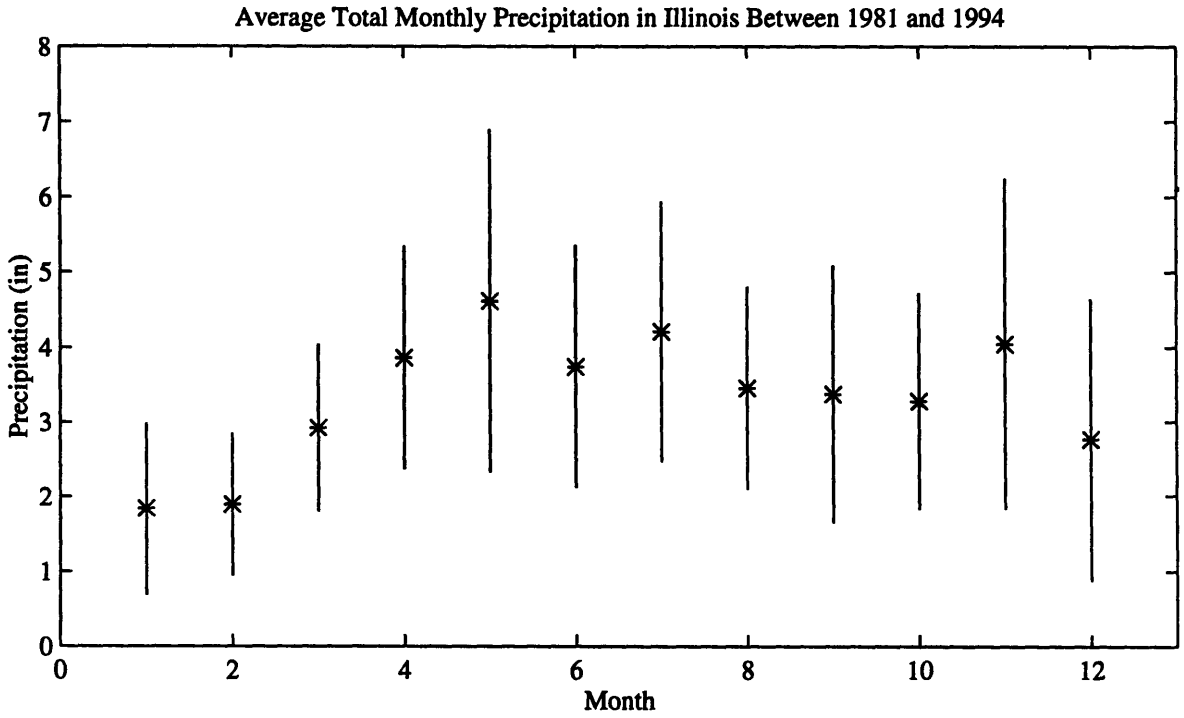

Figure 3.4: Average total monthly precipitation over Illinois, 1981-1994. Stars indicate means of the 14 years; lines extend to plus or minus one standard deviation.

C. Results and Discussion: The Interplay Between Soil Saturation and Subsequent Precipitation Throughout the Year

To relate this data analysis with the modeling discussed in the first chapter, we compared an initial soil condition to subsequent precipitation, much like a modeler would test for precipitation sensitivity to soil water. For a given day, say April 1, we looked at the average soil saturation within the state for each of the available 14 years. We then calculated the total precipitation in the subsequent 21 days for each of the 14 years, in this case, April 2 through April 23. Twenty-one days is time enough for the system to go through a few wetting and drying soil cycles, and a few convective storm cycles, so our results will be indicative not of a single weather event, but of a short climatic period. A linear regression was then performed on these two 14

year series, and the coefficient of determination, r^2, was recorded as an indicator of the percentage of rainfall variability that can be explained by the soil water initial condition. This analysis was performed for all 365 days of the year. The dots in Figure 3.5 show that the r^2 values reach as high as 0.7 for the top 10 cm. Even after a 21 day smoothing, more than 40% of the variability in rainfall can be explained by a simple linear correlation between initial soil saturation and subsequent rainfall. This correlation was damped at greater depths, but was still significant during the summer down to a depth of 90 cm.

The level of significance lines of Figure 3.5 are computed using an F-distribution for the r^2. (The 5% level of significance line for an F distribution with 1 and 12 degrees of freedom in the numerator and denominator, respectively, is 4.75. This yields an r^2 of 0.2836. The 10% line is at $F(1,12) = 3.18$, which yields an r^2 of 0.2095. See Johnston (1984) for details.) These lines apply to the daily measurements, not to the smoothed lines. The significance lines for the smoothed data will be lower since the variability will go down as the inverse of the length of the averaging window. All Figures 3.5a-c show the daily r^2 is stronger during the summer than the rest of the year, though there is also a local peak during April, as well. At the shallower depths, the linear correlation stays above the 10% level of significance line from the end of May to early August, and for much of April. During the rest of the year, the correlation between soil moisture and subsequent precipitation is not significant. We find three possible explanations for these results showing that there is a significant linear relation between soil saturation and subsequent precipitation conditions during this

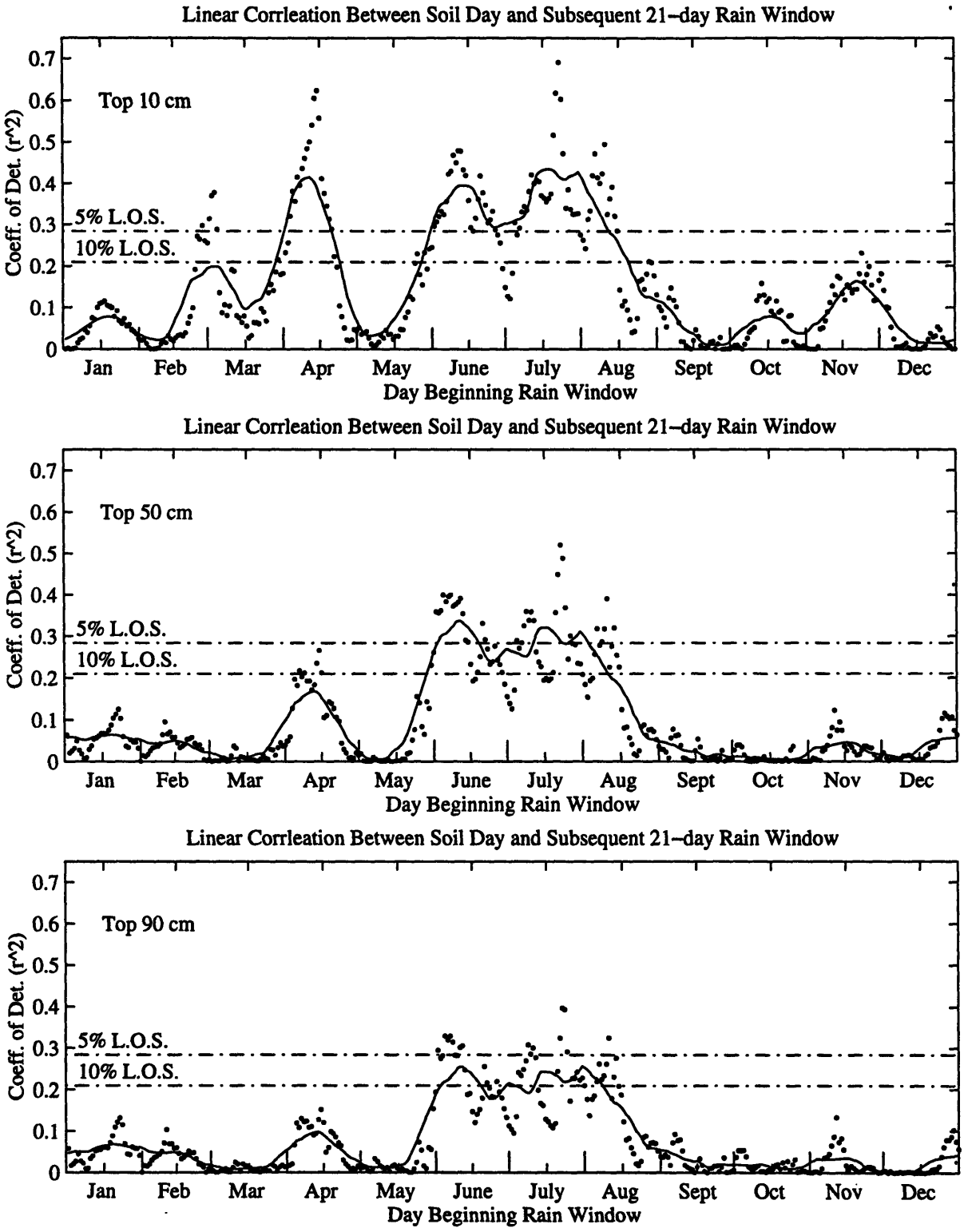

Figure 3.5: Linear correlation between initial soil saturation and precipitation in the subsequent 21 days for a) top 10 cm, b) top 50 cm, and c) top 90 cm. Solid line is 21-day moving average. Level of significance lines refer to the daily values (not the smoothed line).

summer period. First, it is possible that the relationship is due to a persistent large scale atmospheric forcing that sustains or enhances a persistence in rainfall between adjacent time periods, and through the correlation between concurrent rainfall and soil saturation, results in the observed correlation between soil saturation and subsequent rainfall. Second, the correlation could be a reflection of a feedback process in which initial soil moisture affects rainfall, which then affects soil moisture, etc. Finally, we must consider a combination of these two mechanisms.

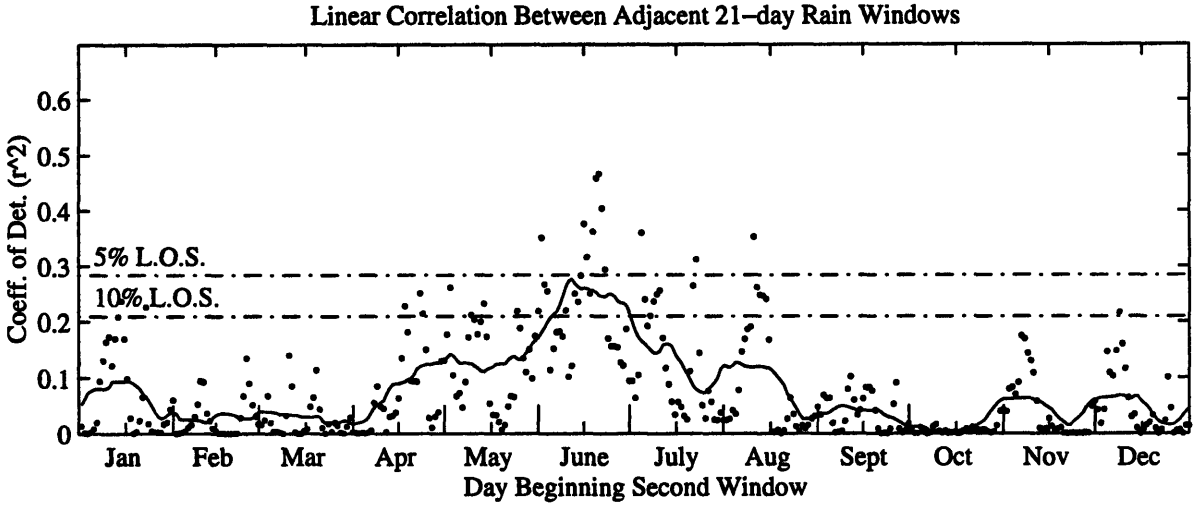

Figure 3.6: Linear correlation between adjacent 21-day precipitation windows; 21-day smoothing. Solid line is 21-day moving average. Level of significance lines refer to the daily values (not the smoothed line).

If large-scale atmospheric processes drive the system at hand, persistence in atmospheric conditions would first be reflected in rainfall persistence, as shown in Figure 3.6. Here, persistence in rainfall is measured by the correlation between the total precipitation in adjacent 21-day windows. Figure 3.7 then shows the correlation between a 21 day rainfall window and soil saturation at the end of the window. If precipitation forces soil saturation at the end of a given window (Figure 3.7), and if precipitation is also linearly correlated with precipitation in the next time window (Figure 3.6), soil saturation may, merely as a direct consequence of this rainfall forcing, also be significantly correlated with subsequent precipitation (Figure 3.5). In this case,

we would expect the rainfall persistence to be greater than the correlation between soil saturation and subsequent precipitation.

In a scenario in which soil moisture is a driving force affecting rainfall, we would expect the state of the soil moisture reservoir to affect rainfall directly. In this case, the correlation between soil saturation and subsequent rainfall should outweigh the correlation between rainfall in adjacent windows. Figures 3.8a-c are plots of the smoothed lines of Figures 3.5a-c superimposed on the smoothed precipitation persistence line of Figure 3.6. From this figure, we can see that for autumn and winter, the correlation between rainfall and prior soil moisture is comparable to the correlation between serial precipitation windows. This suggests that persistence due to large-scale atmospheric forcing can account for much of the observed linear correlation between soil moisture and subsequent rainfall during these seasons. Throughout June, July and August, and for a portion of the spring, however, rainfall is better correlated with prior soil moisture than with prior rainfall. This suggests that during the summer, feedback from soil moisture is the more likely physical explanation. At no point, however, can we rule out the possibility that a combination of the two given explanations is responsible for the observations. These results are consistent with the GCMs discussed earlier, and with the regional study of Pan et al. (1995).

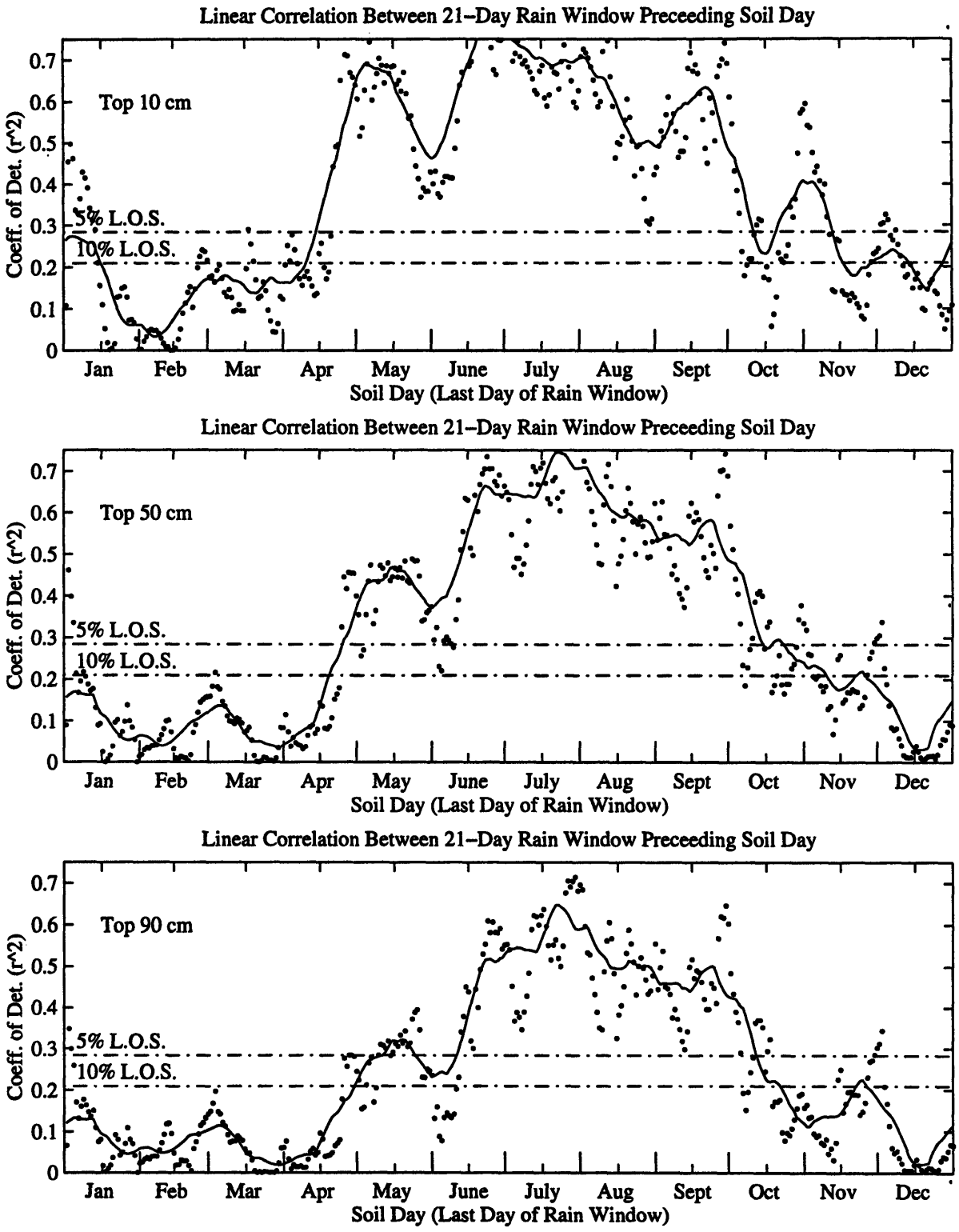

Figure 3.7: Linear correlation between 21-day total precipitation and soil saturation at the end of the 21 days for a) top 10 cm, b) top 50 cm, and c) top 90 cm. Solid line is 21-day moving average. Level of significance lines refer to the daily values.

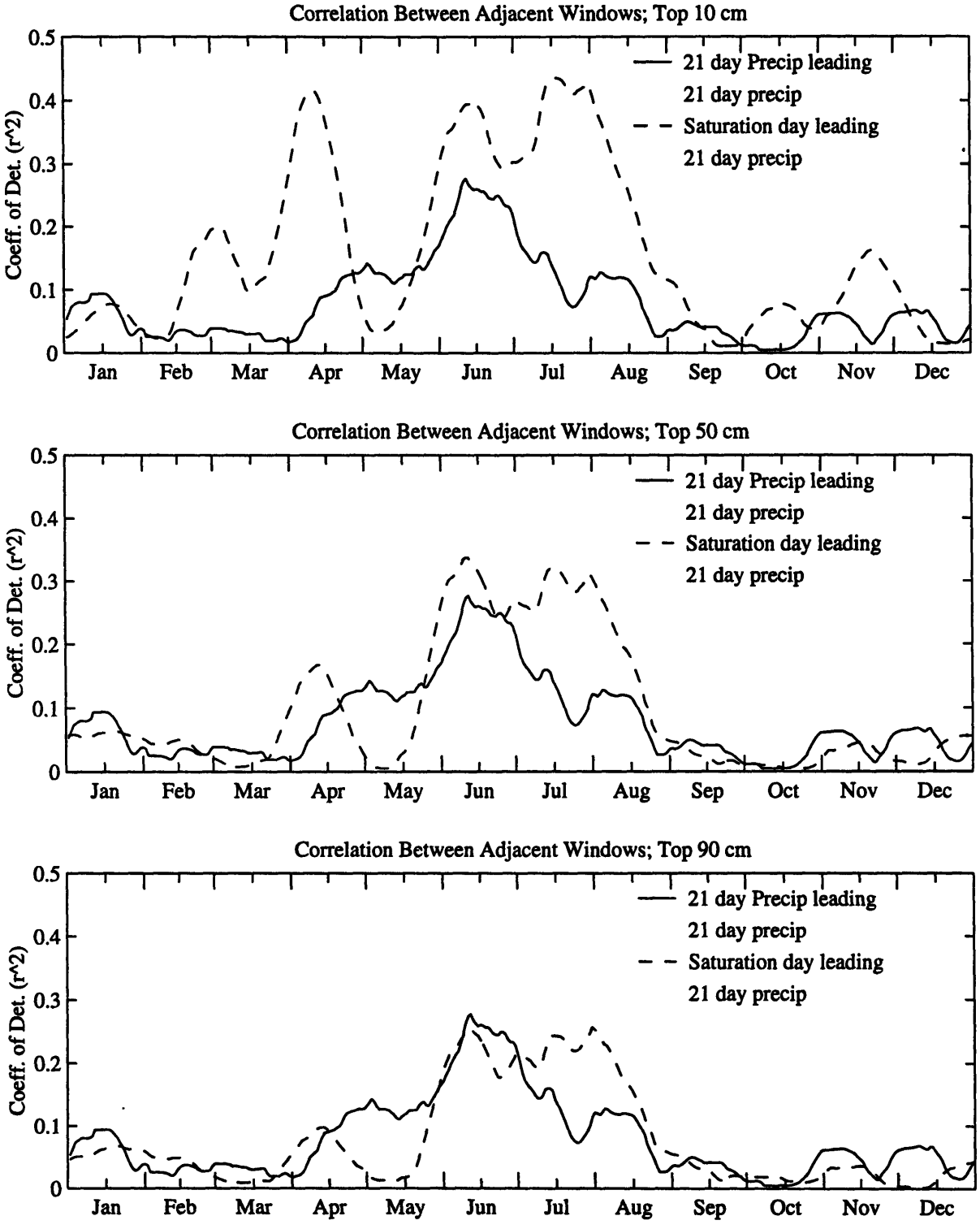

Figure 3.8: Comparison of smoothed lines of the linear correlation between adjacent precipitation windows (solid line from Figure 3.6) and of the linear correlation between soil saturation and subsequent precipitation (dashed lines from Figures 3.5a-c).

D. Results and Discussion: Focus on Spring and Summer Connections

Given the results of the analysis for the entire year, it seems pertinent to focus on the summer months. An analysis similar to the one described above was performed, comparing the correlation between an initial soil condition and total precipitation during the rest of the summer. Assuming that summer is taken to end on August 23, Figure 3.9 shows the r^2 for every initial condition day from May 1 to July 31. Similarly, Figure 3.10 shows the results for the case where summer is taken to end on September 19, with initial condition days moving from May 1 to August 31.

Again, the linear correlation is significant for much of the summer. Figure 3.9 shows a maximum of $r^2 > 0.5$ at the end of June, while Figure 3.10, with summer lasting until September 19, reaches this same r^2 level in mid-July. Figure 3.11 shows the 14 data points used to obtain these r^2 values for the June 25 initial condition and August 23 end of summer. The number beside each data point denotes the year of the event, and the r^2 is given in the upper left corner. Though the non-extreme years show little pattern, we see that the most extreme years, 1988 and 1993, fit the expected pattern of a dry (wet) spring being followed by a dry (wet) summer. If the two variables were completely unrelated, then the probability of both of these events randomly occurring within one data set would be quite low.

The dashed horizontal and vertical lines in Figure 3.11 divide the data into three spring soil moisture classes: high, normal, and low, and into three summer rainfall classes: again, high, normal and low. The lines are calculated by taking the average of the 14 data points ± one standard deviation. These groupings show that during these 14 years, no abnormally dry spring was followed by an abnormally wet summer, and vice versa. Though 14 years is not enough data

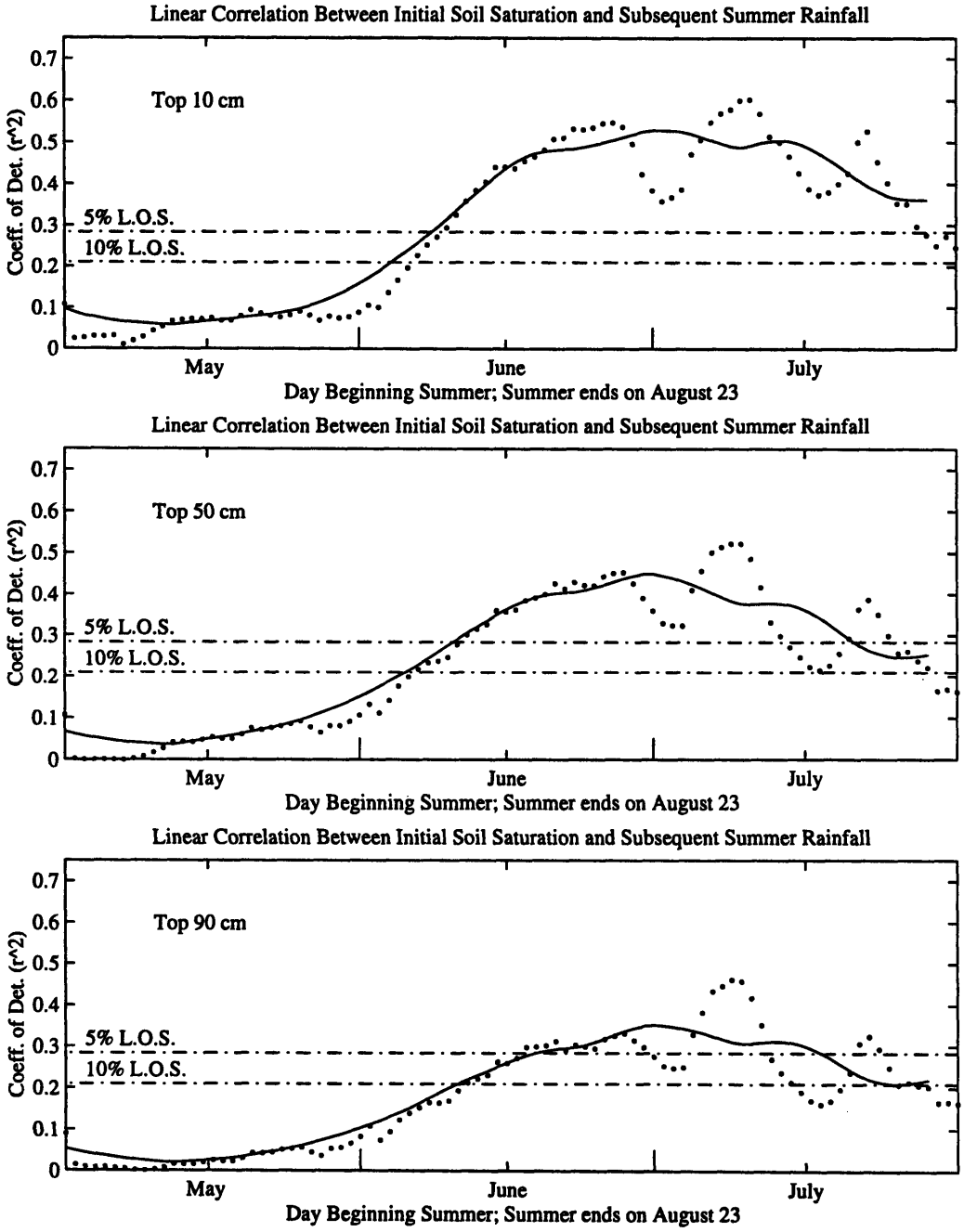

Figure 3.9: Linear correlation between initial soil saturation and precipitation in the rest of the summer (through August 23) for a) top 10 cm, b) top 50 cm, and c) top 90 cm. Solid line is 21-day moving average. Level of significance lines refer to the daily values (not the smoothed lines).

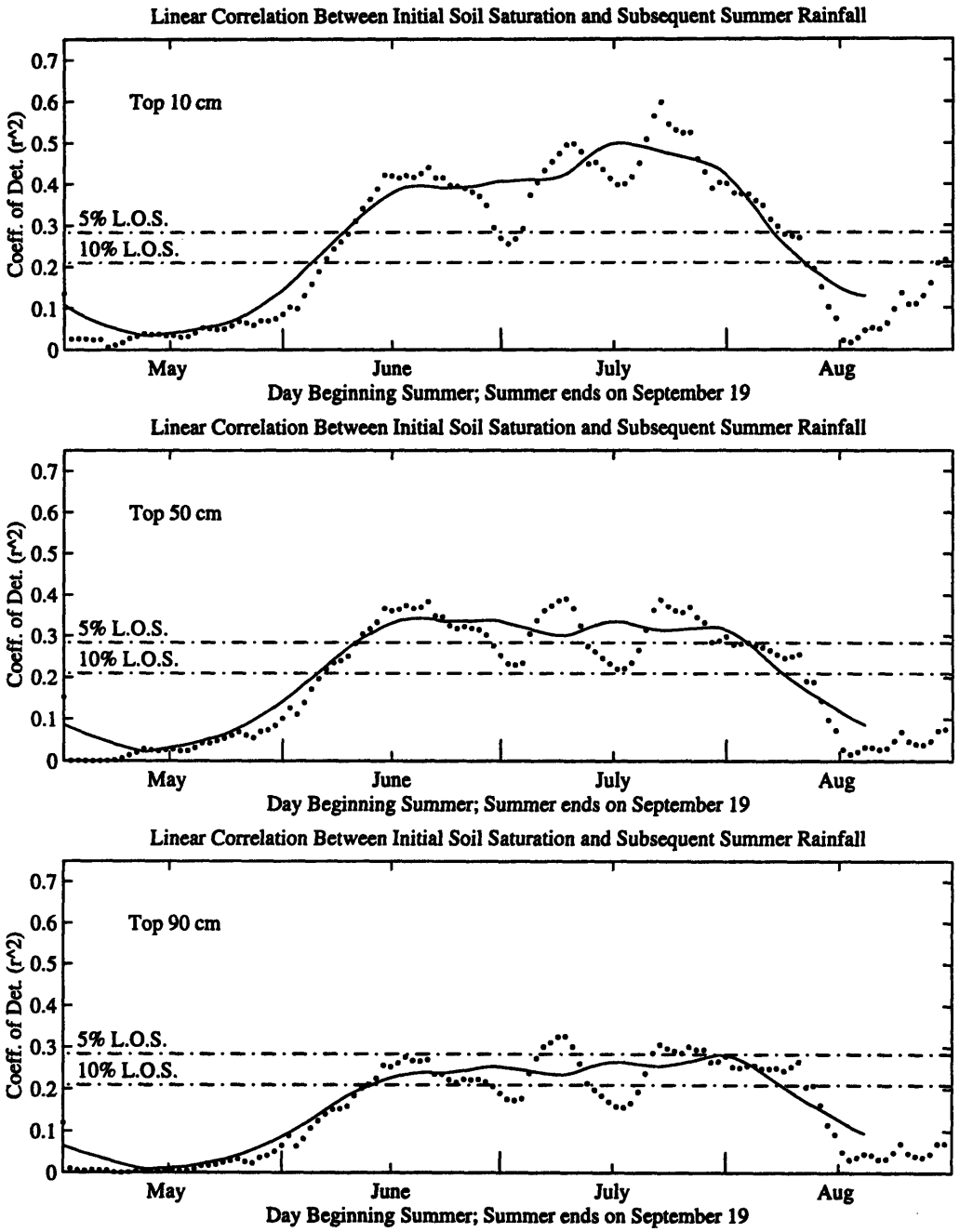

Figure 3.10: Linear correlation between initial soil saturation and precipitation in the rest of the summer (through September 19) for a) top 10 cm, b) top 30 cm, and c) top 90 cm. Solid line is 21-day moving average. Level of significance lines refer to the daily values (not the smoothed lines).

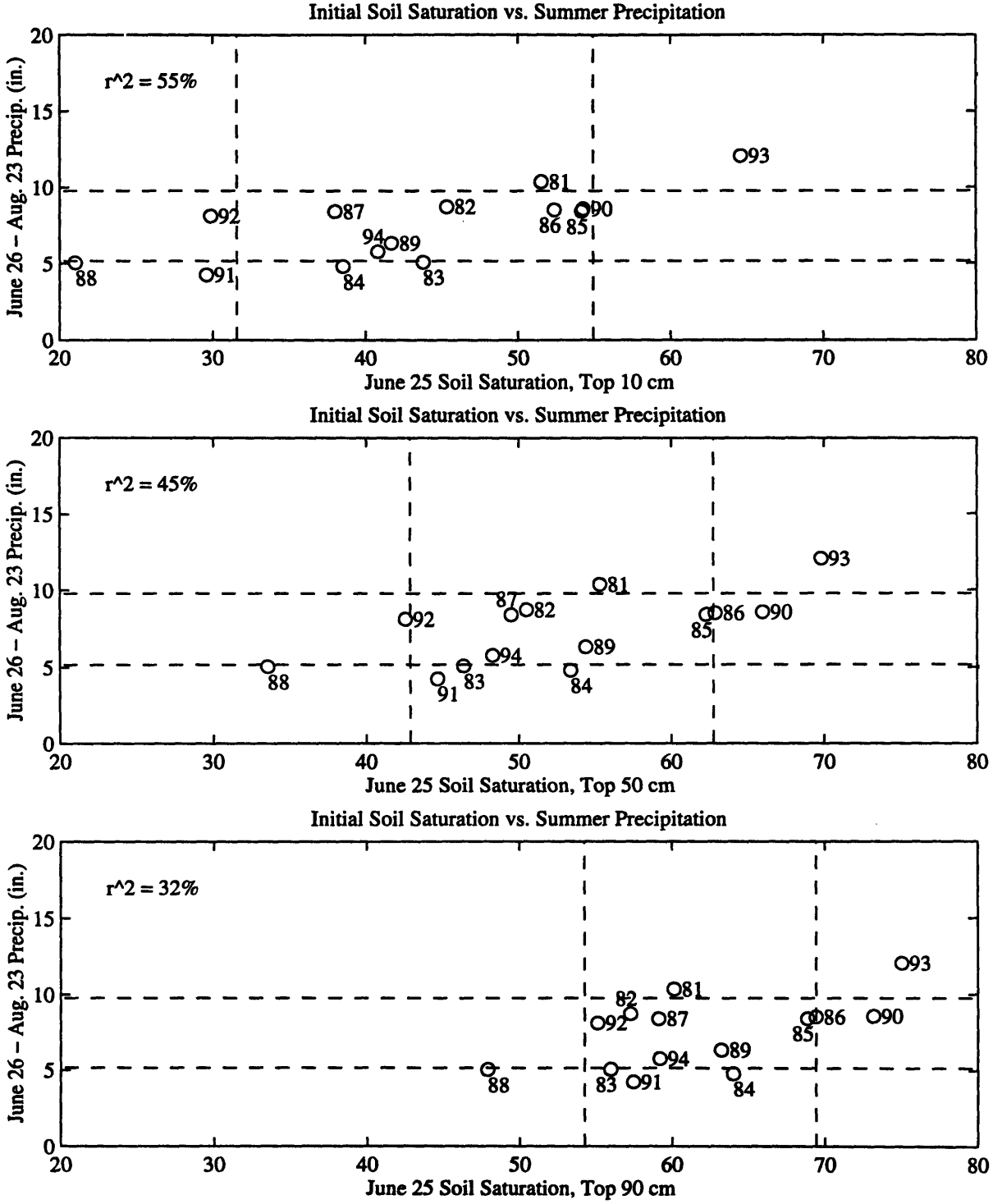

Figure 3.11: Average Initial soil saturation on June 25 for a given year versus summer (July 1 to August 23) precipitation for each year. Numbers beside each data point indicate sample year. Dotted lines are means of the 14 years ± one standard deviation, separating data into low, normal, and high categories of soil saturation and summer precipitation.

on which to base final conclusions, it is more data than has ever been collected and analyzed in this manner to date.

E. Discussion of Results

This study tests the hypothesis that soil saturation is positively correlated with subsequent precipitation by analyzing a 14 year soil moisture data set from the state of Illinois. The linear correlation between an initial soil saturation condition and subsequent rainfall is significant during the summer months, reaching a peak of $r^2 > 0.4$ in mid-June. This result is consistent with the hypothesis that knowledge of late spring/early summer soil moisture conditions can aid in the prediction of drought or flood years, but it does not necessarily prove that feedback from anomalous soil moisture reservoirs is the cause of anomalous summer conditions. Further analyses indicate that from early June to mid-August, persistence in rainfall cannot fully account for the observed correlations, suggesting the likelihood of a physical feedback mechanism linking early summer soil saturation with subsequent precipitation.

Though these conclusions are striking, they must be accepted with some restraint: the observed results suggest that though the physical feedback is significant, it is by no means the only pertinent physical process. Furthermore, the data set is limited in both spatial and temporal resolution. The 14 years comprising this data set have very few non-normal events from which we can make inferences regarding the association between soil moisture and subsequent summer rainfall. Additionally, the aerial coverage is quite small: the entire mid-western United States would provide a much more comprehensive study region. However, despite these deficiencies, this data set is by far the largest of its kind that is readily available for analysis.

Observations made here should be useful to those working on the dynamics of droughts and floods for mid-latitude continental interiors. The results of many GCMs (Shukla and Mintz (1982); Oglesby (1991); Rind (1982); Trenberth et al. (1988); Atlas et al. (1993); Oglesby and Erickson (1989)) and Regional studies (Pan et al. (1995); Huang et al.(1996)) are consistent with those observed in the Illinois data set: extreme soil moisture availability (or lack thereof) acts as either a feedback mechanism maintaining the wet (or dry) conditions established in the beginning of each summer, or as a flag indicative of some large-scale process that is affecting both the soil moisture and the precipitation regime.

Neither these observations nor the modeling studies discussed earlier answer the question of how these links between soil moisture and precipitation are forged. The subsequent chapters will address two stages of the physical link between soil water and rain water: Chapter 3 will address the relationships between soil saturation and boundary layer conditions, while Chapter 4 will focus on boundary layer conditions and rainfall.

Chapter 4: The Relationships Between Soil Saturation and Boundary Layer Conditions

The observed relationship between soil saturation and subsequent rainfall, detailed in the previous chapter, highlights the importance of investigating possible physical mechanisms linking these two variables. The analyses described in this chapter attempt to address the first of two intermediary steps between soil and rainfall: the relationship between soil saturation and boundary layer conditions, as indicated by surface measurements. Chapter 5 will be directed towards the link between boundary layer conditions and rainfall.

A. The NCDC Surface Airways Hourly Dataset

Surface meteorological data was obtained from the National Climatic Data Center's (NCDC's) Surface Airways Hourly Dataset TD-3280. Only eight stations are located within Illinois. These eight are supplemented by five additional stations: Paducah, Kentucky, just over the Ohio River at the Southern tip of the state; Milwakee, Wisconsin, approximately 60 km north of the northeastern corner of Illinois, and three additional stations in western Indiana, 40, 100, and 110 km east of Illinois. See Figure 4.1 for station locations.

Given the paucity of data within the approximately 300 km by 650 km control volume of Illinois, the inclusion of this supplemental information was deemed beneficial to the statistical validity of the analysis. The Kentucky station is only nominally outside of Illinois, and the other four are in the predominately downwind direction of Illinois, and can therefore be an indicator of

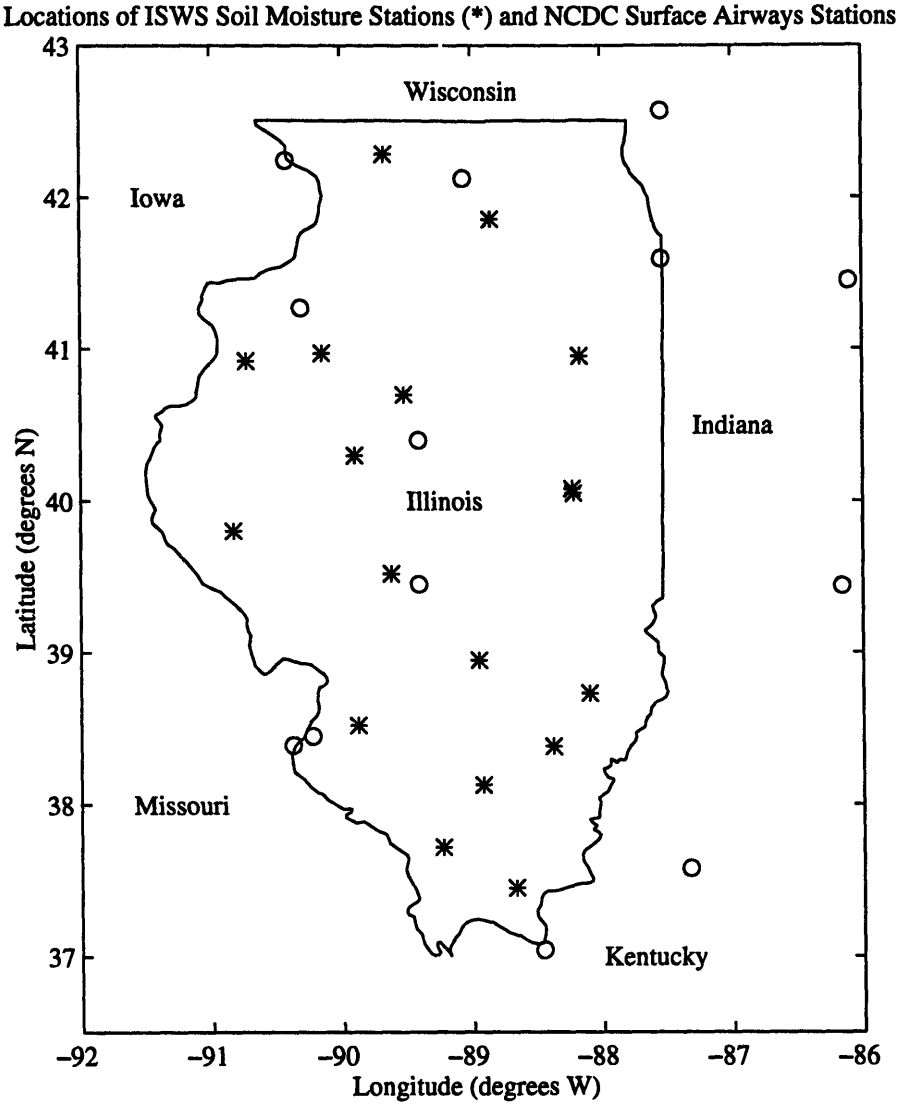

Figure 4.1: Locations of ISWS soil moisture stations and NCDC Surface Airways Hourly Dataset stations. Solid line is the Illinois state boundary.

the influence of soil saturation on boundary layer air as it is advected out of our study area. The averaging of data both within and downwind of the soil moisture study area is intended to address two of the difficulties of working with real data: the complications of advection, and the limitations of data collection and availability.

Surface parameters obtained from the NCDC hourly dataset include temperature, T, wet-bulb temperature, T_w, pressure, P, and relative humidity, f. From these quantities, wet-bulb depression, $T_{dpr} = T - T_w$, potential temperature, θ, virtual potential temperature, θ_v, equivalent

potential temperature, θ_E, wet-bulb potential temperature, θ_w, temperature of the lifting condensation level (LCL), T_{LCL}, pressure depth to the LCL, P_{LCL} - P_s, and mixing ratio, w were calculated at each station for each hour. The hourly values of each of these variables were then averaged all 13 stations. The daily minimum, mean, and maximum of each of these twelve variables was then determined, and these 36 quantities were then used in an analysis with the daily soil saturation time series described in the previous chapter.

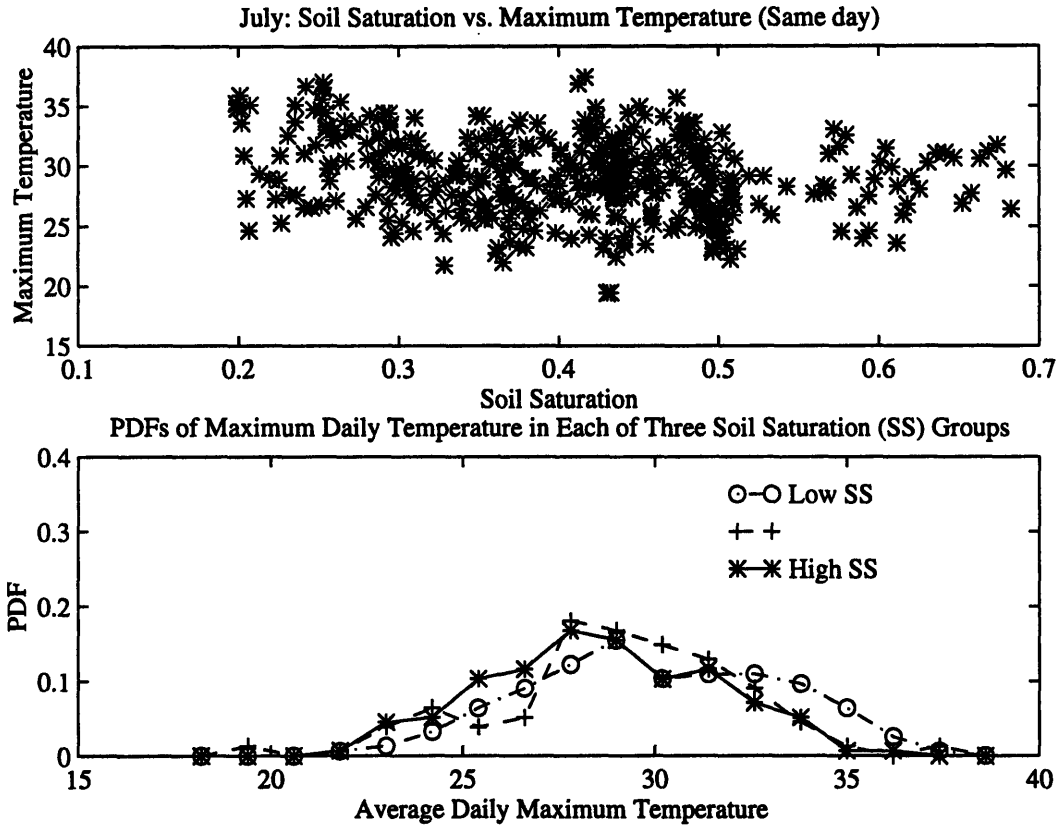

Figure 4.2: Soil saturation (SS) and maximum daily temperature (T) for days during July, during the years 1981 to 1995; a) scatter plot of all data pairs; b) probability density functions (PDFs) for three subsets of the data based on the degree of soil saturation.

B. Presentation of Results

Figures 4.2a-d show the same data in four different ways. Figure 4.2a shows, for the month of July in each of the years for which both soil saturation data and NCDC surface

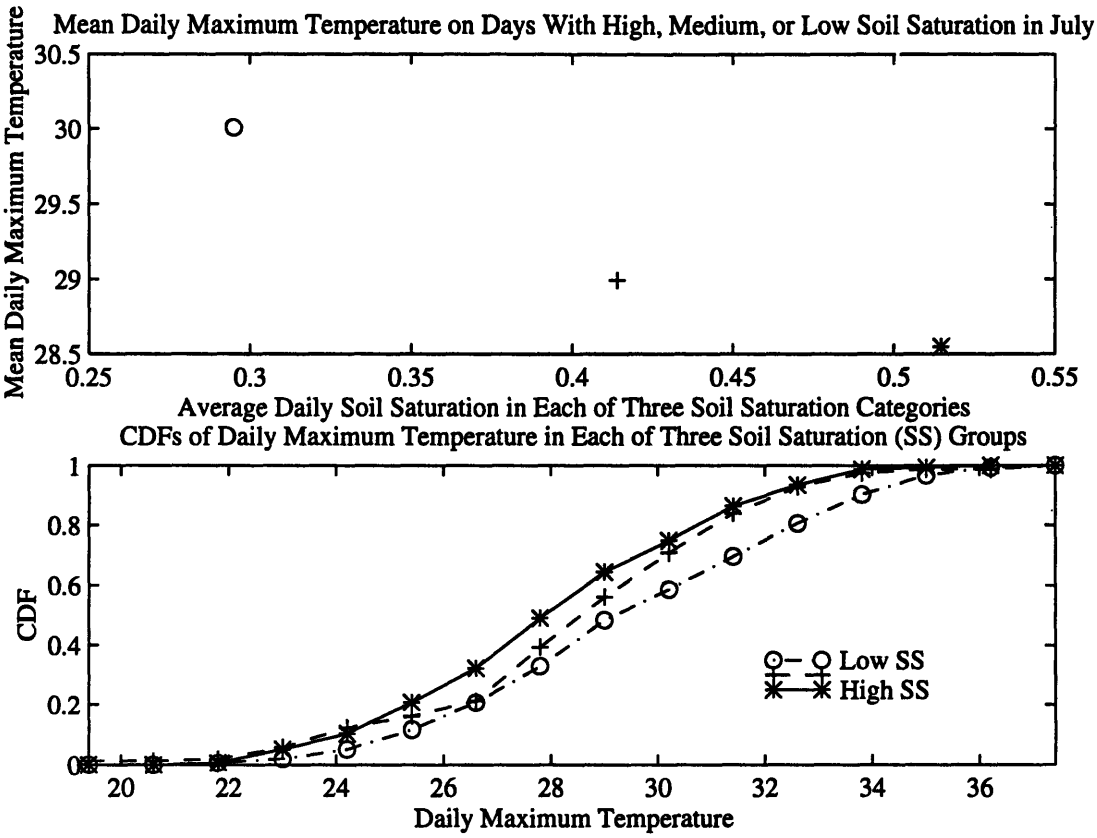

Figure 4.2 (cont.): c) first moments of the PDFs in 4.2b; d) cumulative distribution functions (CDFs) for the PDFs in 4.2b.

observations are available (1981-1995), the state-wide average soil saturation (top 10 cm) on a given day and the state-wide average maximum temperature on the same day. Since soil saturation is only one of many factors which could potentially impact temperature, a strong trend is not indicated by this raw data. Other factors, particularly incident solar radiation at the surface, are responsible for the majority of temperature fluctuations. However, the role of soil moisture can be important for days on which the incident solar radiation is equal. Since daily observations of this quantity were not obtained for Illinois, we are unable to factor out this dependence. Instead, we split the data into three different categories of soil saturation and compared the behavior of surface variables given that soil saturation was high, medium, or low. The 465 data points (15 years, 31 days in July) in Figure 4.2a were split into three groups: the 155 points with the lowest soil saturation, the 155 points with the highest soil saturation, and the 155 points in the

middle. Figure 4.2b shows probability density functions (PDFs) of temperature for each of these three soil saturation groups.

The PDFs show a fair amount of overlap, due to the dominance of factors other than soil saturation, but Figure 4.2c shows that the means of these distributions indicate that, on average, drier soil conditions lead to warmer daily maximum temperatures. The cumulative distribution functions (CDFs) for these distributions are shown in Figure 4.2d. This figure is potentially more revealing than the PDFs: we can see that the CDF of the high soil saturation category increases more rapidly than the other two, indicating that more of the mass of the distribution is at lower temperatures. This effect can also be seen in the PDFs, but the overlap of the lines makes PDFs of these data sometimes difficult to interpret. Results from subsequent analyses with other variable combinations will only be presented in the manner of Figures 4.2c and 4.2d.

C. Analysis of Initial Soil Saturation Followed by 21-Day Average of Boundary Layer Conditions, Averaged Over All of Illinois

The previous section compared daily soil saturation to air temperature on the same day of the soil saturation observation. This approach does not appropriately address the issue of how land surface conditions might impact the boundary layer, because it is not clear if, for example, low soil saturation is the result or the cause of a high air temperature. To address this cause-effect issue, the following analyses were performed with soil saturation on a given day and average boundary layer conditions in the subsequent 21 days. Same-day analyses were also performed for all of the variables presented in this section, and the results were not significantly different. A twenty-one day window was chosen to be consistent with the soil moisture-rainfall analyses presented in Chapter 3. As discussed in that chapter, this approach is meant to mimic the

control a person running a climate model has in setting the initial soil saturation condition in their simulation domain.

The analyses show that when a trend between a given boundary layer variable and soil saturation is strong, this trend is consistent in the minimum, mean and maximum daily value. For most variables, with the exception of relative humidity, the maximum daily values show equal or slightly greater dependence on soil saturation than the mean or minimum. When a trend with soil saturation is not strong, the maximum, mean, and minimum still almost always show consistent relative positions: if the intermediate soil category shows the highest average of daily maximums of the variable in question, followed by the lowest soil category and then the highest, the daily minimum and mean of the variable show this same pattern. To avoid redundancy, only the results with maximum values will be presented here.

Daily maximum relative humidity shows a strong dependence on soil saturation in each of the months May through September, as seen in Figure 4.3. April does not show a distinct dependence on soil saturation. As stated above, relative humidity is the one variable where the minimum and mean show stronger patterns than the maximum. The maximum shows a weaker effect because of the possibility of reaching complete saturation: once this threshold is reached, the measure can go no higher. This makes the range of the maximum relative humidity smaller than that of the minimum and mean, so the slope of the lines connecting the first moments in Figure 4.3 is smaller than that shown by minimum and mean relative humidity plots. Nevertheless, the trend is consistent: wetter soil on an initial day implies that the air in the following 21 days will be closer to saturation. Mixing ratio, however, only shows this dependence during July. June and August both have the highest w associated with the wettest

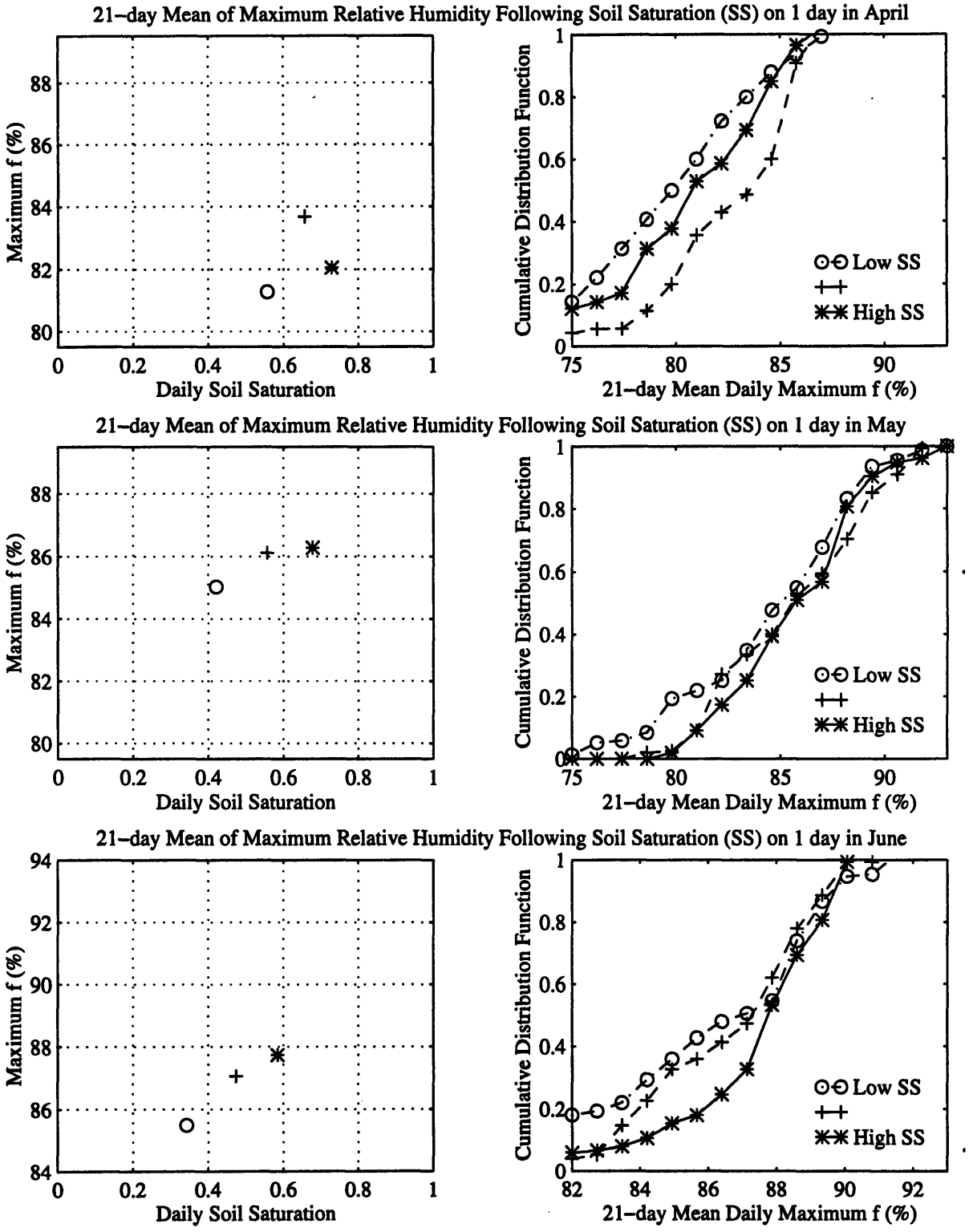

Figure 4.3: First moments and cumulative distribution functions (CDFs) of 21-day mean of maximum relative humidity (f), given that soil saturation (SS) on the day prior to the averaging window is low, medium, or high. Note that April, May and September plots are on one scale, while June, July and August plots are on a different scale: a) April, b) May, c) June.

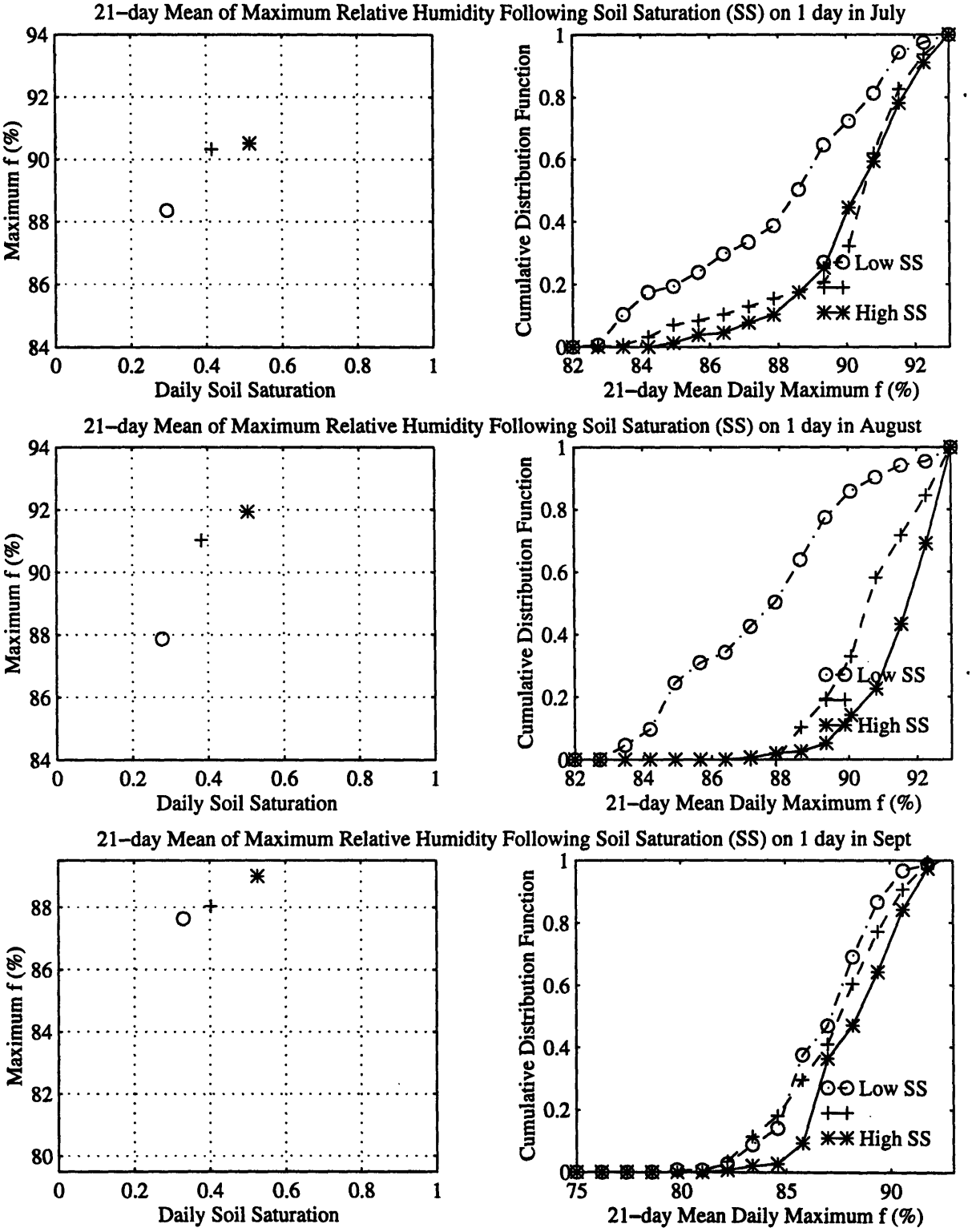

Figure 4.3 (cont.): As above, for d) July, e) August, and f) September.

soils, but the normal and dry soils do not fit this pattern. April and September show a negative correlation with soil moisture, as does May, though the normal soils have a slightly higher mean w than the driest soils. Though wetter soil seems to imply that the air is closer to saturation, it does not necessarily imply higher mixing ratio.

Mixing ratio was calculated from temperature, pressure and relative humidity at each station, for each hour of observations, using the following equations from Rogers and Yau (1989) and Bolton (1980). Relative humidity is defined as $f = w/w_{sat}$, so $w = fw_{sat}$. The saturation mixing ratio, w_{sat}, is determined from the relation:

$$w_{sat} = \varepsilon\left(\frac{e_{sat}}{p - e_{sat}}\right) \tag{4.1}$$

where $\varepsilon = m_v/m = 0.622$ and the saturation vapor pressure is given by:

$$e_{sat}(T) = 6.112\exp\left(\frac{17.67T}{T+243.5}\right) \tag{4.2}$$

The maximum daily temperature dependence on soil moisture demonstrated for the month of July in the above Section B is mimicked by the months of April, May and September (see Figure 4.5). During June and August, however, the pattern is not as strong: the drop in average temperature from the lowest soil saturation category to the intermediate soil saturation category is followed by an increase, rather than a drop, in average temperature between the intermediate and high soil saturation groups. This behavior was also seen in the same-day analysis of temperature and soil saturation, so it is not thought to be a result of the 21-day averaging masking the influence of the initial condition.

As mentioned above, soil saturation exhibits an important influence on air temperature, but it is by no means the dominant influence. We would expect higher soil moisture to mean that

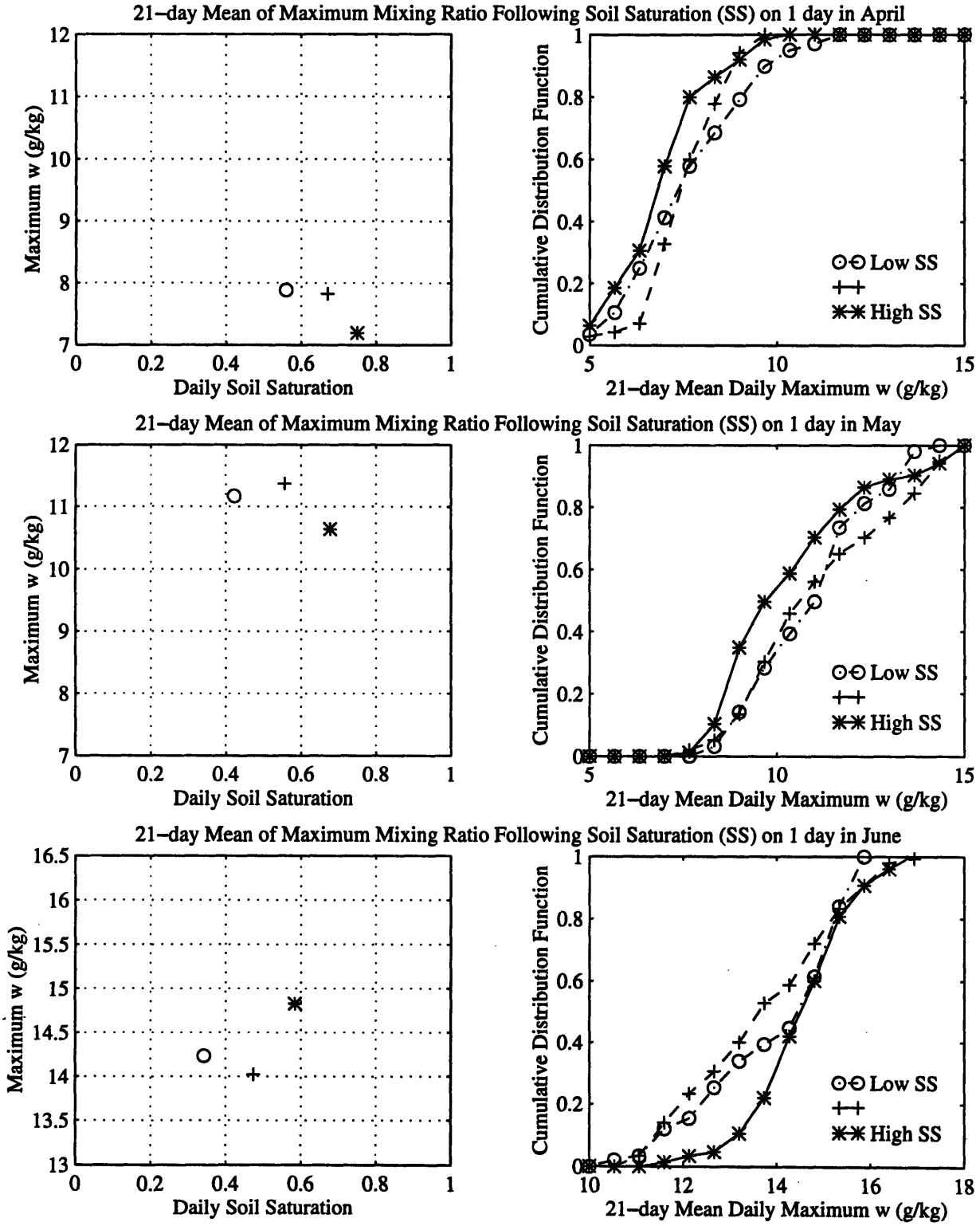

Figure 4.4: As in Figure 4.3, but for mixing ratio (w); a) April, b) May, c) June.

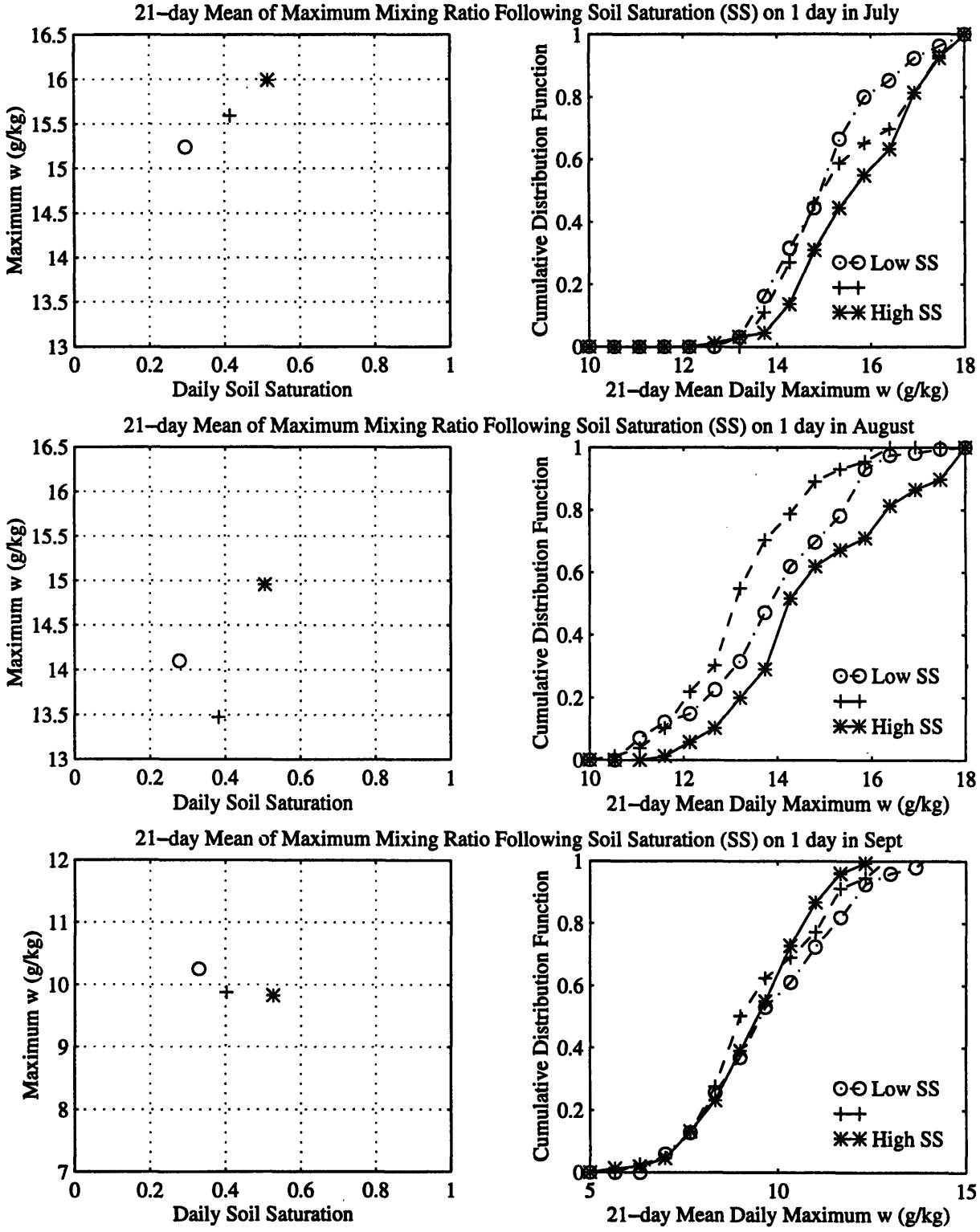

Figure 4.4 (cont.): As above, for d) July, e) August, and f) September.

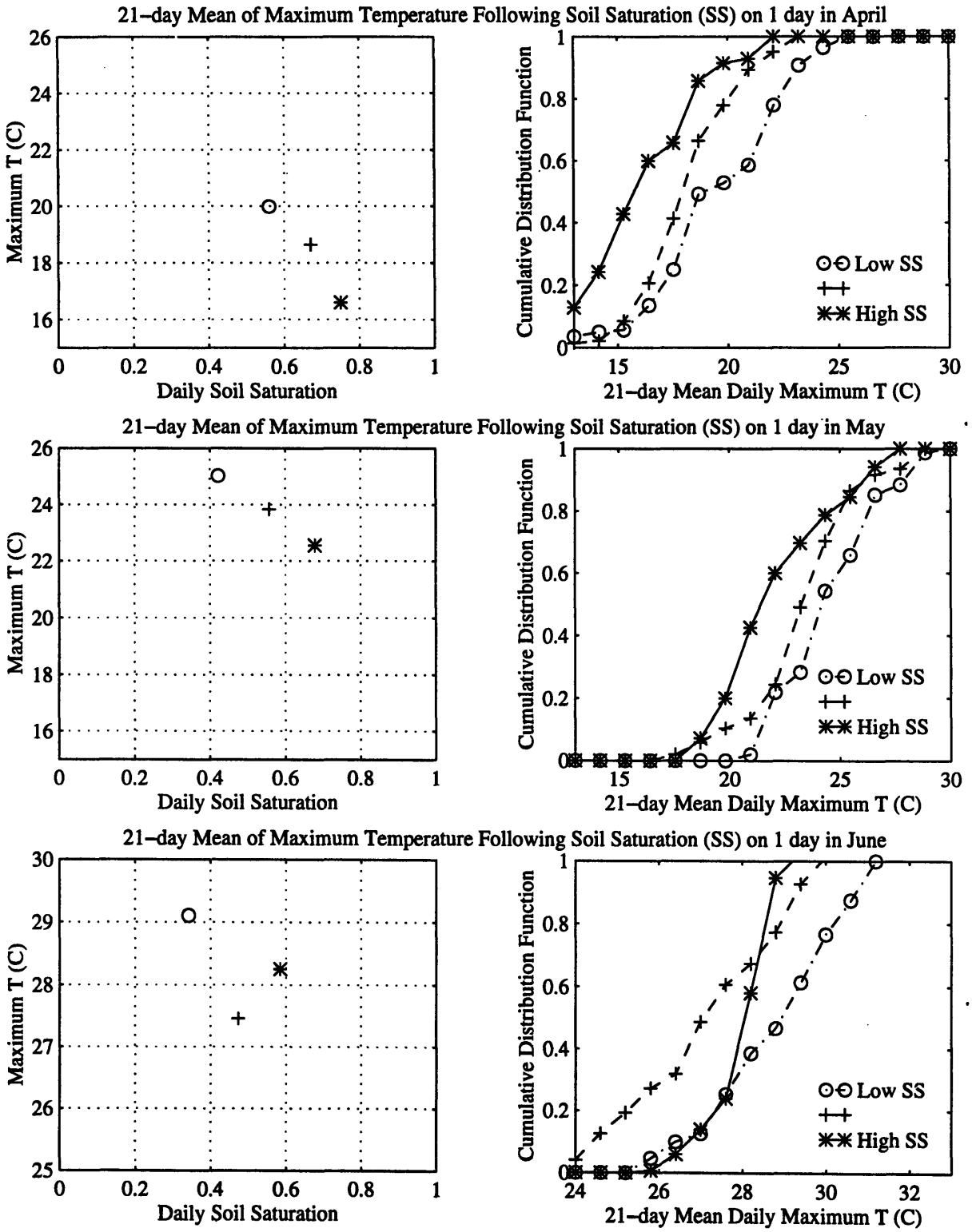

Figure 4.5: As for Figure 4.3 but for air temperature (*T*); a) April, b) May, c) June.

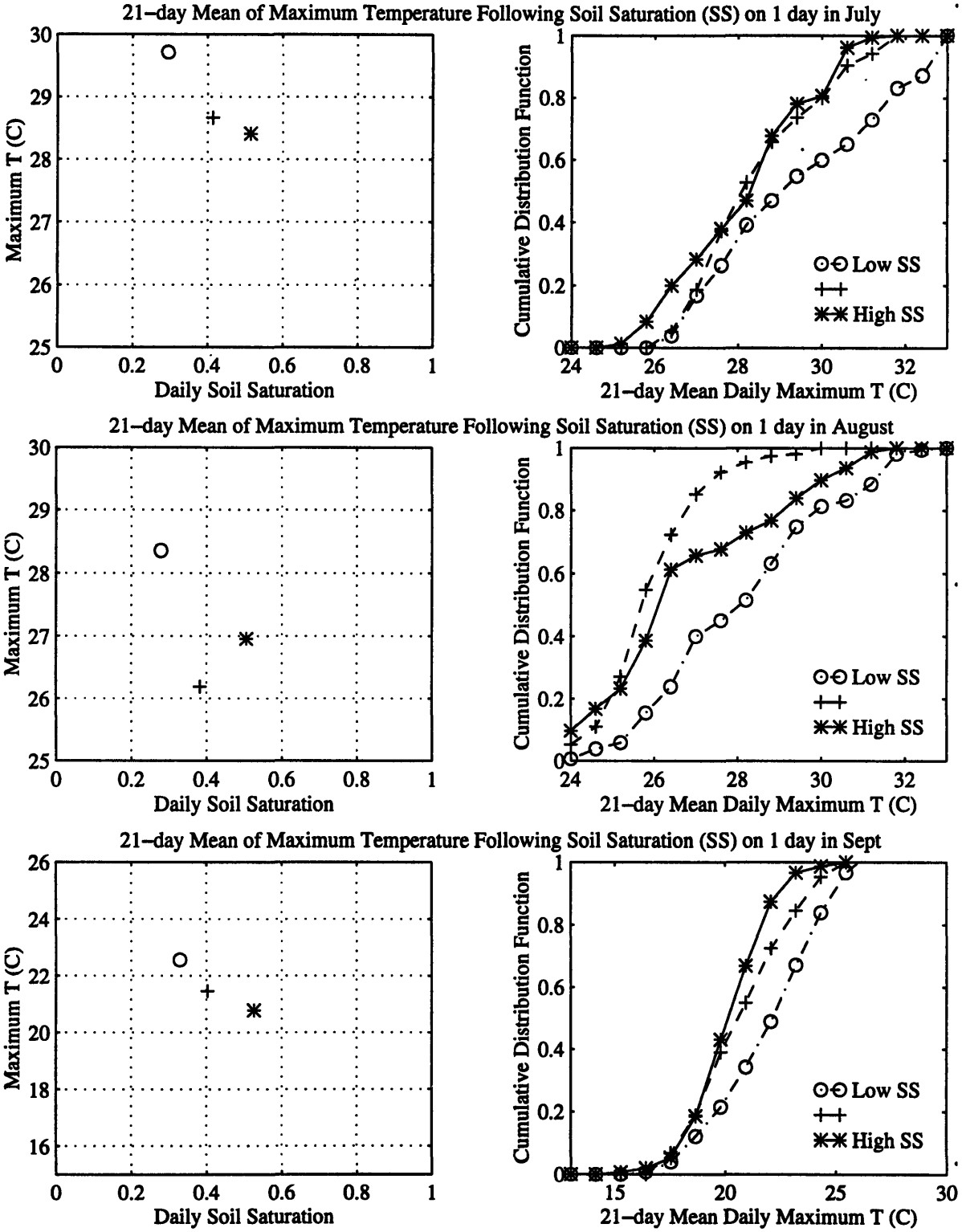

Figure 4.5 (cont.): As above, for d) July, e) August, and f) September.

more of the available energy is used to evaporate water than in a drier soil moisture scenario. This makes less energy available for sensible heating of the air, so we would expect higher soil moisture to lead to a lower Bowen ratio (β = ratio of sensible heat flux to latent heat flux) and a lower air temperature, given equivalent incident solar radiation at the surface. This qualifier is an important one that cannot always be assumed to be a given. Differences in incident solar radiation may be a significant factor in the ambiguity of the soil moisture–temperature relationship during June and August. In the FIFE data analysis of Betts and Ball (1995), their study of the effects of soil moisture on the boundary layer only takes into account days with net radiation above a given threshold, thereby acknowledging the potential significance of this forcing mechanism.

Another important factor which may be influencing the temperature behavior is the threshold dependence of evapotranspiration on soil moisture, as discussed in Chapter 2, and as pointed out by Betts and Ball (1995): "Above some soil moisture threshold, evapotranspiration depends primarily on atmospheric parameters, rather than soil moisture controls on vegetative conductance (p. 25,686)." Clearly, this cannot explain the mean temperature increase from the normal to the wettest soil category, but it can partially account for the non-negative trend.

Minimum, mean and maximum daily pressure are all entirely independent of both soil saturation and month (April through September). Each of the three quantities remain essentially constant over the combinations of months and soil saturations studied, with means of approximately 990 mb, 995 mb, and 998 mb.

Potential temperature, θ, is given by

$$\theta = T_K \left(\frac{1000}{p} \right)^{0.2854(1-0.28x10^{-3}w)}, \qquad (4.3)$$

where p is pressure, w is mixing ratio in g/kg, and T_K is temperature in degrees Kelvin (Bolton, 1980). Since w is usually on the order of 10-25 g/kg, its influence on θ is very small. Given that pressure is independent of soil saturation, we expect that the observed patterns in potential temperature should be very similar to those seen in the normal air temperature. The results were, indeed, nearly identical to those seen with normal air temperature and are not shown here.

The virtual temperature, T_v, accounts for the fact that moist air is lighter than dry air at the same pressure and temperature. It is approximately given by $T_v \approx T(1+0.608\text{x}10^{-3}w)$, where w is again in g/kg, and is generally very close to T (Emanuel, 1994). The virtual potential temperature, θ_v, is the potential temperature associated with T_v. The behavior of these variables is negligibly different from that of temperature. These results are not shown here.

The wet-bulb temperature, T_w, is a function of both the air temperature and the water vapor content of the air. It is defined as the temperature to which air may be cooled by evaporating water into it at a constant pressure, until saturation is reached (Rogers and Yau, 1989). The dew point temperature, T_{dew}, is defined as the temperature at which saturation is reached by cooling a parcel with pressure and mixing ratio held constant (Rogers and Yau, 1989). The T_w is, by definition, between the T_{dew} and the T since it includes evaporating water into the parcel: this leads to an increase in mixing ratio and a decrease in temperature due to the latent heat consumed by evaporation. Hot, dry air, then, will have a lower T_w than hot, moist air, since more evaporation and more evaporative cooling is needed to reach saturation. Given constant solar radiation, soil moisture increases are expected to lead to increased mixing ratio and decreased temperature. These changes do not independently affect T_w, but in general, increased mixing ratio would tend to increase the wet-bulb temperature, while decreased temperature would

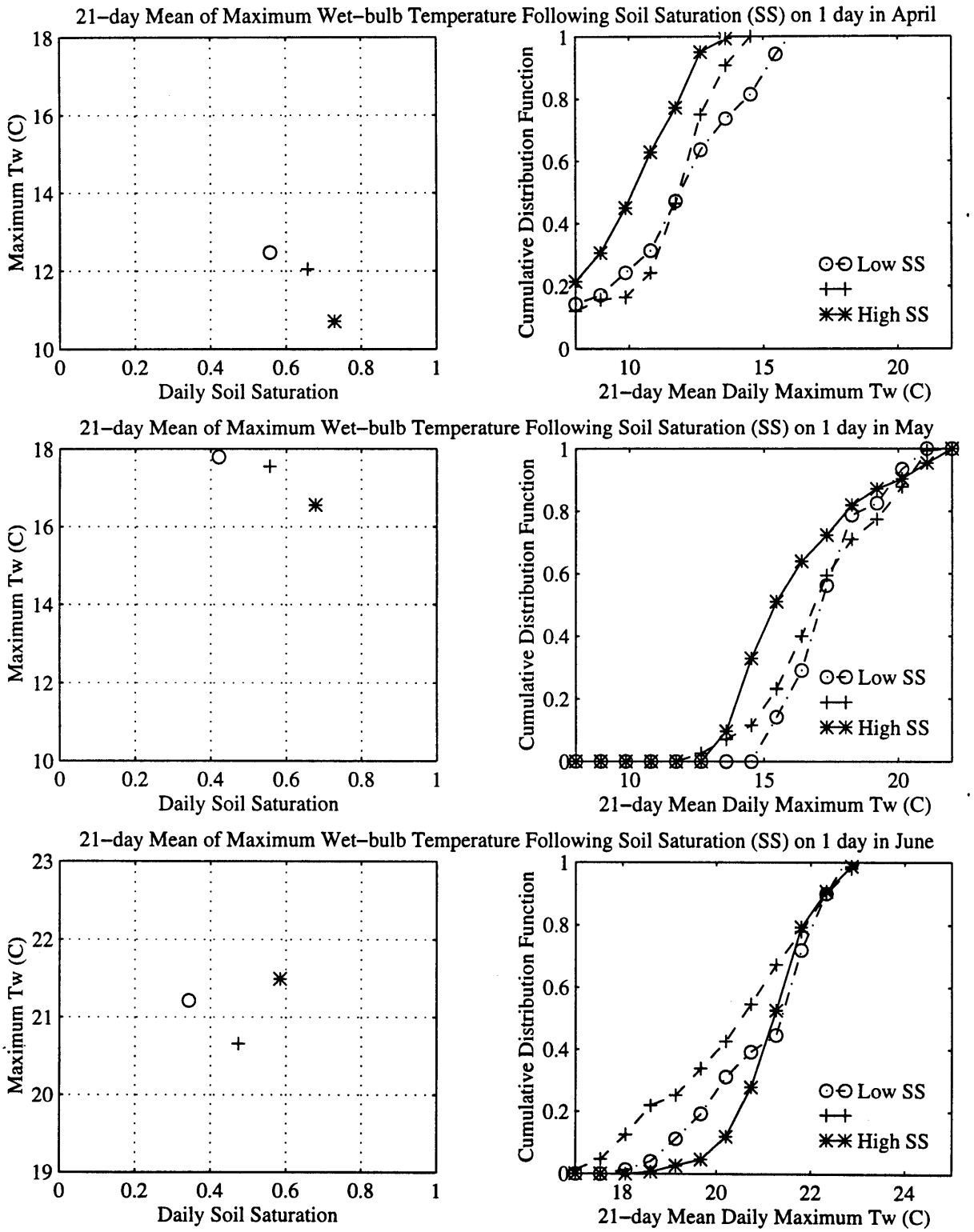

Figure 4.6: As for Figure 4.3 but for wet-bulb temperature (T_w); a) April, b) May, c) June.

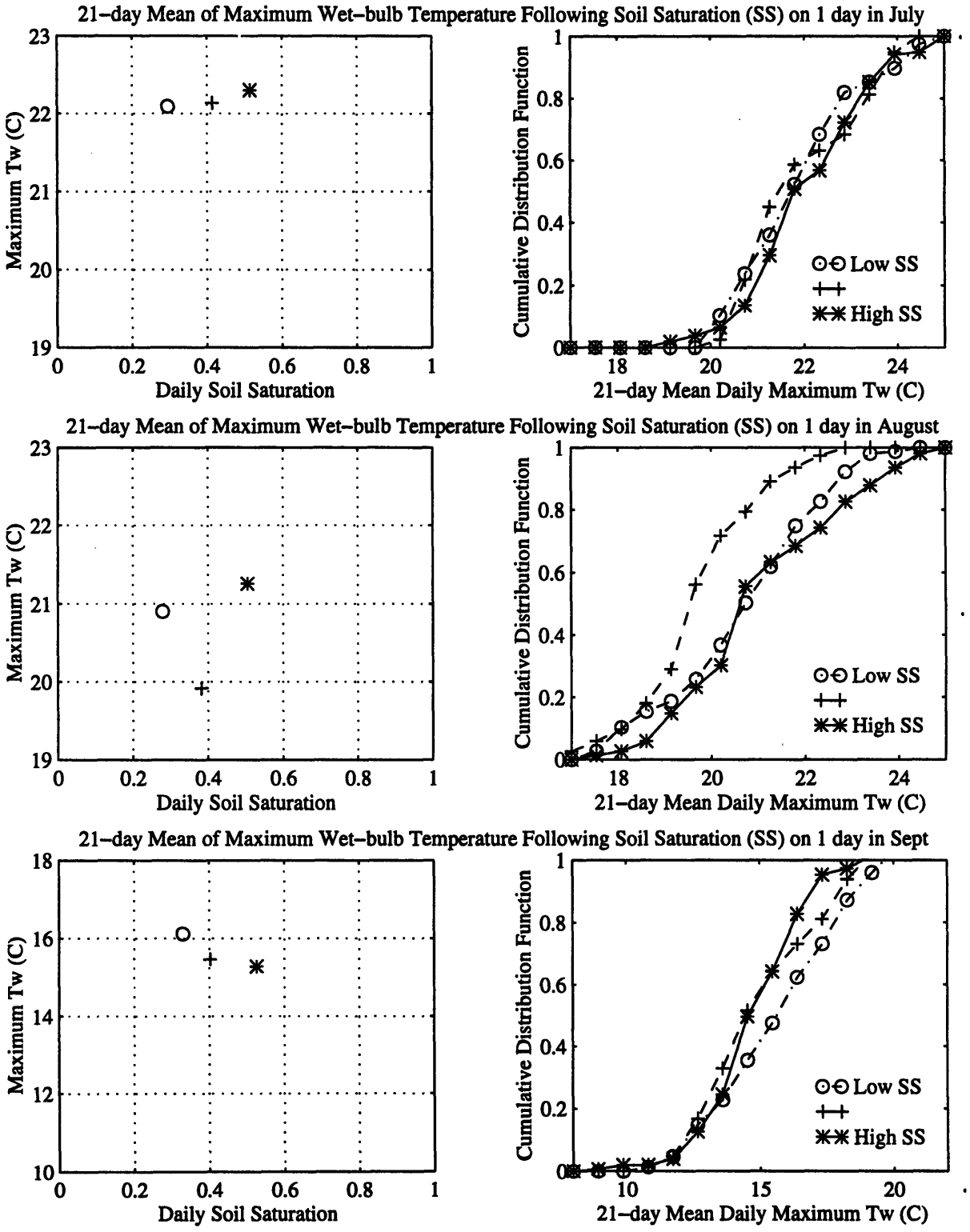

Figure 4.6 (cont.): As above, for d) July, e) August, and f) September.

tend to decrease T_w. The non-linearity of the relationship between these variables and wet-bulb temperature, and the uncertainty about the extent of the effect of soil moisture changes on temperature and mixing ratio makes it makes it difficult to anticipate the role of soil saturation on T_w. The data (Figure 4.6) show that for the months of June and August, days with wet soils are followed by days with a wet-bulb temperature that is approximately 0.5 °C greater than days with dry soils, and 1-1.5 °C greater than days in the intermediate soil saturation category. During July, the driest soil has the lowest, and the wettest soil has the highest, subsequent mean daily maximum wet-bulb temperature. The difference between the two means is less than 0.5 °C: much smaller than the 1.5-2 °C ranges we see in the opposite trends in April and May, both of which have the highest wet-bulb temperatures after days with the driest soils. September also shows this negative trend, but the range is less than 0.5 °C.

The wet-bulb depression, $T_{dpr} = T - T_w$, shows the strongest and most consistent trend of any of the variables studied (Figure 4.7). Whether the mean, minimum or maximum wet-bulb depression was analyzed, wetter soils were consistently followed by 21 days with a lower mean wet-bulb depression. The difference in daily maximum, mean, and minimum T_{dpr} between the wettest and driest soils was between 2 and 3 °C, 1 and 1.5 °C, and 0.3 to 0.7 °C, respectively, in each of the months April through September.

The strength of the negative correlation between soil moisture and wet-bulb depression can be explained by considering the anticipated effects of soil moisture on temperature and mixing ratio: the variables which ultimately affect T_{dpr}. As stated above in the discussion of wet-bulb temperature, we expect increased soil moisture to lead to increased mixing ratio and decreased temperature. This would have the effect of closing the gap between T_{dew} and T: at saturation,

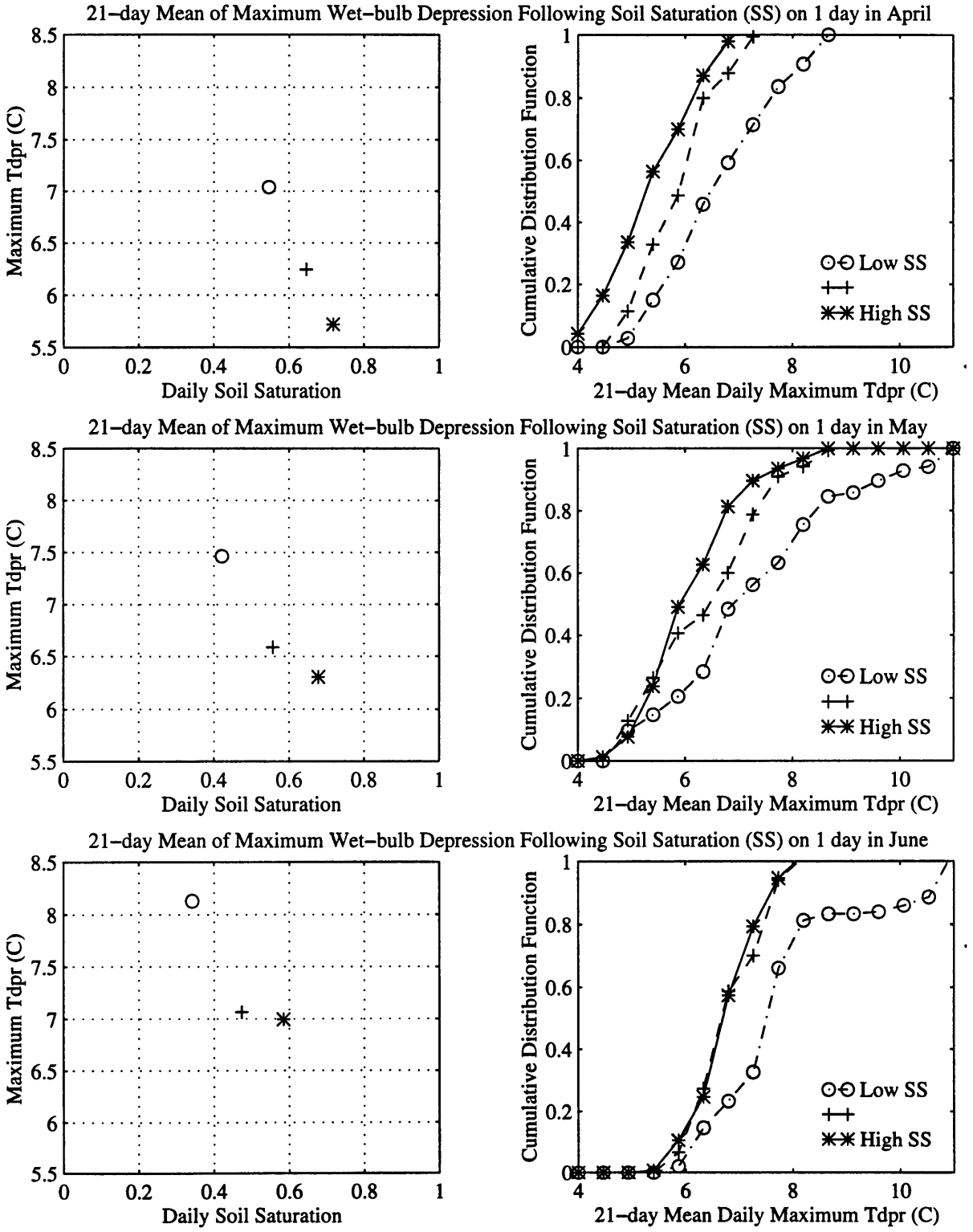

Figure 4.7: As for Figure 4.3 but for wet-bulb depression (T_{dpr}); a) April, b) May, c) June.

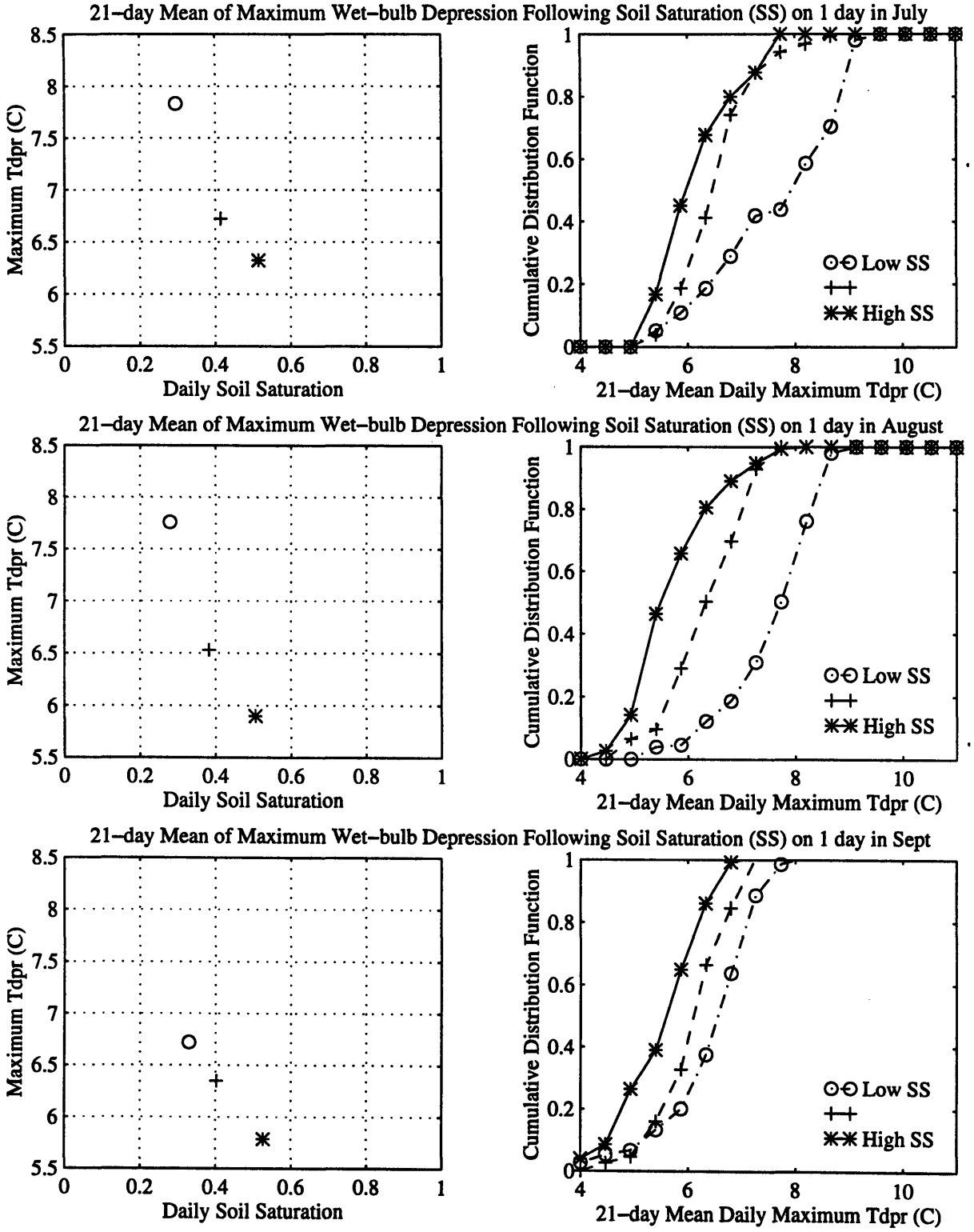

Figure 4.7 (cont.): As above, for d) July, e) August, and f) September.

$T_{dew} = T_w = T$. Since, by definition, whenever the air is unsaturated T_w lies between the dew-point and the air temperature, an increase in soil moisture which should lead to a decrease in T - T_{dew} will also lead to a decrease in T - T_w. The wet-bulb depression, in a sense, amplifies the impacts that soil moisture has on the temperature and humidity of the air. Weak correlations between these other two variables lead to stronger correlations with wet-bulb depression.

It is interesting to note that in five of the six months (September being the exception), the difference between the mean wet-bulb depressions associated with dry and normal soils is greater than the difference between the mean wet-bulb depressions associated with normal and wet soils. This is probably due to the moisture threshold controls on evapotranspiration previously discussed in regard to the results of the temperature analyses.

The temperature at the lifting condensation level, T_{LCL}, is calculated from the formula of Bolton, (1980):

$$T_{LCL} = 55 + \frac{1}{\frac{1}{T_K - 55} - \frac{\ln(f/100)}{2840}} \tag{4.4}$$

During June, July and August, the T_{LCL} is highest, by up to 2 K, after days with wet soils (Figure 4.8). In July, this temperature is lowest after days with dry soils, making for a consistent dependence on soil saturation: as soil saturation increases, the T_{LCL} also increases, indicating lower cloud base heights. This is consistent with the earlier results regarding relative humidity and wet-bulb depression: as more water is available in the soil, the air is closer to saturation, and a parcel lifted from the surface reaches saturation at a lower altitude (higher pressure, higher temperature). During August, however, the lowest soil saturation category shows mean T_{LCL}'s that are approximately 1 K higher than that in the intermediate soil saturation category, and in

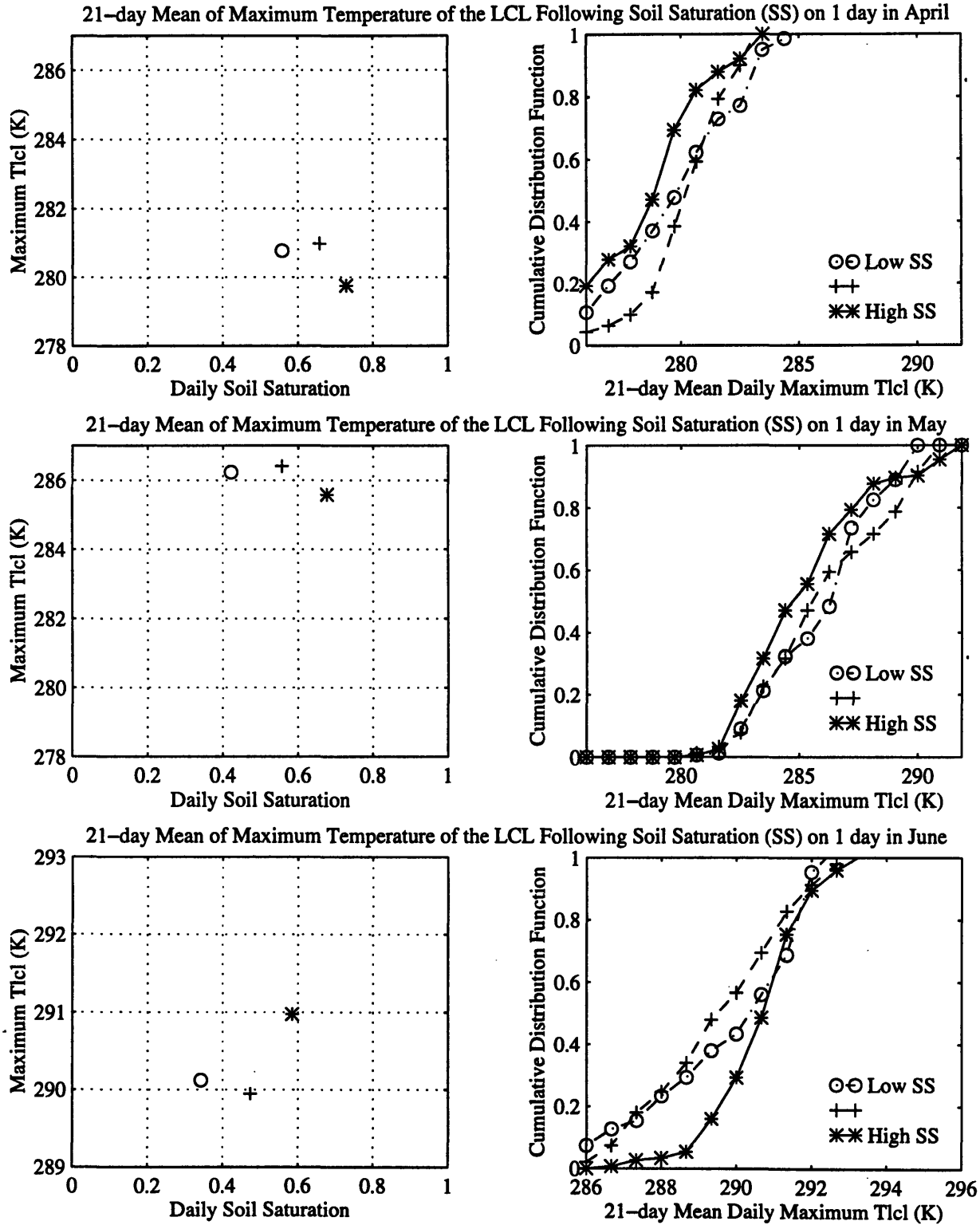

Figure 4.8: As for Figure 4.3 but for temperature of the lifting condensation level (T_{lcl}); a) April, b) May, c) June.

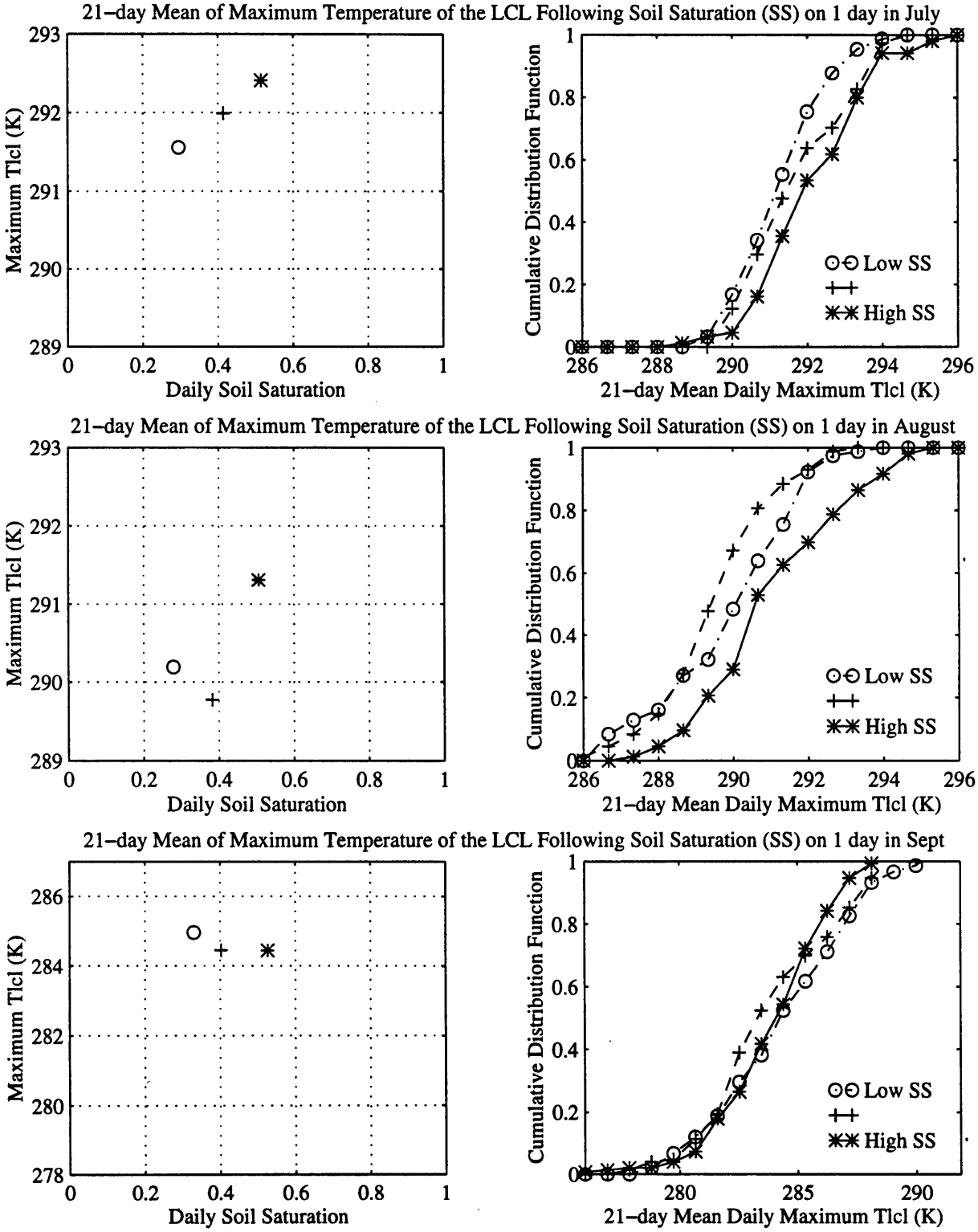

Figure 4.8 (cont.): As above, for d) July, e) August, and f) September.

June the dry and intermediate soils yield equivalent T_{LCL}'s. In April and September, the lowest T_{LCL} is associated with the wettest soils, and the highest T_{LCL} with the driest soils. The May pattern is closest to these two, but the intermediate soils have a slightly higher maximum T_{LCL} than the driest soils.

The temperature of the LCL is an indication of the subcloud layer depth, but it includes no information about the condition of the LCL relative to the surface. A more appropriate quantity to describe the cloud base height is the pressure depth of this layer, i.e., the pressure at the surface minus the pressure at the LCL: P_{LCL} - P_s. P_{LCL} is approximated from surface measurements by calculating the saturation pressure of a surface air parcel. We know from Equation 4.1 that

$$P = \varepsilon \frac{e_{sat}}{w_{sat}} + e_{sat} \tag{4.5}$$

where w_{sat} is calculated from the surface observations of P and T, but e_{sat} is calculated using T_{LCL}.

The work of Betts and Ball (1995) and Betts et al. (1996) supports the theory that dry soil conditions lead to increased sensible heat flux and increased parcel buoyancy. This leads to a deeper and drier mixed layer, which suggests a larger pressure depth to the LCL. Indeed, Figure 4.9 shows that, in each of the months, the deepest boundary layers are associated with the driest soils. Similarly, in April, May, July, and September, the shallowest boundary layers are associated with the wettest soils. This is not true in June and August, however. This pattern is quite consistent with the temperature results shown in Figure 4.5. Since the depth to the LCL is closely related to parcel buoyancy, this correspondence is internally consistent.

The equivalent potential temperature, θ_E, is often used as a measure of entropy in the boundary layer. It is defined as the temperature that a parcel of air would have if all the moisture

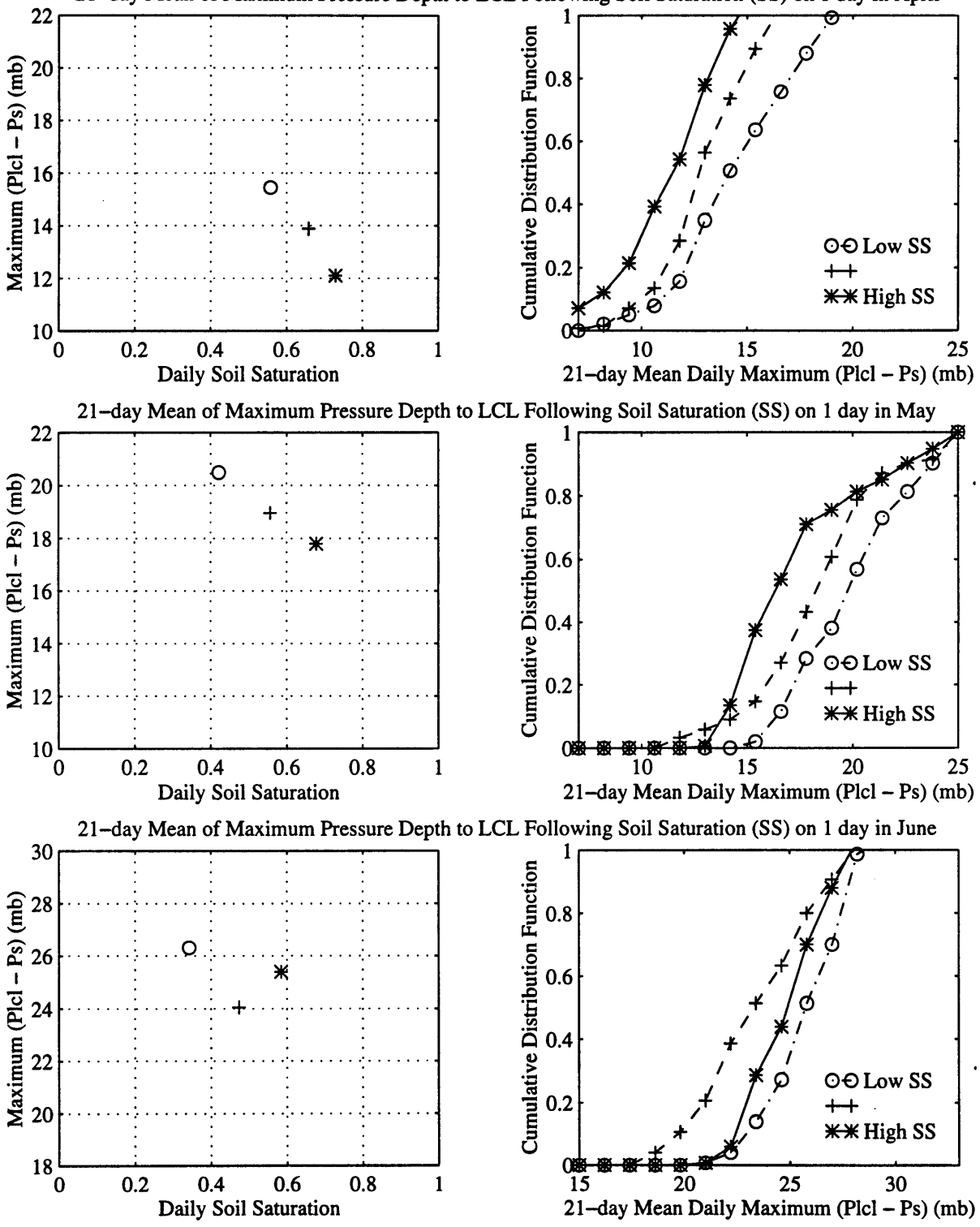

Figure 4.9: As for Figure 4.3 but for pressure depth to the lifting condensation level (P_{lcl} - P_s); a) April, b) May, c) June.

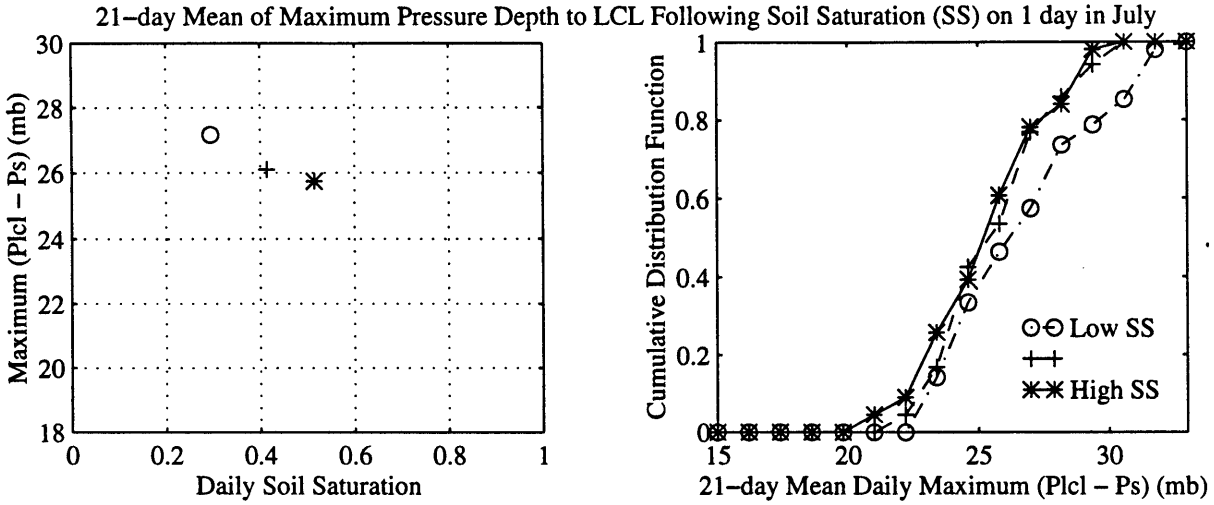

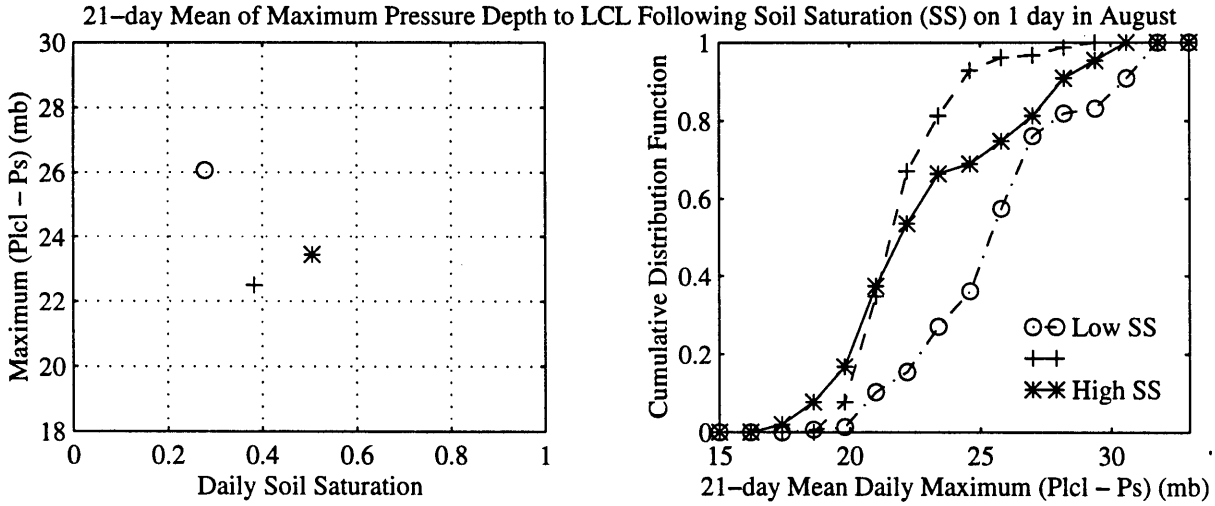

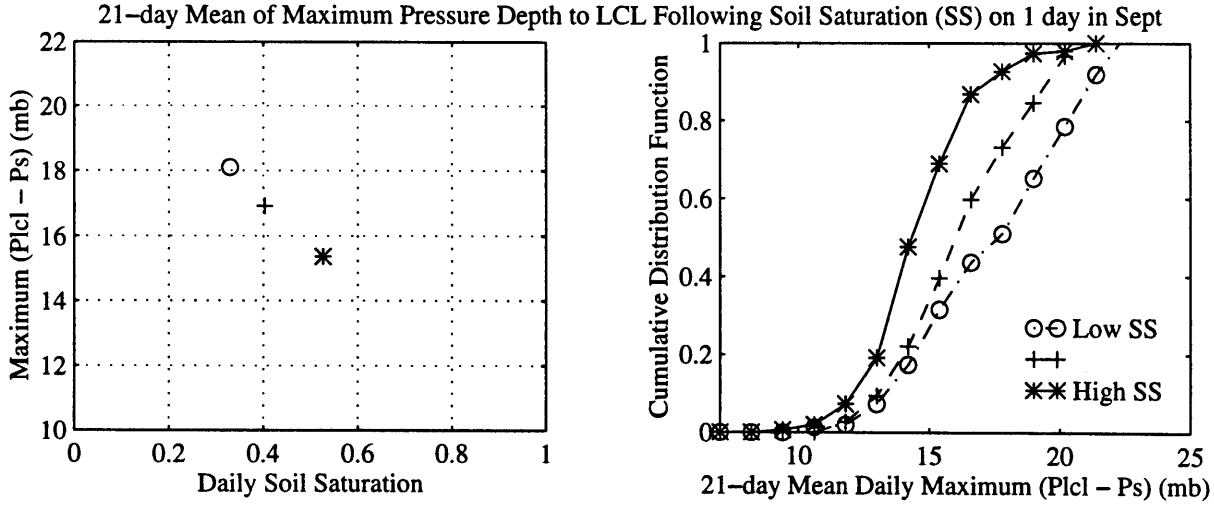

Figure 4.10 (cont.): As above, for d) July, e) August, and f) September.

were condensed out pseudoadiabatically, and then the sample was taken dry adiabatically to a pressure of 1000 mb (Rogers and Yau, 1989). It is calculated following Bolton (1980):

$$\theta_E = T_K\left(\frac{1000}{P}\right)^{0.2854(1-0.28x10^{-3}w)} \exp\left[\left(\frac{3.376}{T_L} - 0.00254\right)w(1+0.81x10^{-3}w)\right] \tag{4.6}$$

The behavior shown in Figure 4.10 closely mimics that of the wet-bulb temperature shown in Figure 4.6, but the temperature differences are amplified on the θ_E scale. The results of the analysis between the wet-bulb potential temperature, θ_w, (which is calculated by substituting T_w for T in Equation 4.2) and soil moisture also mimics the patterns of T_w and θ_E, as expected by the one-to-one relationship between θ_w and both of these other variables. Figure 4.11 shows these results. This correspondence between θ_E, θ_w, and T_w is consistent with the discussion in Chapter 2: all three variables are measures of the boundary layer entropy, or the moist static energy in the boundary layer.

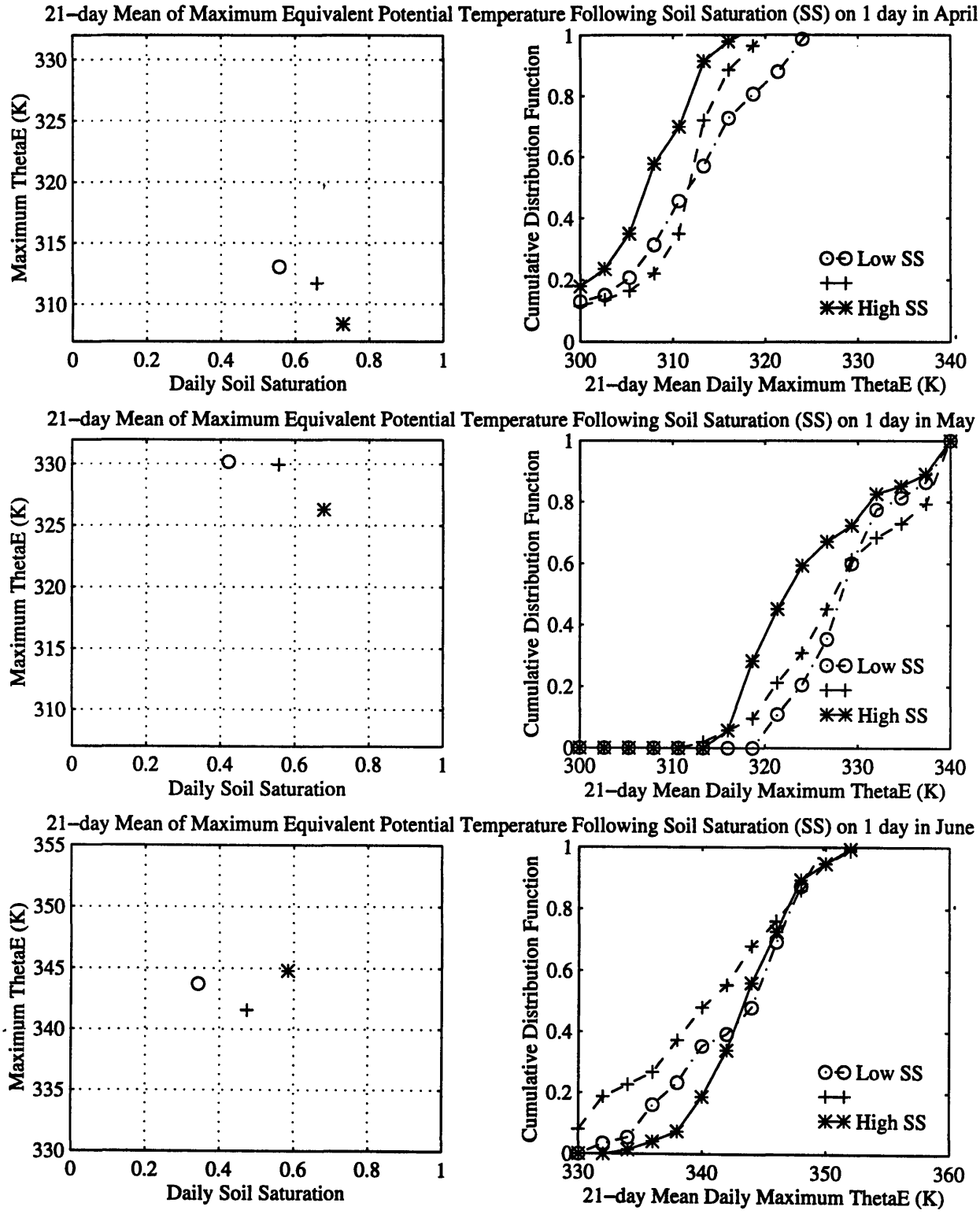

Figure 4.10: As for Figure 4.3 but for equivalent potential temperature (θ_E); a) April, b) May, c) June.

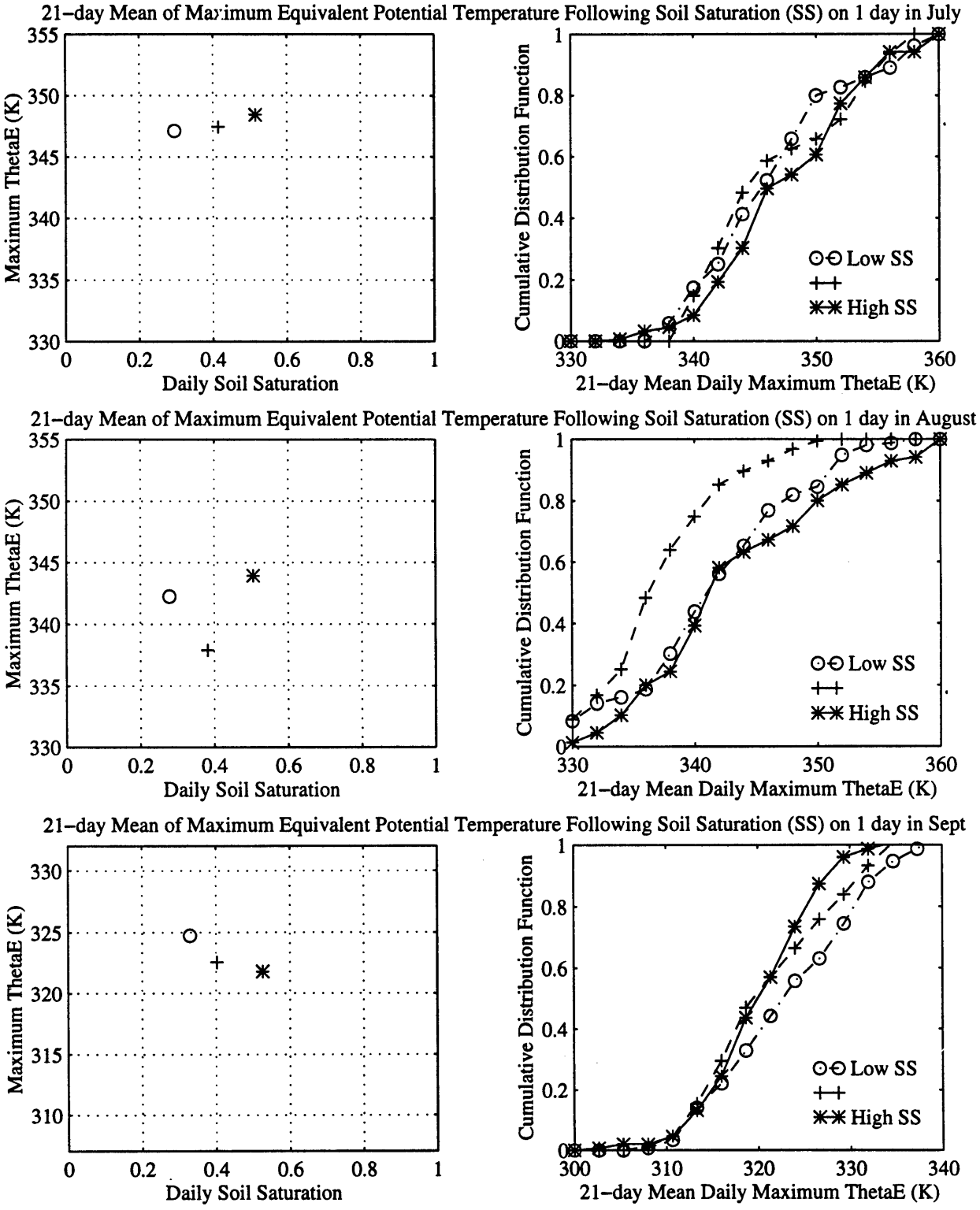

Figure 4.10 (cont.): As above, for d) July, e) August, and f) September.

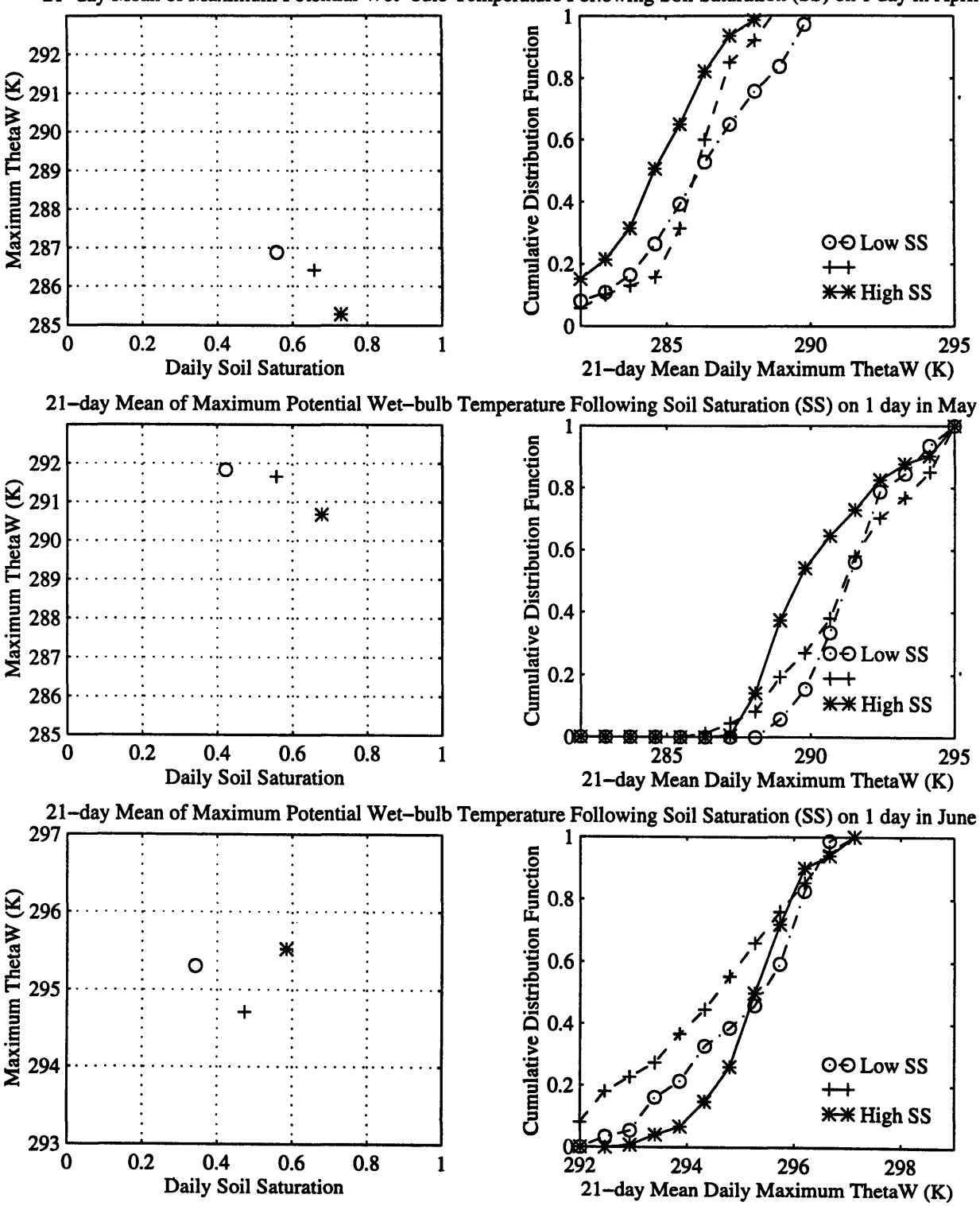

Figure 4.11: As for Figure 4.3 but for wet-bulb potential temperature (θ_w); a) April, b) May, c) June.

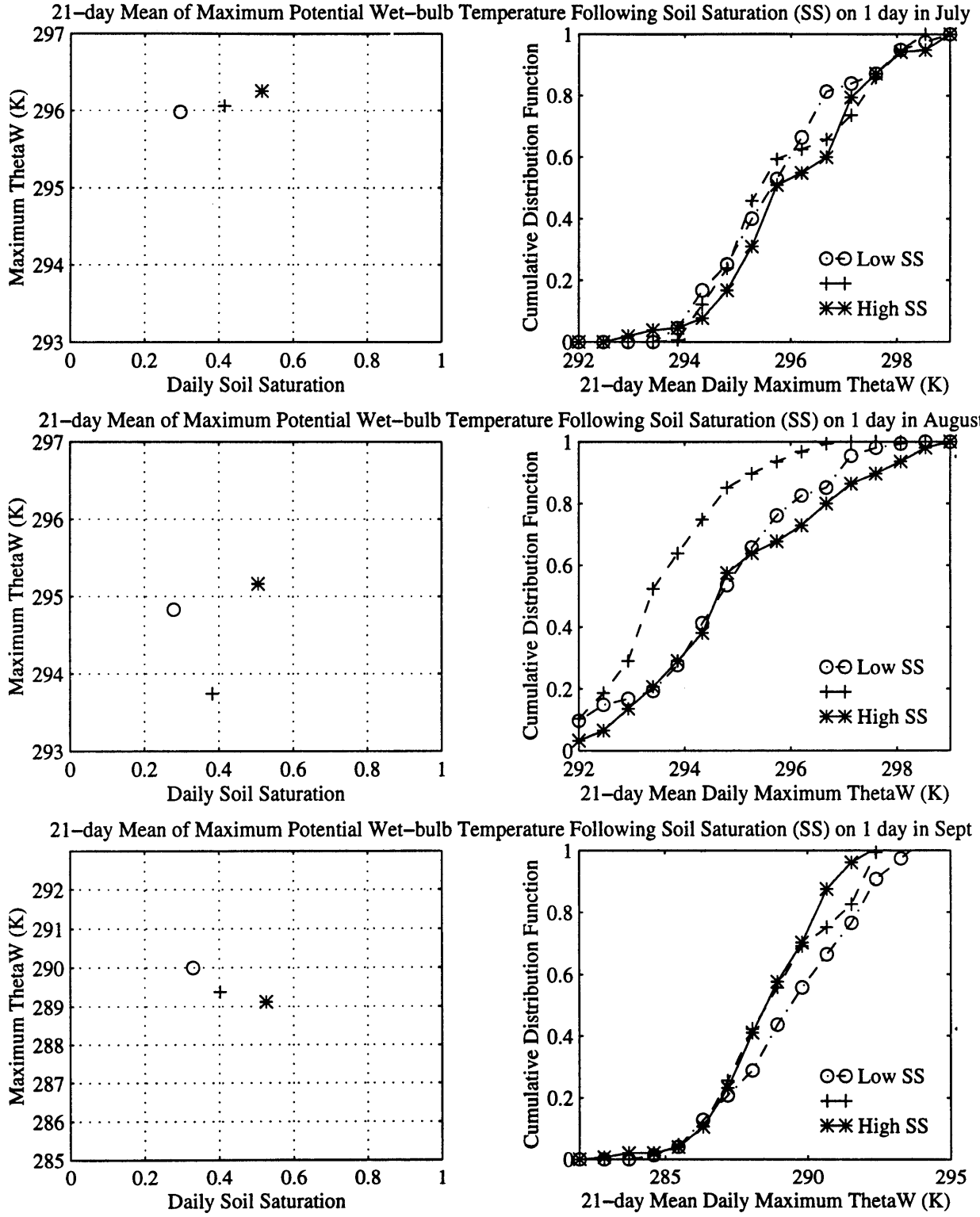

Figure 4.11 (cont.): As above, for d) July, e) August, and f) September.

D. Analysis of the Linear Correlation Between Soil Saturation and Subsequent Boundary Layer Conditions Throughout the Year

To test the annual cycle of any linear correlation which might be present between soil saturation and any of the boundary layer variables considered, time series of the correlation coefficients between soil saturation and the minimum, mean, and maximum daily values of each of the 12 variables were generated for the full year. This procedure was similar to that described in Chapter 3: for each day of the year, the linear correlation between the 15 years of data pairs (soil saturation on that day, and the mean of the variable in question over the following 21 days) was quantified by the coefficient of determination (r^2). (The procedure described in Chapter 3 tested pairs which consisted of soil saturation on a given day and the subsequent 21-day total rainfall, rather than the mean daily rainfall.) The results for relative humidity and wet-bulb depression are shown in Figures 4.12 and 4.13, respectively, for the minimum (top plot), mean (middle plot), and maximum (bottom plot). Figures 4.14 through 4.20 show the results of only the maximum of each of the other variables: the minimum and mean for each variable show very similar results. Each of these plots is calculated using soil saturation in the top 10 cm. The level of significance lines are computed by relating the r^2 to an F-distribution with 1 and 15 degrees of freedom, as described in Chapter 3. The 5% level of significance yields an r^2 of 0.2643, while the 10% level of significance yields an r^2 of 0.1945.

Only relative humidity (Figure 4.12) and wet-bulb depression (Figure 4.13) show a significant linear correlation with soil saturation in all of the daily minimum, mean, and maximum. These correlations are strongest from mid-May through mid-September, but mid-April, early October, and late November all show local peaks with significant correlations. As stressed in Chapter 3, the level of significance lines on these correlation time-series figures are calculated for

the individual data points. The solid line, representing a 21-day moving average, is significant at lower r^2, due to the averaging process.

A few other variables have brief periods of significance. The minimum, mean, and maximum temperature of the lifting condensation level (Figure 4.17) are all significant for a week or two at the end of June, and again at the end of November. The maximum daily temperature (Figure 4.15), and the maximum pressure depth to the LCL (Figure 4.18) pass above the 10% level of significance line for a few weeks at the beginning of May, and again at the end of August, lasting past the middle of September.

It should be stressed that these figures show only the degree of linear correlation between soil saturation and each of the boundary layer quantities: non-linear relationships, such as threshold behavior, will not be captured by this analysis. The negative correlation between soil moisture and measures of parcel buoyancy (T, θ, T_v, P_{LCL}-P_s) seen during the spring and fall in the previous section is captured in the linear correlation analysis presented here, but the possible threshold dependence of evapotranspiration on soil moisture cannot be captured by the linear correlation coefficient. This accounts for the June-August drop in the r^2 in the daily maximums of these variables.

The negative correlations seen in Section C between the measures of boundary layer entropy (θ_E in Figure 4.10, θ_w in Figure 4.11, and T_w in Figure 4.6) and soil moisture during the spring and fall were not strong enough to show up in the linear correlation analysis of this section. Nevertheless, it is revealing to see that wet-bulb depression and relative humidity have such a strong summertime relationships with soil saturation.

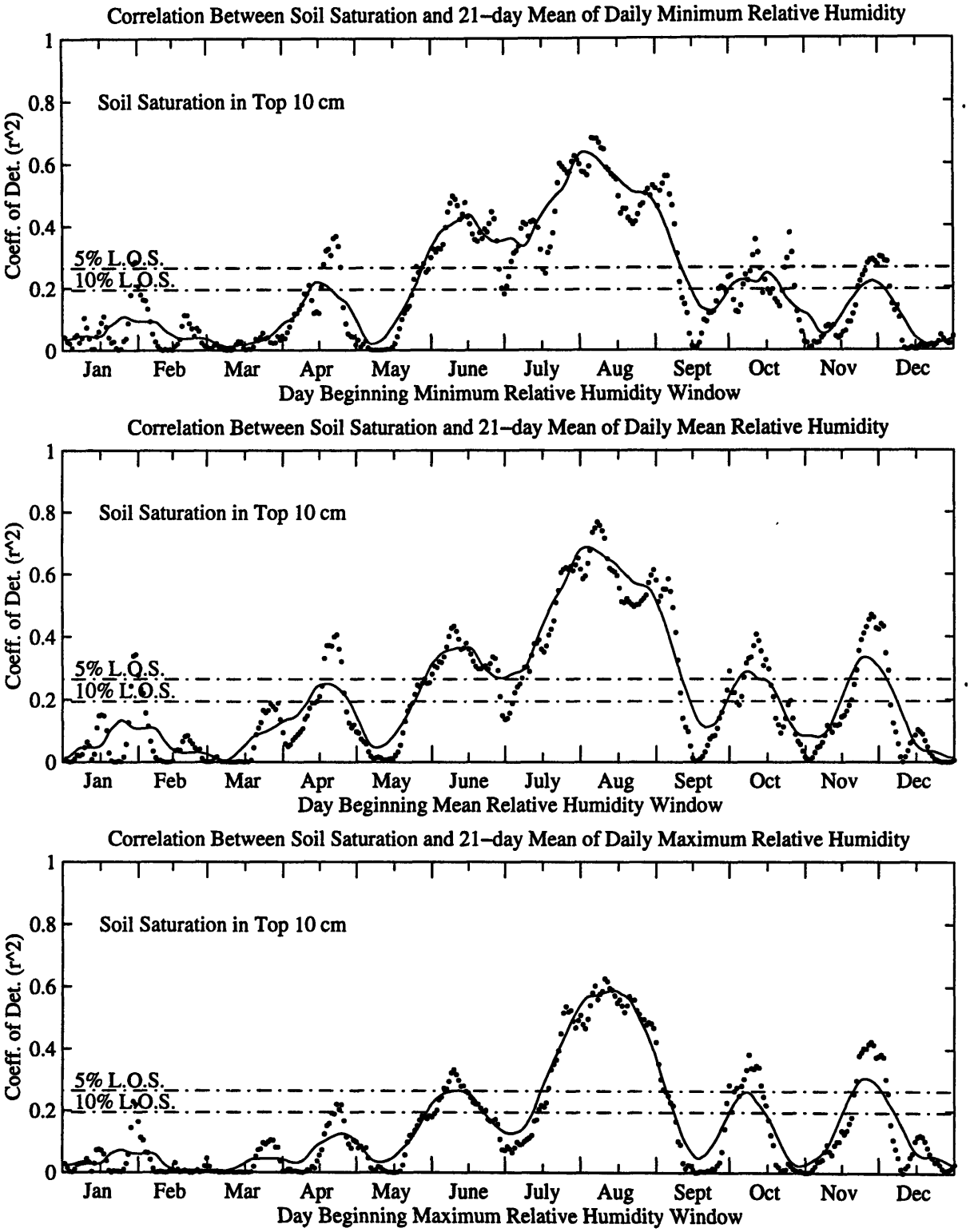

Figure 4.12: Linear correlation between initial soil saturation (SS) and average (a) minimum daily, (b) mean daily, and (c) maximum daily relative humidity (*f*) in the subsequent 21 days, as measured by the coefficient of determination (r^2). Solid line is 21 day moving average. "LOS" lines are 5 and 10% level of significance lines for the r^2 variable (not the smoothed line).

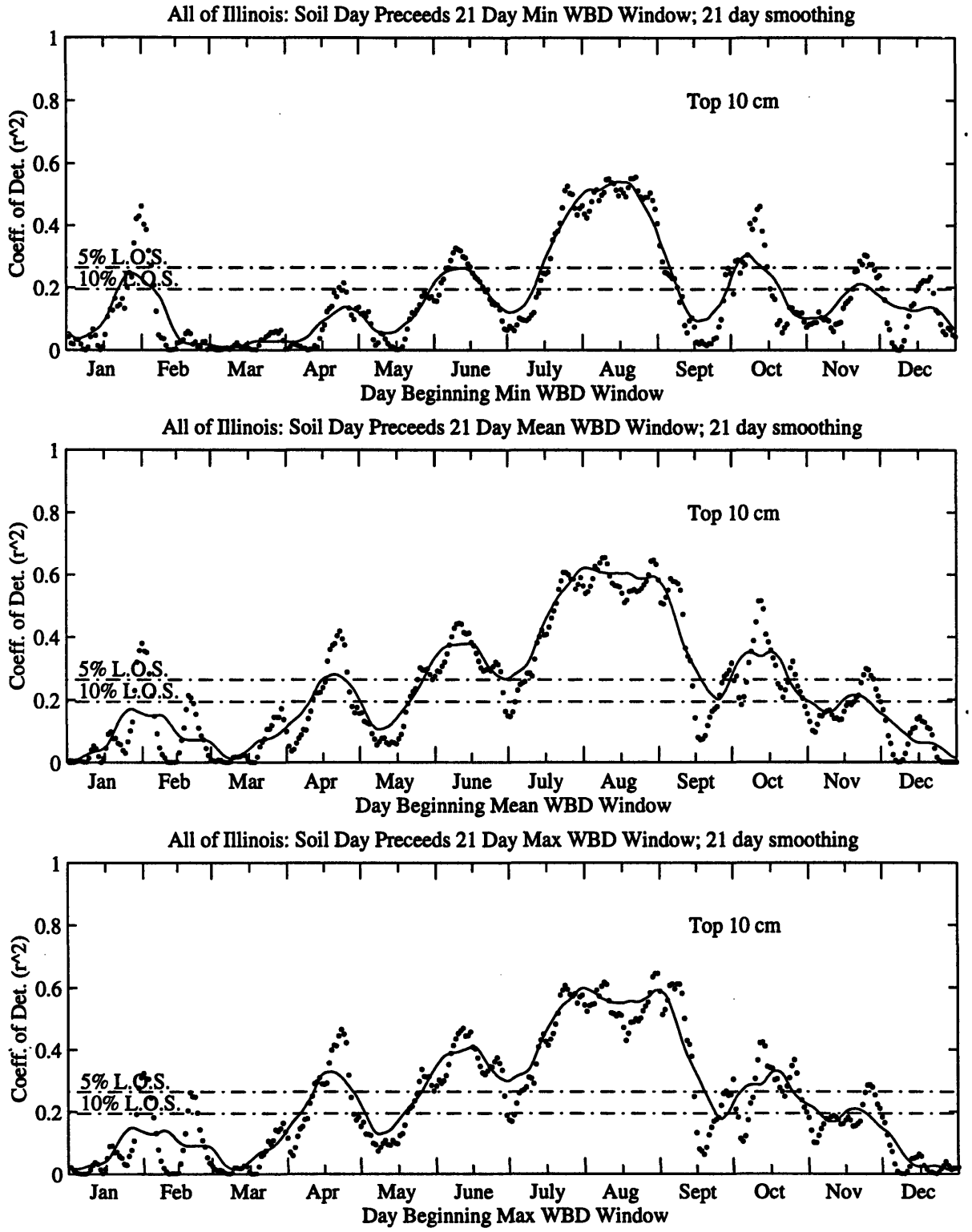

Figure 4.13: As for Figure 4.12, but for wet-bulb depression (T_{dpr}).

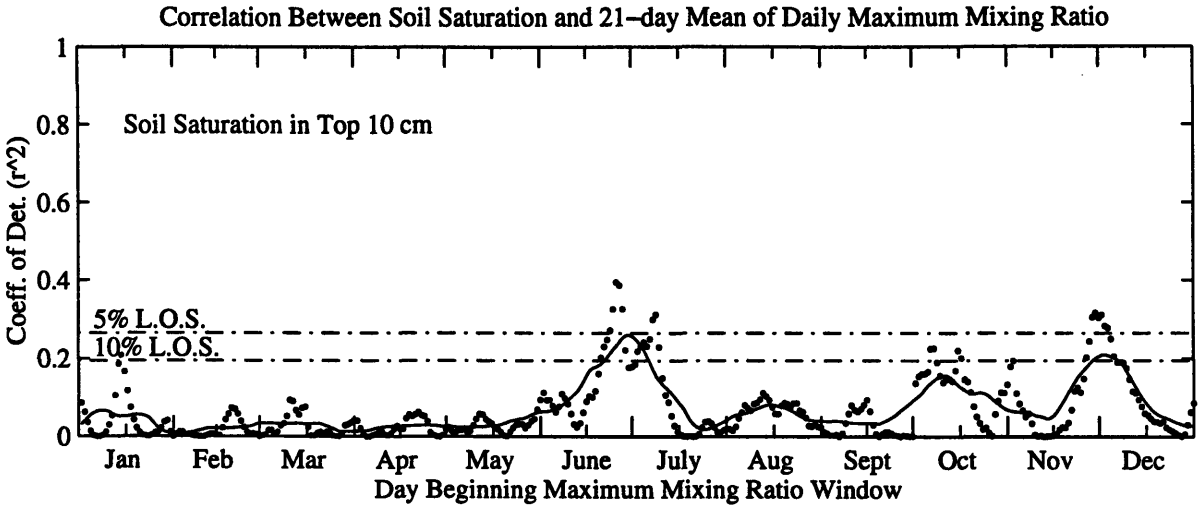

Figure 4.14: As for Figure 4.12c but for maximum daily mixing ratio (w).

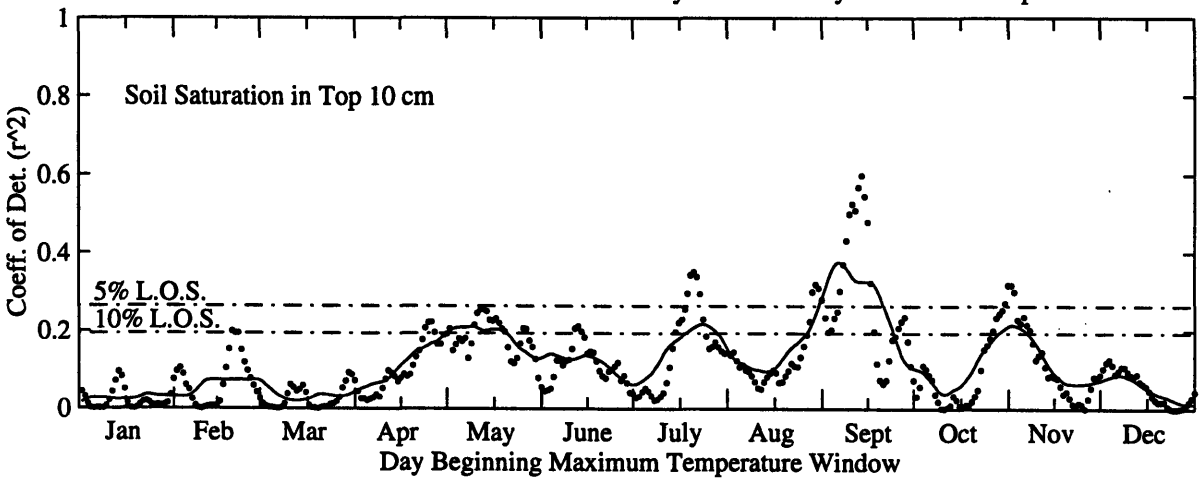

Figure 4.15: As for Figure 4.12c but for maximum daily air temperature (T).

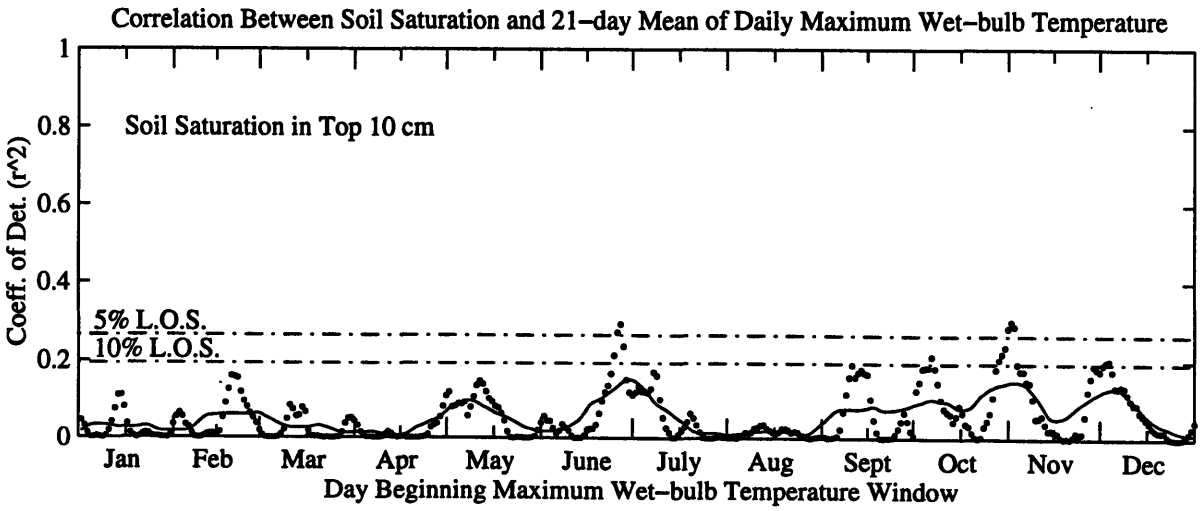

Figure 4.16: As for Figure 4.12c but for maximum daily wet-bulb temperature (T_w).

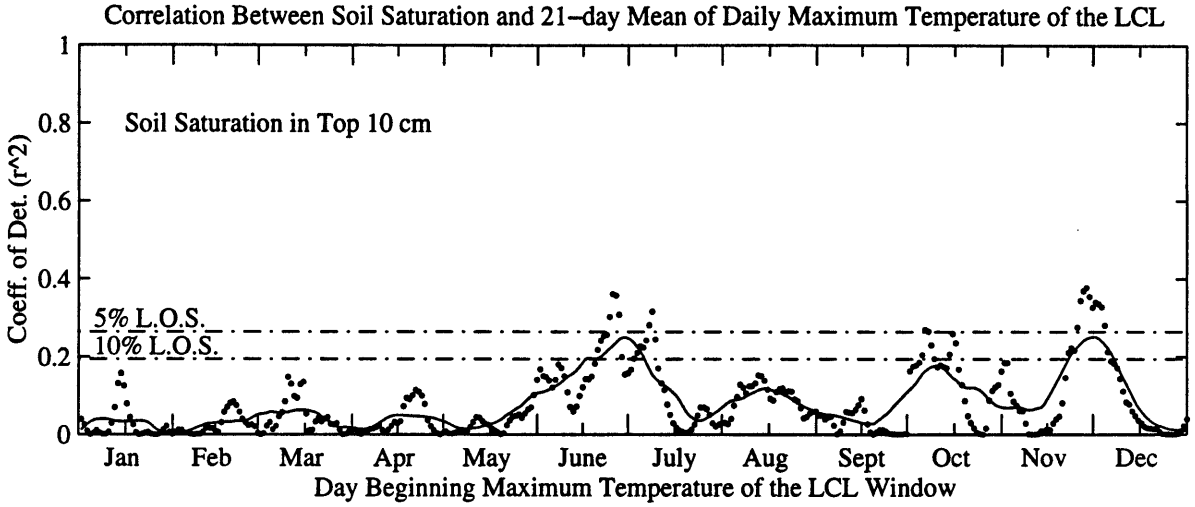

Figure 4.17: As for Figure 4.12c but for maximum daily temperature of the lifting condensation level (T_{LCL}).

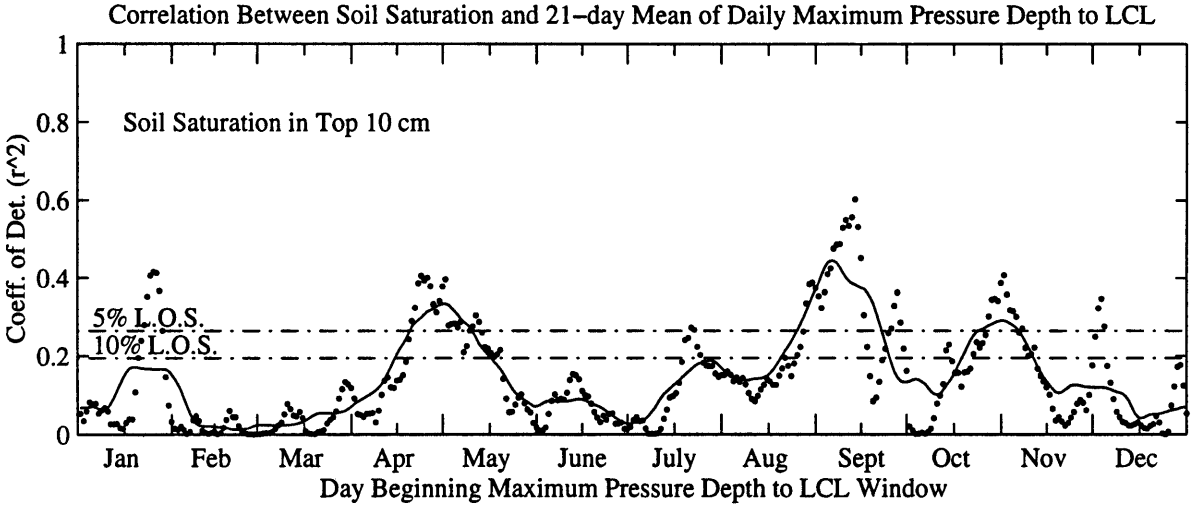

Figure 4.18: As for Figure 4.12c but for maximum daily pressure depth to the lifting condensation level (P_{LCL} - P_s).

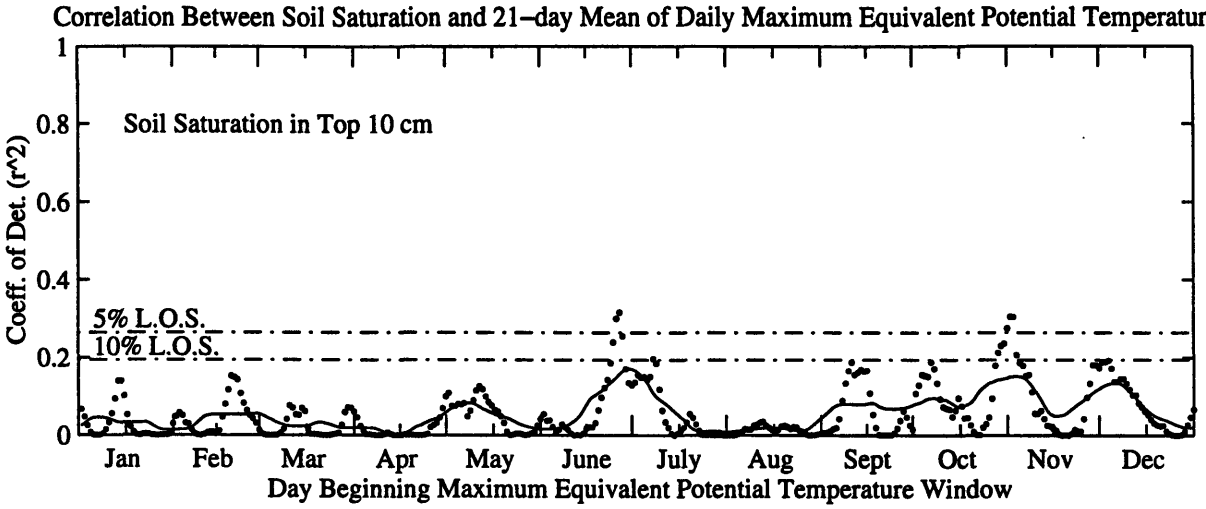

Figure 4.19: As for Figure 4.12c but for maximum daily equivalent potential temperature (θ_E).

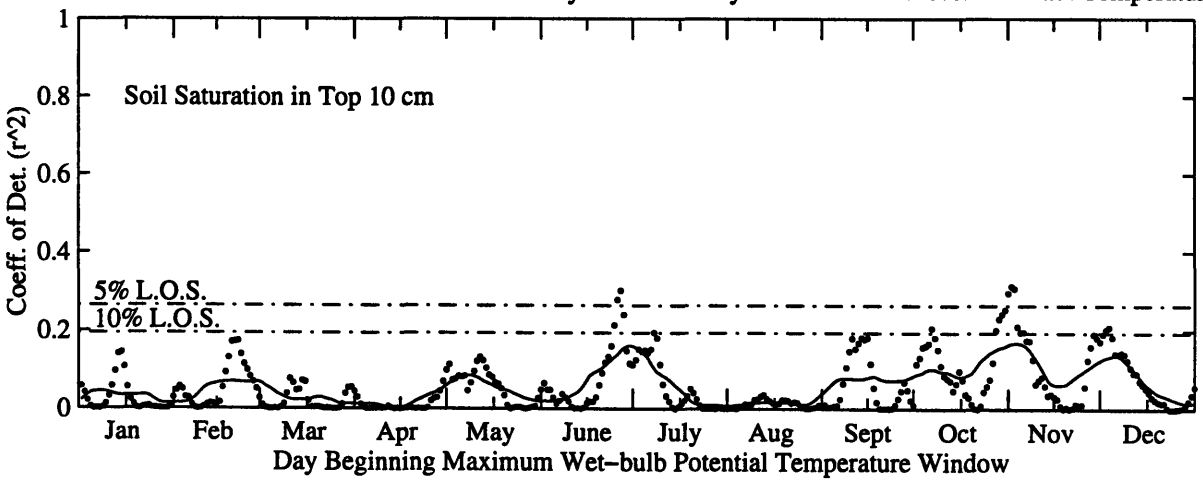

Figure 4.20: As for Figure 4.12c but for maximum daily wet-bulb potential temperature (θ_w).

Figures 4.21 and 4.22 show the correlation between wet-bulb depression and soil saturation averaged over deeper depths: the top 50 cm in Figure 4.21, and the top 90 cm in Figure 4.22. The summertime significance of this correlation is seen in both plots, but it is damped with depth.

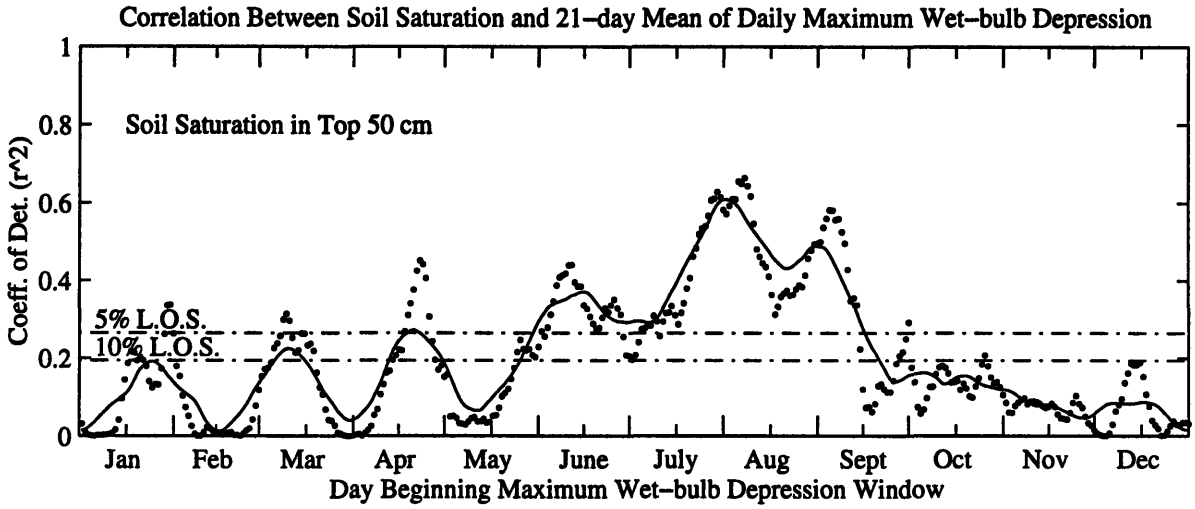

Figure 4.21: As for Figure 4.12c but for initial soil saturation in the top 50 cm and average maximum daily wet-bulb depression (T_{dpr}) in the subsequent 21 days.

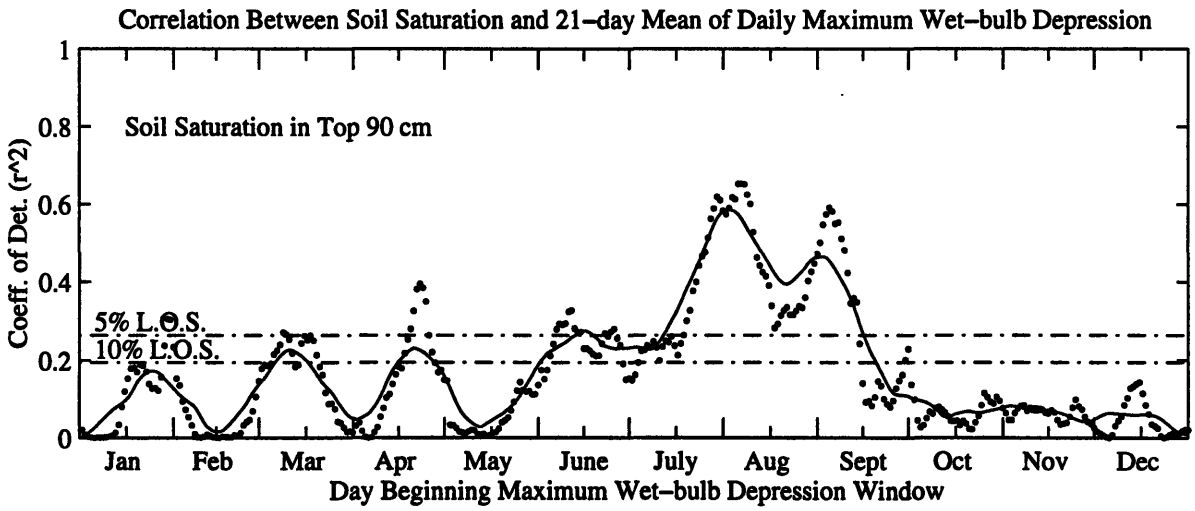

Figure 4.22: As for Figure 4.12c but for initial soil saturation in the top 90 cm and average maximum daily wet-bulb depression (T_{dpr}) in the subsequent 21 days.

E. Discussion of Results

This chapter focused on the relationships between soil moisture conditions and subsequent boundary layer conditions, as described by observations of near-surface air. There were three main classifications of variables analyzed:

1) Measures which are functions of both the temperature and the degree of saturation:
   - relative humidity, f, and
   - wet-bulb depression, T_{dpr};
2) Measures of buoyancy:
   - temperature, T,
   - potential temperature, θ,
   - virtual potential temperature, θ_v, and
   - pressure depth to the Lifting Condensation Level, P_{LCL} - P_s; and
3) Measures of moist static energy:
   - wet-bulb temperature, T_w,
   - wet-bulb potential temperature, θ_w, and
   - equivalent potential temperature, θ_E.

Additional variables included in the analysis were mixing ratio, q, which is a measure of the water content, but contains no information about the air temperature (or, therefore, about the relative humidity), and the temperature of the Lifting Condensation Level, T_{LCL}, which is related to the depth of the boundary layer, but contains no information about the pressure at the LCL, or the pressure or temperature of the surface relative to the LCL.

The first category of variables, measures of temperature and saturation, showed a strong and clear dependence on initial soil saturation. The results show that days with wetter soil moisture conditions tend to be followed by days with surface air closer to saturation.

Neither the buoyancy nor the energy variables show such a clear relationship to initial soil moisture conditions. Days with dry soils are, on average, followed by periods of greater buoyancy than either the normal or wet soil days, but the wet soil days tend to be followed by periods of greater buoyancy than the normal soil days. This is potentially due to the fact that lack

of moisture at the surface can be the limitation for evaporation when soils are dry, but once the soil is wetter than some threshold, the moisture source is no longer the controlling factor on evaporation.

The energy variables show less of the expected trends than the buoyancy variables. As discussed in Chapter 2, previous studies have shown a positive association between soil moisture and moist static energy in the boundary layer (e.g., Betts and Ball, 1995: higher soil moisture leads to higher θ_E). The results presented here, however, show a negative correlation between soil moisture and the energy variables during the spring and fall, a very slight positive correlation in July, and mixed results in June and August.

Though these results are quite illustrative of the strong impact the soil conditions can have on the wet-bulb depression of near-surface air, further analyses are needed to more accurately determine the relationships between the land surface and the whole boundary layer. It is not clear if surface observations are appropriate indicators of the conditions throughout the boundary layer; further analyses should include upper air data. Nor is it clear that the limitations of the soil moisture dataset discussed in Chapter 3 and/or the limited number of hourly surface observations stations are not dampening the strength of the theoretical relationships between soil moisture and moist static energy of the boundary layer discussed in the Chapter 2.

Despite these data limitations, the analyses in this chapter clearly show that soil moisture has a positive impact on the wet-bulb depression of near-surface air during the summer months. This correlation become significant in mid-May, and persists through mid-September, almost perfectly matching the time period of significance of the soil moisture–rainfall correlation discussed in Chapter 3.

The soil moisture–wet-bulb depression correlation is strongest with the daily maximum T_{dpr}, rather than the minimum or mean. The maximum T_{dpr} usually occurs a few hours after the noontime peak of solar forcing, corresponding to the usual time of occurrence of local convective storms. The next chapter will discuss this temporal dependence of the mechanisms initiating rainfall, and will then investigate the question of what boundary layer conditions are most favorable for convective rainfall during the summer.

Chapter 5: The Relationships Between Boundary Layer Conditions and Rainfall

A. The EarthInfo NCDC Hourly Rainfall Database

The hourly rainfall data used in this analysis was obtained through EarthInfo, Inc. This dataset is a subset of the National Climatic Data Center's (NCDC's) TD-3240 file, with hourly precipitation records for many stations throughout the United States beginning in 1948. Within Illinois, there were 82 stations with consistent hourly rainfall records. The locations of these stations are shown in Figure 5.1. Also shown in this figure are the locations of the Surface Airways Stations discussed in Chapter 4. These data will again be used to quantify the hourly conditions of the boundary layer.

B. The Diurnal Cycle of Rainfall in Illinois

There are three main mechanisms of initiating rainfall in Illinois: the Low Level Jet, which brings air north from the Gulf of Mexico during the night when the boundary layer over the Great Plains has collapsed (Carlson and Ludlam, 1966; Bonner, 1968; McCorcle, 1988), synoptic systems associated with the Jet Stream from the north and west, and locally triggered small-scale convective storms. It is this third type of storm that is the focus of this study on the effects of soil moisture on rainfall in Illinois; however, it is very difficult to isolate these events from the synoptic scale events. Small-scale convective storms generally are due to local instabilities in the vertical distribution of temperature and humidity. Eltahir and Pal (1996) present a detailed discussion of

the triggering mechanisms leading to the release of energy associated with convective rainfall events.

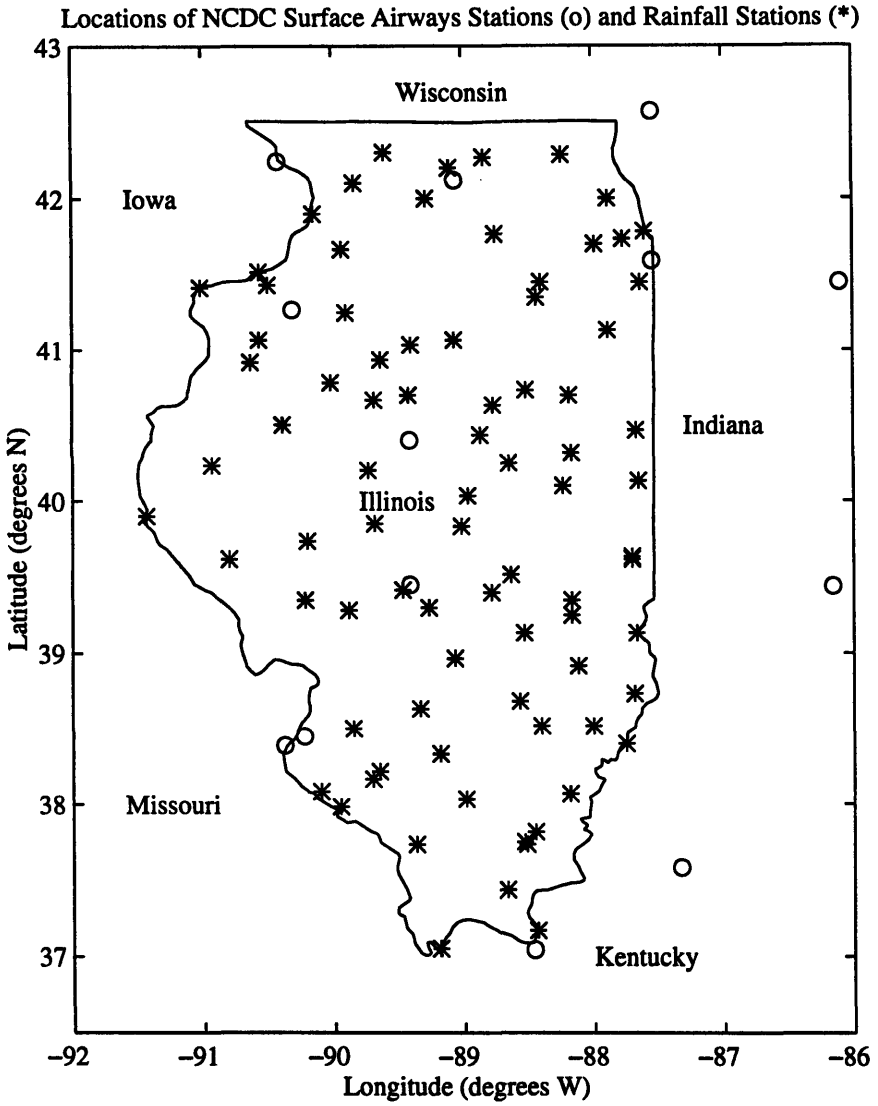

Figure 5.1: Locations of the NCDC Hourly Rainfall Stations (*) and the NCDC Surface Airways Stations (o). Solid line is the Illinois state boundary.

Figure 5.2 shows the diurnal cycle of rainfall during the years of this analysis, 1981 to 1995, for each of the months between April and September. It is clear from the left-most column that there is very little evidence of a diurnal cycle in the average depth of rainfall per hour. In tropical climates, most of the rainfall occurs during afternoon thundershowers, and the average depth of rain during the afternoon hours can be many times that of nighttime hours (see, for

example, Eltahir and Pal, 1996). In Illinois, however, the largest range for any month shows the maximum average hourly rainfall rate is at most only two times the minimum rate (0.01 to 0.02 cm per hour), and the minimum comes at mid-day, rather than during the night, as in the tropical case. During August and September, there is virtually no dependence on time of day. Clearly, the situation in Illinois is quite different from that of the tropics, even during the summer.

The plots in the middle column of Figure 5.2 show, for each month, the average duration of storms initiated during each hour of the day. Similarly, the right-most plots show the probability of storm initiation for each hour of the day. In general, the average storm duration peaks in the early morning hours, while the probability of storm initiation peaks in the afternoon. These two plots combine to explain the lack of a diurnal cycle in the depth of rainfall: early morning (after midnight) storms are long but fairly rare, while late afternoon storms are short but more frequent. April, May, June and July show a minimum in rainfall depth near mid-day, when neither the storm duration nor the probability of initiation is peaked. August and September show less of a diurnal cycle in storm duration or likelihood of initiation than the earlier months. This is reflected in the near-constant average rainfall depth throughout the day.

The long early morning storms are likely the result of large-scale forcing by the Low Level Jet, which originates over the Gulf of Mexico, and carries warm, moist air onto the continent when the boundary layer is not present (Carlson and Ludlam, 1966; Bonner, 1968; McCorcle, 1988). The late afternoon storms are likely the convective storms we wish to investigate. The analyses presented in this chapter will focus on boundary layer conditions, as described by surface observations, between 2 and 6 PM, and rainfall in the hour following each surface observation, i.e., 3 to 7 PM. We focus on rainfall in the hour after a given surface observation to avoid

contamination of boundary layer data by rainfall events. Since convective rainfall is a threshold process, where energy is stored until some factor lifts the air past an energy barrier, we discard any data observed while rainfall was occurring. This allows us to focus on role that the boundary layer plays in triggering rainfall events.

Also removed from the analysis are hours preceding large-scale events, defined by continuous rainfall for more than five hours. This is an attempt to remove the synoptic influence from the data. The five hour threshold was varied between three and eight hours, with little to no change in the results. This is consistent with the above analysis of the diurnal cycle of rainstorm duration: very few large-scale storms occur during the afternoon.

Figure 5.2: The diurnal cycle of rainfall depth, storm duration, and probability of initiation for April and May.

Figure 5.2 (cont.): The diurnal cycle of rainfall depth, storm duration, and probability of initiation for June and July.

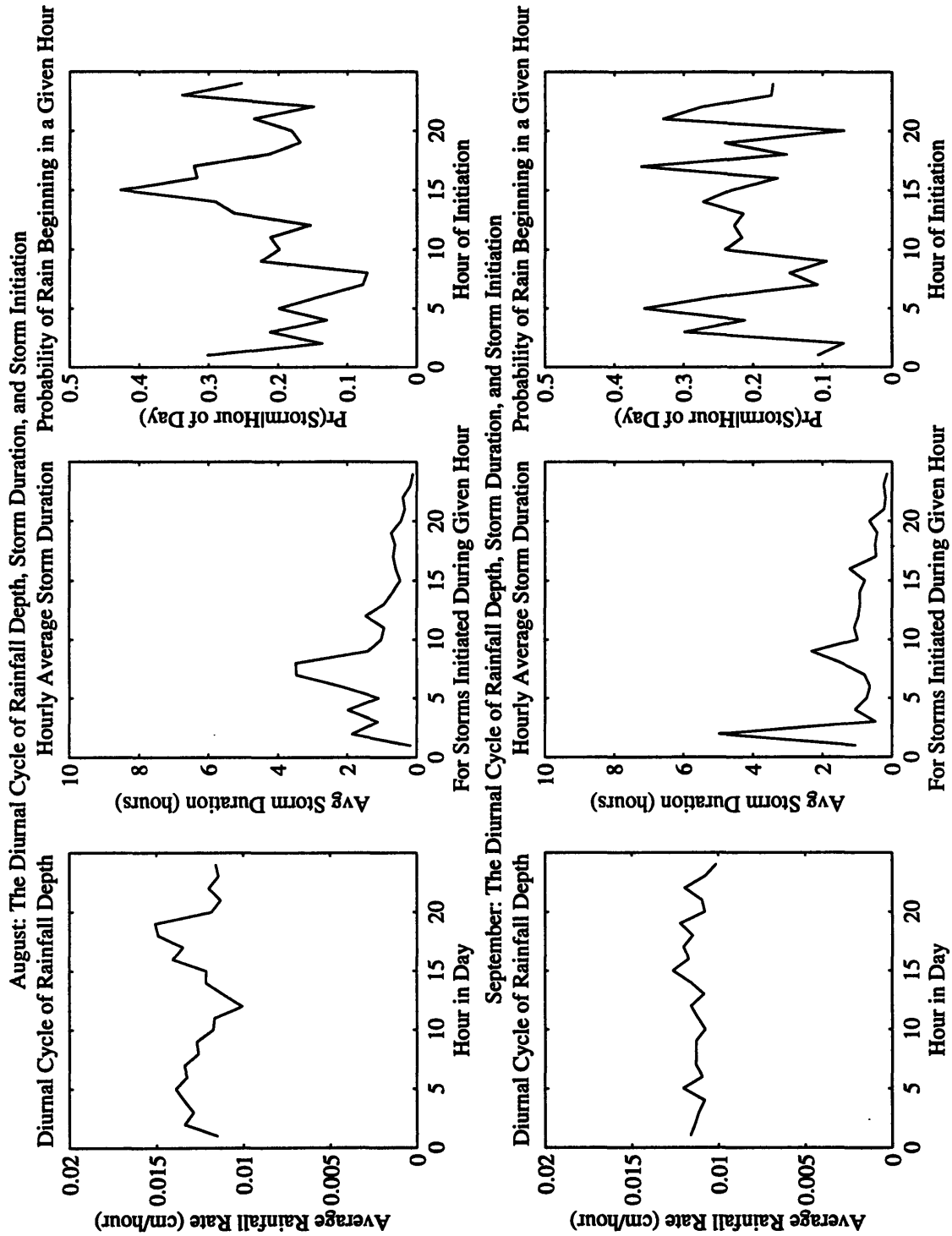

Figure 5.2 (cont.): The diurnal cycle of rainfall depth, storm duration, and probability of initiation for August and September.

C. *Analysis of Afternoon Storm Events and the Preceding Boundary Layer Conditions*

The pressure at the ground surface is often a good indicator of the synoptic setting of the region: low pressure centers are associated with cyclonic flow, which causes convergence, lifting, and, quite often, rainfall. Figure 5.3 shows that the afternoon hours of 2 to 6 PM are not free of this dependence. The right-most columns show the probability of the initiation of rainfall after an hour with pressure in a given bin, centered around each astrix. The raw data, shown in the left-most columns of Figure 5.3, are grouped such that each of ten bins has an equal number of data points. Ten bins was chosen arbitrarily, but was used consistently in all the subsequent analyses to minimize the bias that can be introduced by the bining process. After removal of the above-mentioned data points, still remaining were between 1190 and 1640 valid observations each month. The number of data points in each bin ranged from 119 in April to 164 in September. The raw data are presented in all subsequent analyses so that the effects of bining are clear. However, many of the data points have zero rainfall and are overlain on the raw data plots.

The middle columns in Figure 5.3 show the average depth of rain per hour, given that rainfall did indeed occur, associated with the ten bins in the probability of initiation plots. Little association between pressure and average depth of rain in the subsequent hour is observed. The probability of initiation plots, however, show that, during each month, rainfall is more likely to begin after hours with a low pressure than after hours with a relatively high pressure. This suggests that though other boundary layer conditions may be associated with occurrence of rainfall, as the results presented herein will demonstrate, the synoptic influence may assist in triggering rainfall events and cannot be neglected. This will be discussed in greater detail in the next section.

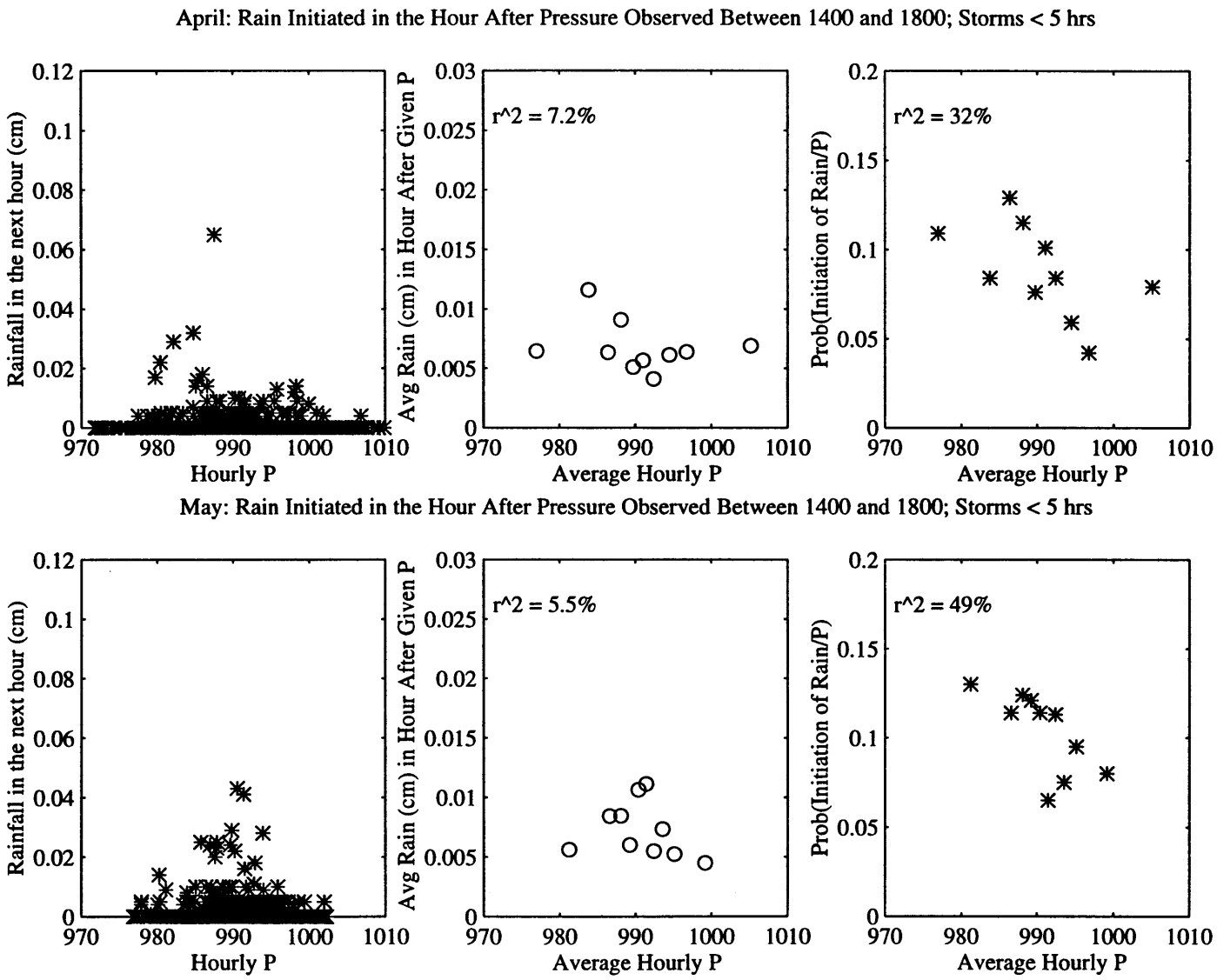

Figure 5.3: Correlations between hourly pressure (*P*) and rainfall during April and May.

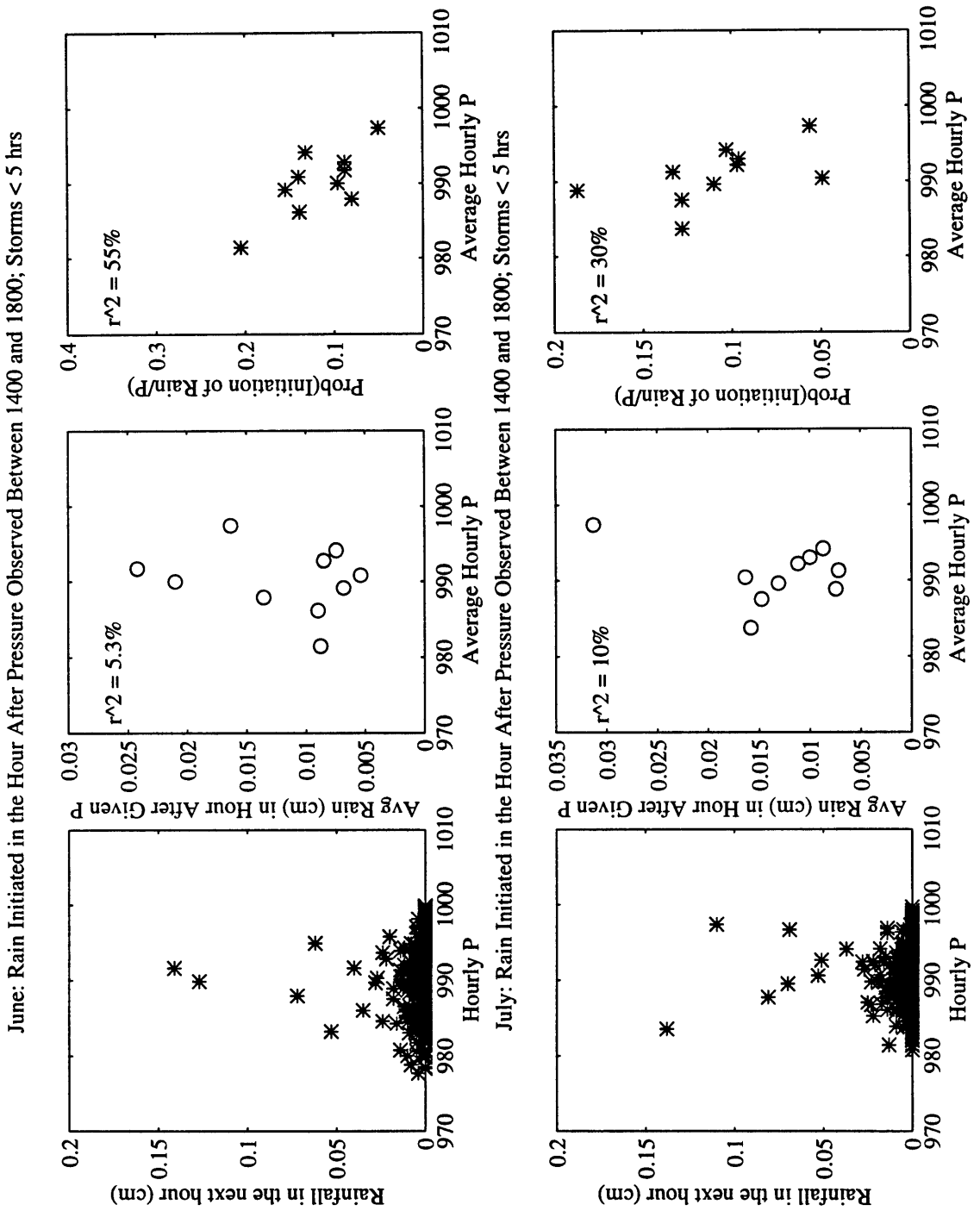

Figure 5.3 (cont.): Correlations between hourly pressure (*P*) and rainfall during June and July.

Figure 5.3 (cont.): Correlations between hourly pressure (*P*) and rainfall during August and September.

Please note in all Figures 5.3 through 5.13 that the axes scaling are variable. The spring and fall months (April, May, and September) have the same x-axis scaling for each variable, as do the summer months (June, July, and August). The two groups often have different x-axis ranges. The y-axes are scaled according to the results, so careful attention should be paid to these limits.

Relative humidity is shown in Figure 5.4 to have a strong association with the initiation of rainfall in the subsequent hour during all of the six months studied. The linear correlation between relative humidity and the probability of initiation of rainfall is strongest during the summer months of June, July and August, when the r^2's are all between 79 and 83%. The average depth of rain in the hour following an observation shows almost no association with relative humidity.

Figure 5.5 shows that mixing ratio displays a similarly close association with the likelihood of rainfall as relative humidity, but it tends to be a better predictor of rainfall depth in the subsequent hour. The r^2s of the probability of occurrence are quite high in June and August, lower during spring and fall, and quite low in July. The month of July exhibits some interesting behavior at both extremes of low and high mixing ratio. Between about 10 and 16 g/kg, there is a strong positive correlation between *w* and the probability of initiation of rain, with probabilities changing from approximately 0.07 to 0.17. The two bins beyond 16 g/kg, however, show that rainfall is less likely to begin in these very wet circumstances. The highest *w* bin, centered near 20 g/kg, has dropped down to a probability of about 0.08: as low as the bin centered near 11 g/kg. The August data also show this drop in probability for the highest *w* group, but the transition is much less extreme: from about 0.18 to 0.17.

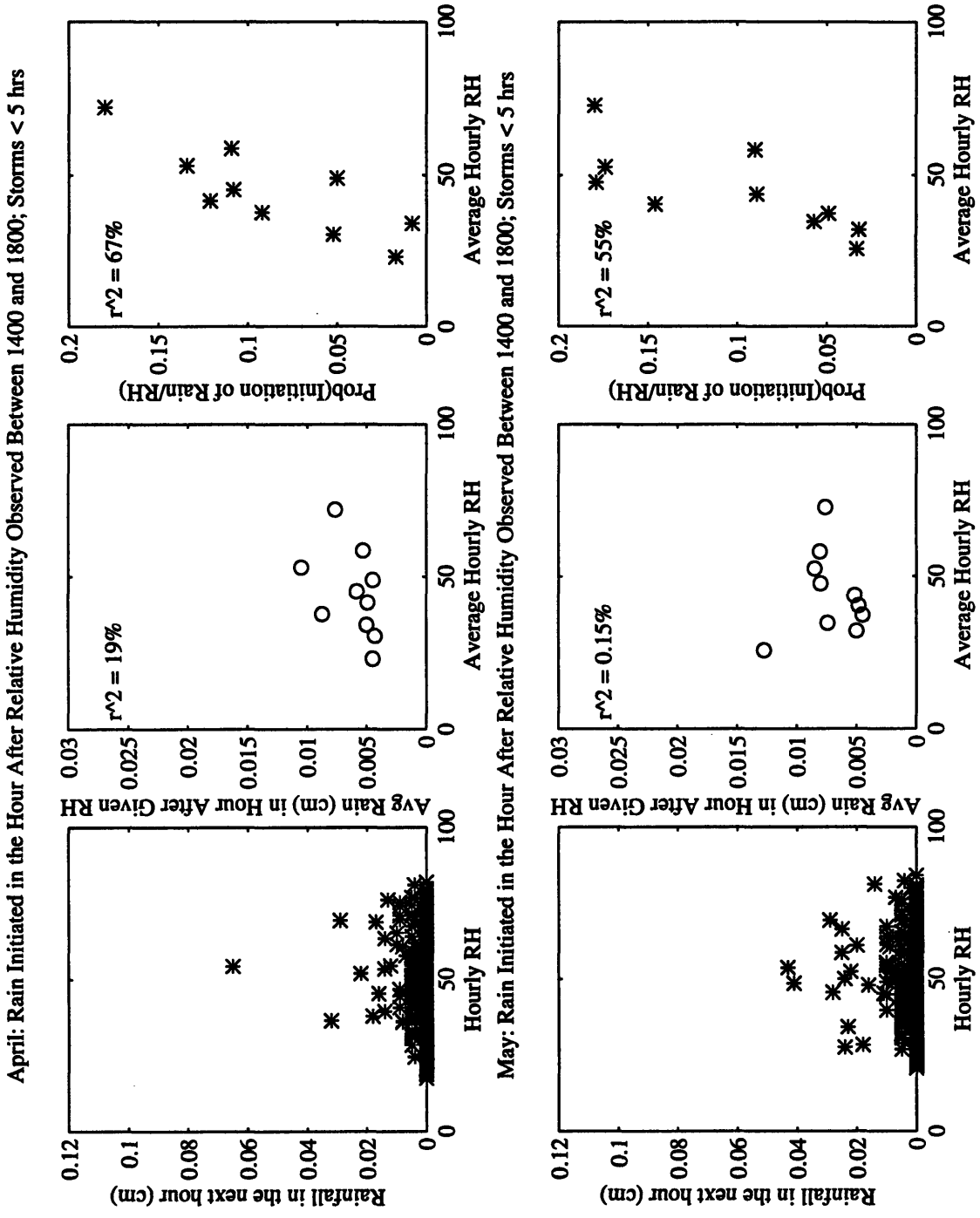

Figure 5.4: Correlations between hourly relative humidity (*f*) and rainfall during April and May.

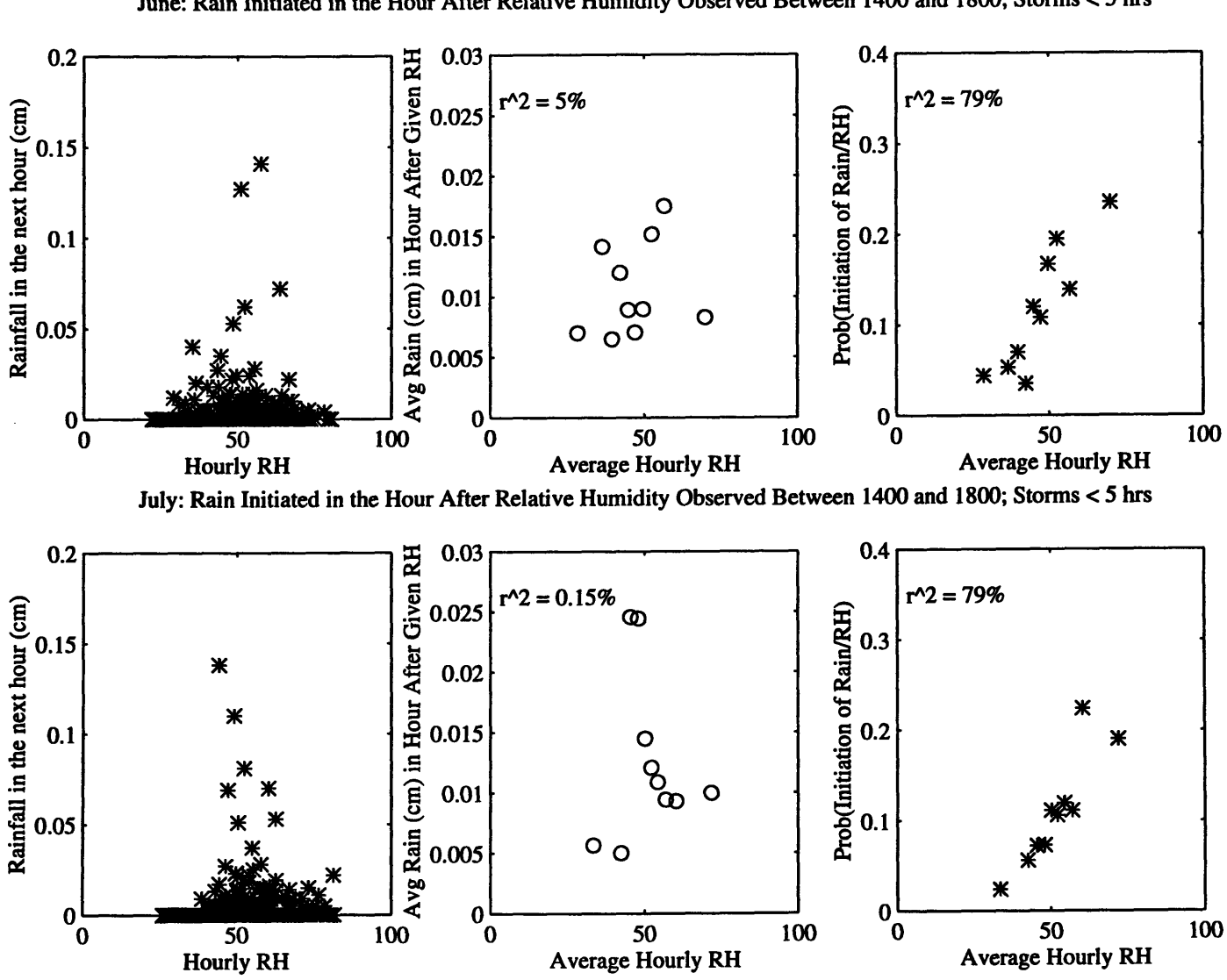

Figure 5.4 (cont.): Correlations between hourly relative humidity (*f*) and rainfall during June and July.

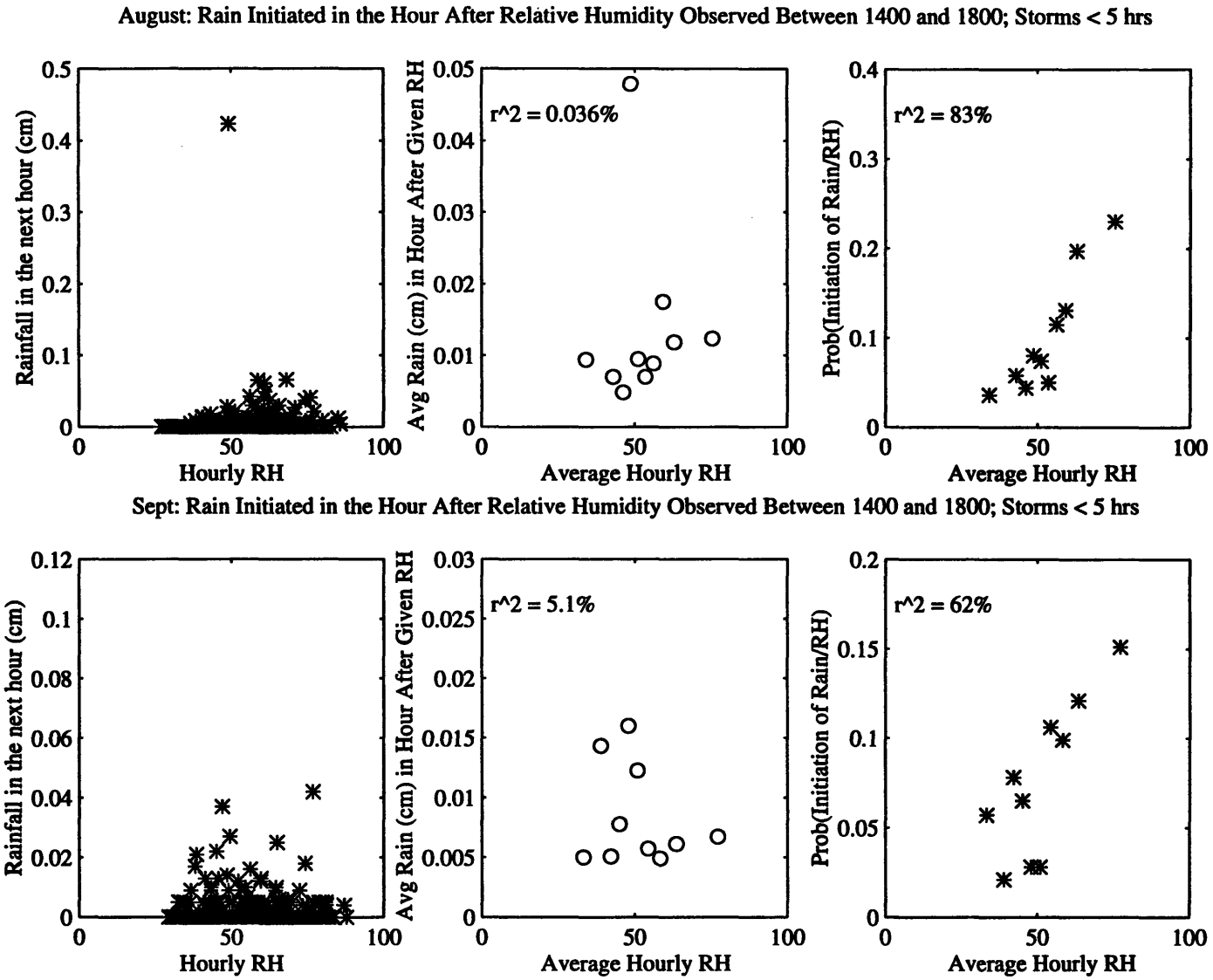

Figure 5.4 (cont.): Correlations between hourly relative humidity (*f*) and rainfall during August and September.

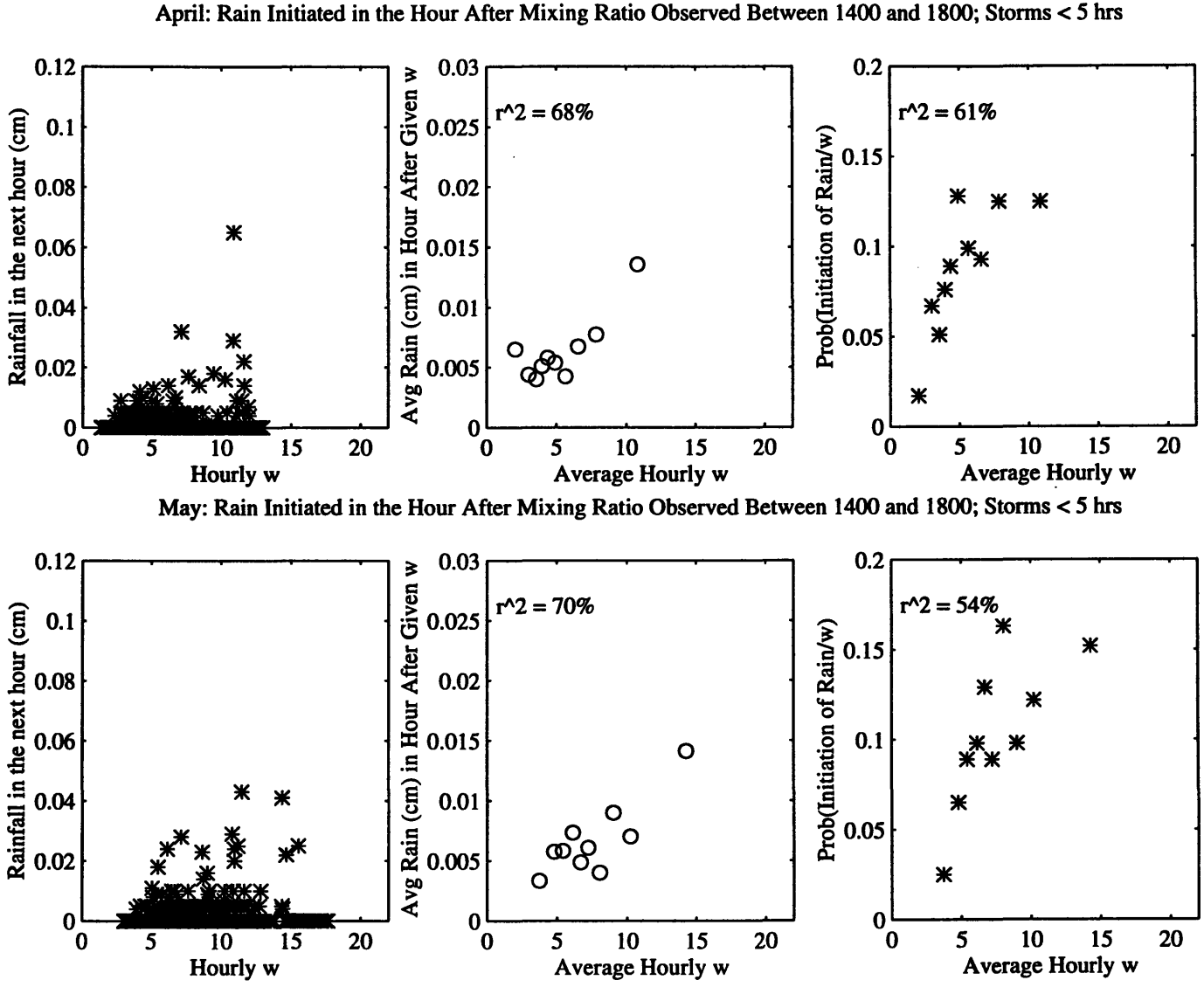

Figure 5.5: Correlations between hourly mixing ratio (w) and subsequent rainfall during April and May.

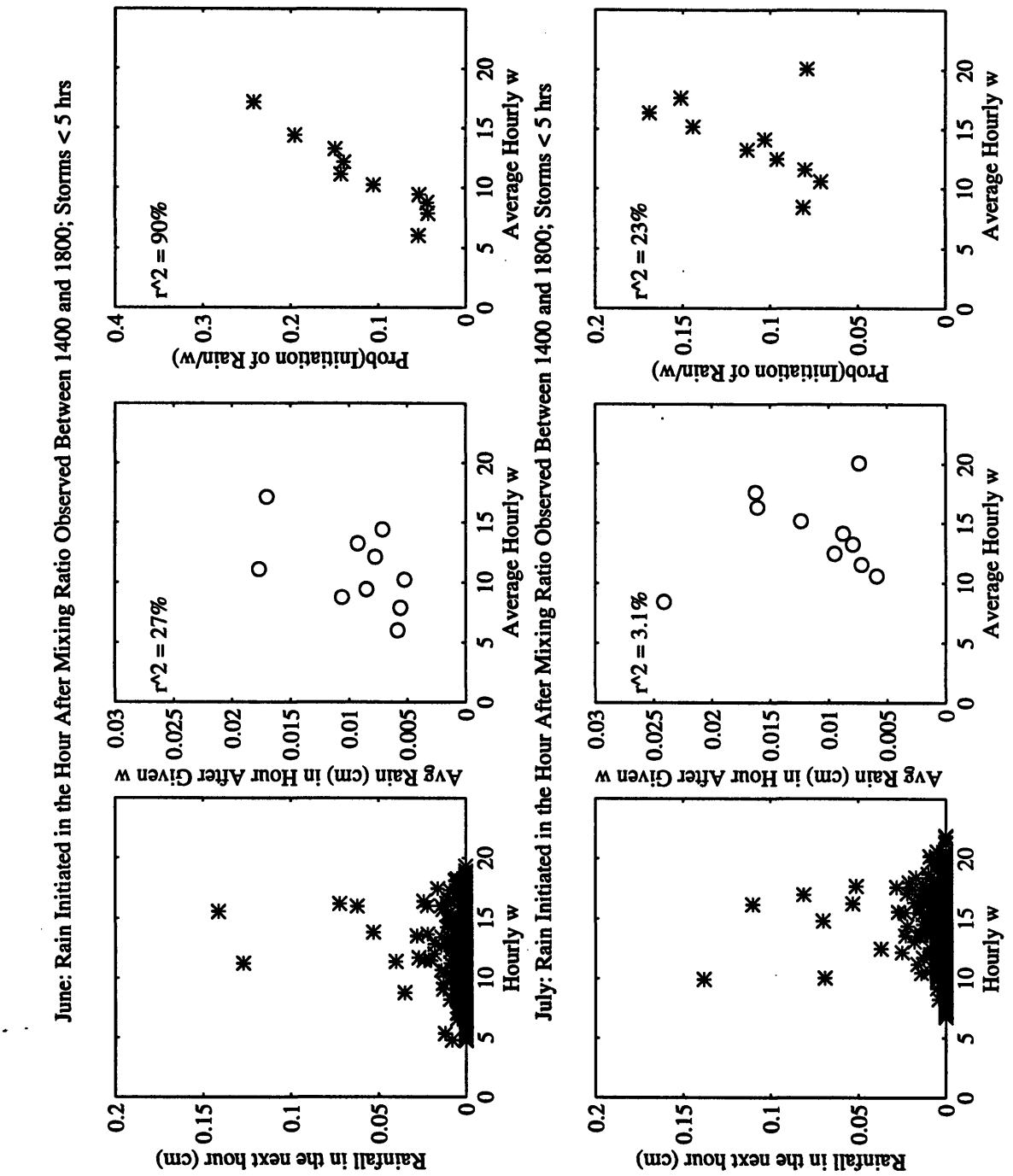

Figure 5.5 (cont.): Correlations between hourly mixing ratio (w) and rainfall during June and July.

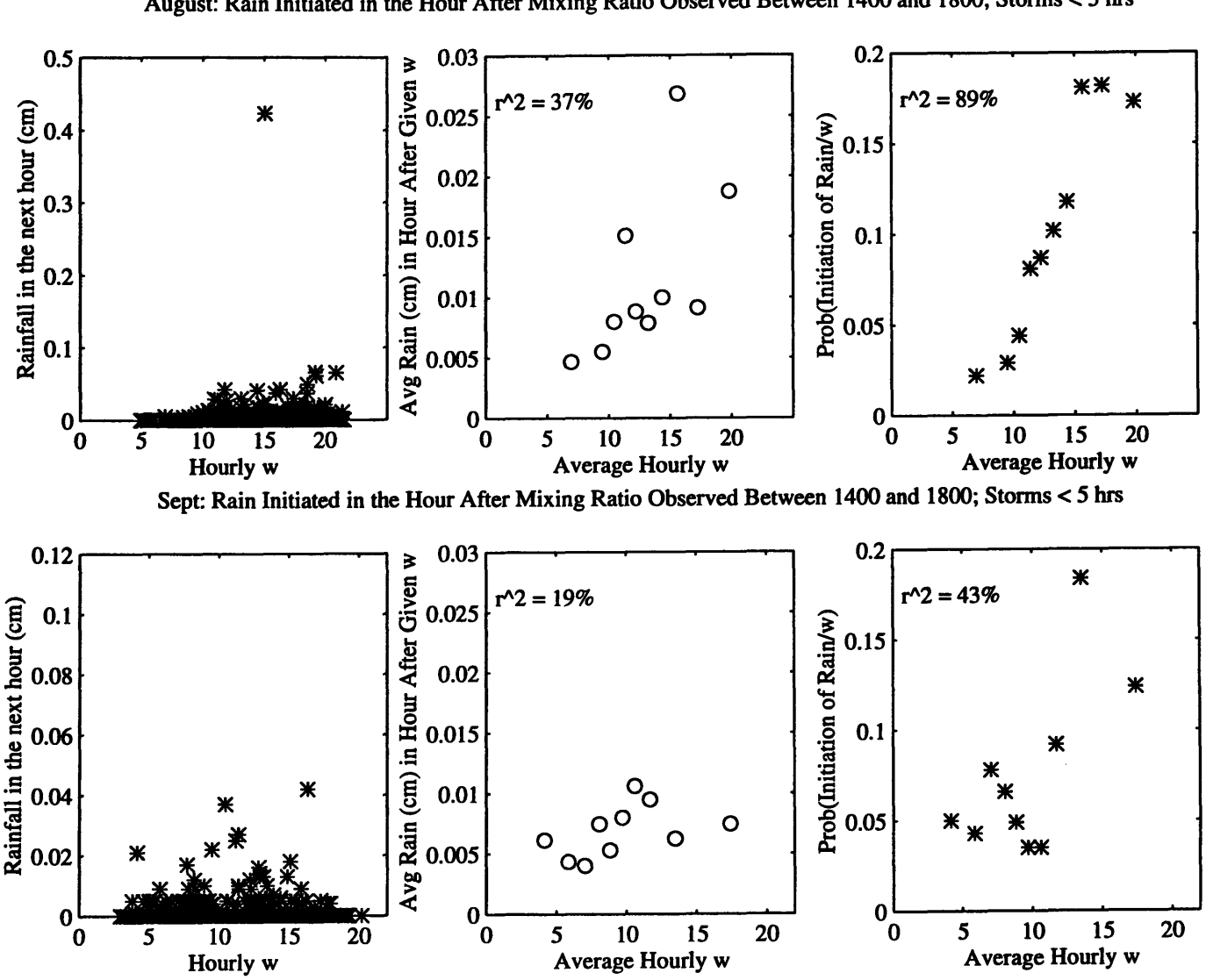

Figure 5.5 (cont.): Correlations between hourly mixing ratio (*w*) and rainfall during August and September.

At the low end of the observations of mixing ratio, the positive linear trend is also broken in June and August, as well as in July. Below w's of approximately 8 g/kg, the probability of rainfall initiation is nearly constant. Both of these deviations from linearity are seen in other variables presented in this chapter. Possible causes will be discussed in the next section.

The studies of Williams and Renno (1993) and Eltahir and Pal (1996) showed a dependence between rainfall and wet-bulb potential temperature, θ_w, and wet-bulb temperature, T_w, respectively. Both focused on tropical regions, but, as Carlson and Ludlam (1966) point out, during the summer the mid-latitudes often acquire much of the behavior of the tropics. Figure 5.6 shows that there is, indeed, a strong relationship between T_w and subsequent rainfall during June and August. Between approximately 15 and 25 °C there is a strong positive linear trend in the probability of storm initiation. July shows a similar trend (but with much more scatter) in this range, but the lowest probability of rainfall is associted with the largest T_w of approximately 26 °C. Below 15 °C, the probability is nearly constant in June. The fall and spring months show very little pattern in the probability of initiation, but some positive dependence on T_w is evident in the average depth of rain per hour in these months, as well as in June and August.

As stated in Chapter 4, the equivalent potential temperature, θ_E, is a measure of the moist static energy of the boundary layer, and is conserved in dry and moist adiabatic transformations. It is closely related to the development of cumulus and cumulonimbus convection, and is often used as an indicator of boundary layer depth and growth (Betts and Ball, 1995). There is a one-to-one relationship between θ_E and θ_w, and the results for θ_E in Figure 5.7 and for θ_E in Figure 5.8 are very similar. As with T_w, both θ_E and θ_w show particularly good correlations with probability of rainfall occurrence during June and August, while during July the one anomalous highest bin

throws off a scattered but positive linear trend. April, May and September also have similar rainfall initiation patterns in θ_w and θ_E as in T_w. The average depth of rain after surface observations of θ_E or θ_w shows weak positive association in all months except July. This is also consistent with wet-bulb temperature results.

Figure 5.9 shows that wet-bulb depression is good at predicting storm occurrence in all months, with r^2's between 45 and 83%, but especially in May (83%), June (76%), and July (77%). Given the results of Chapter 4 showing the strong connection between soil moisture and subsequent wet-bulb depression, this is an important result for the determination of a physical pathway connecting soil moisture and rainfall. This will be discussed in greater detail in the next section. Though wet-bulb depression is a good predictor of rainfall occurrence, it is not, however, as robust a predictor of subsequent rainfall depth.

Another good predictor of storm occurrence is the temperature of the Lifting Condensation Level (LCL) (see Figure 5.10). A positive linear correlation explains between 70 and 85% of the variability in storm initiation during April, May, June, and August, and 47 and 42% in July and September, respectively. It is also a fairly robust indicator of average rainfall depth in the next hour in April, May, June, and August. The correlation shows that rainfall is more likely to occur when the LCL is at higher temperatures than at lower temperatures. July exhibits the same anomalous behavior at the highest T_{LCL}'s that was noted in the highest q, T_w, and θ_w bins. Threshold behavior is demonstrated by the near-constant initiation probabilities at T_{LCL}s less than about 280 K in the summertime.

Peppler and Lamb (1989) analyzed the correlation between rainfall and what they called SSITPs: Static Stability Indicies and Related Thermodynamic Parameters. They determined that

the variables which were most closely related to tropospheric static stability over central North America were not typical buoyancy parameters, but were related to the pressure of the LCL. The results with T_{LCL} found here show a similarly high correlation: a high LCL temperature implies a lower LCL pressure and a lower cloud base height.

Interestingly, this strong association between T_{LCL} and rainfall does not carry over to the pressure depth of the LCL. Figure 5.11 shows June, August and September (except for the lowest bin) with a scattered positive trend between P_{LCL} - P_s and probability of rainfall. July, however, shows a negative trend. April and May do not show clear trends in the probability of initiation, but show much stronger correlation with average hourly rainfall depth than the other months.

As discussed in Chapter 4, the pressure depth to the LCL is, in a sense, a measure of buoyancy. The soil moisture–boundary layer analyses results showed that this variable responded to soil moisture in a very similar manner as temperature, potential temperature, and virtual potential temperature. This correspondence between these four variables is also seen in their relationship to rainfall in the following hour. Figure 5.12 shows the results for temperature, but results for potential temperature and virtual potential temperature are not shown. The patterns in Figure 5.12 are very similar to those in Figure 5.11 for the pressure depth to the LCL. Of note is July's even stronger negative correlation between probability of initiation of rain T (r^2 = 68%).

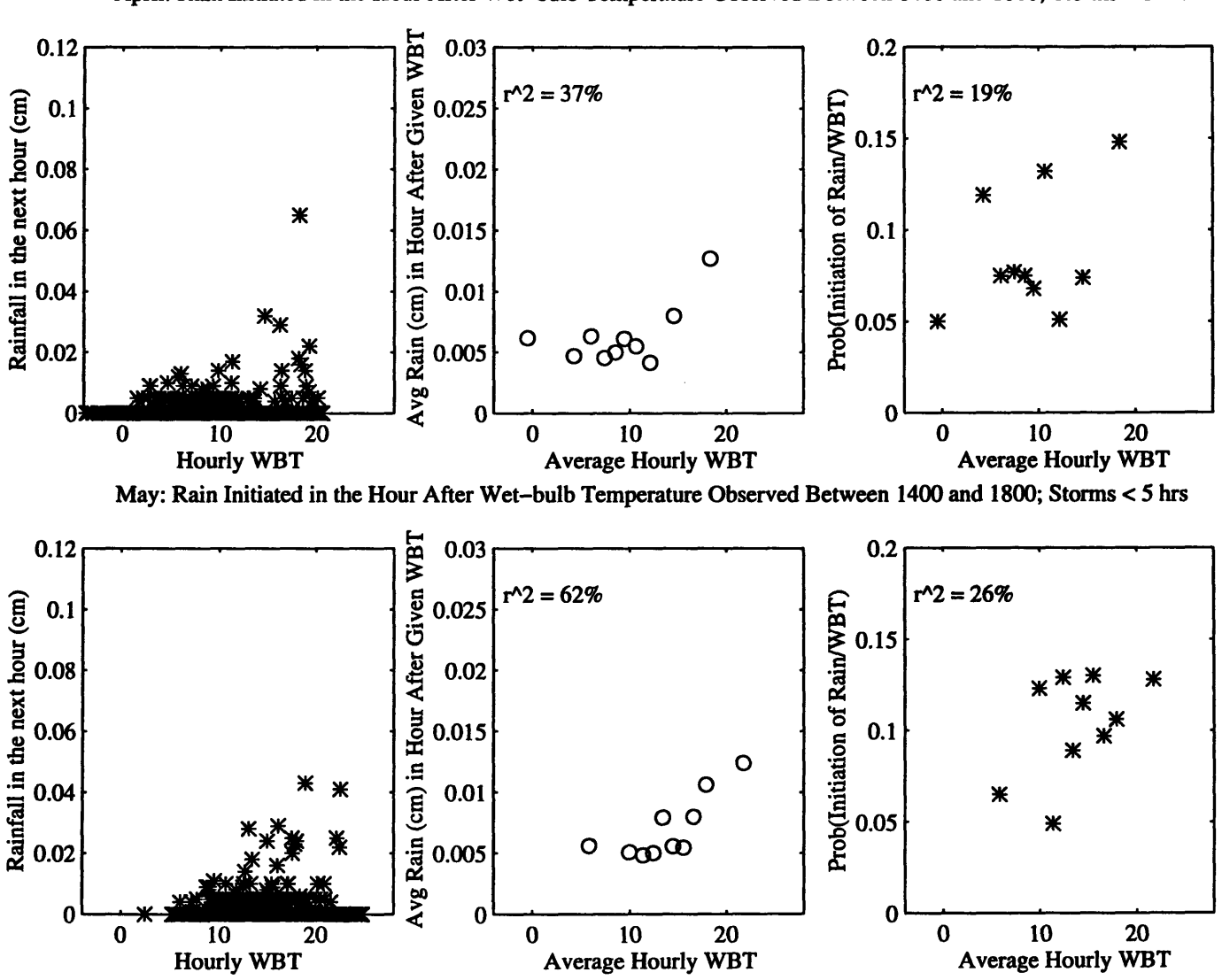

Figure 5.6: Correlations between hourly wet-bulb temperature (T_w) and rainfall during April and May.

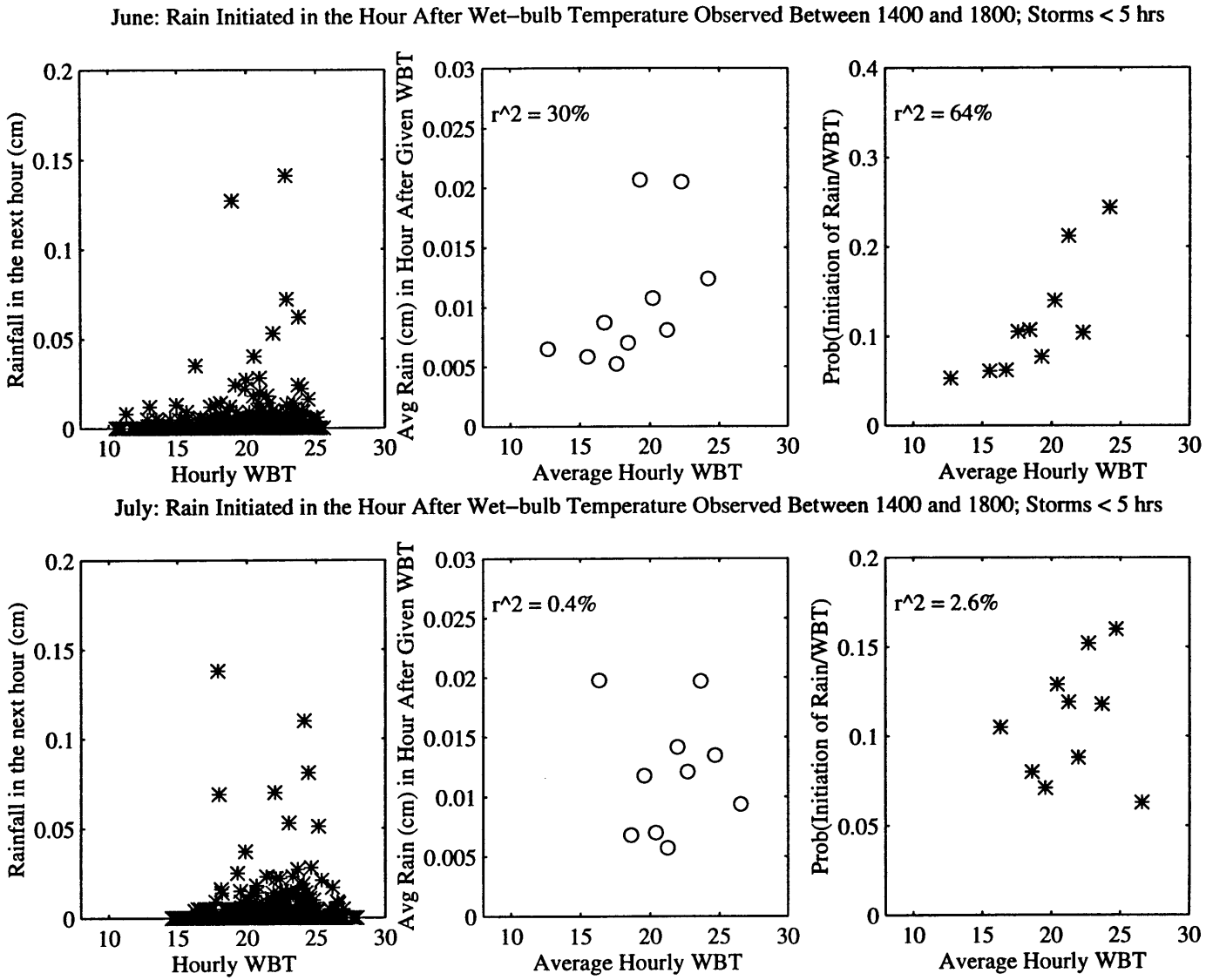

Figure 5.6 (cont.): Correlations between hourly wet-bulb temperature (T_w) and rainfall during June and July.

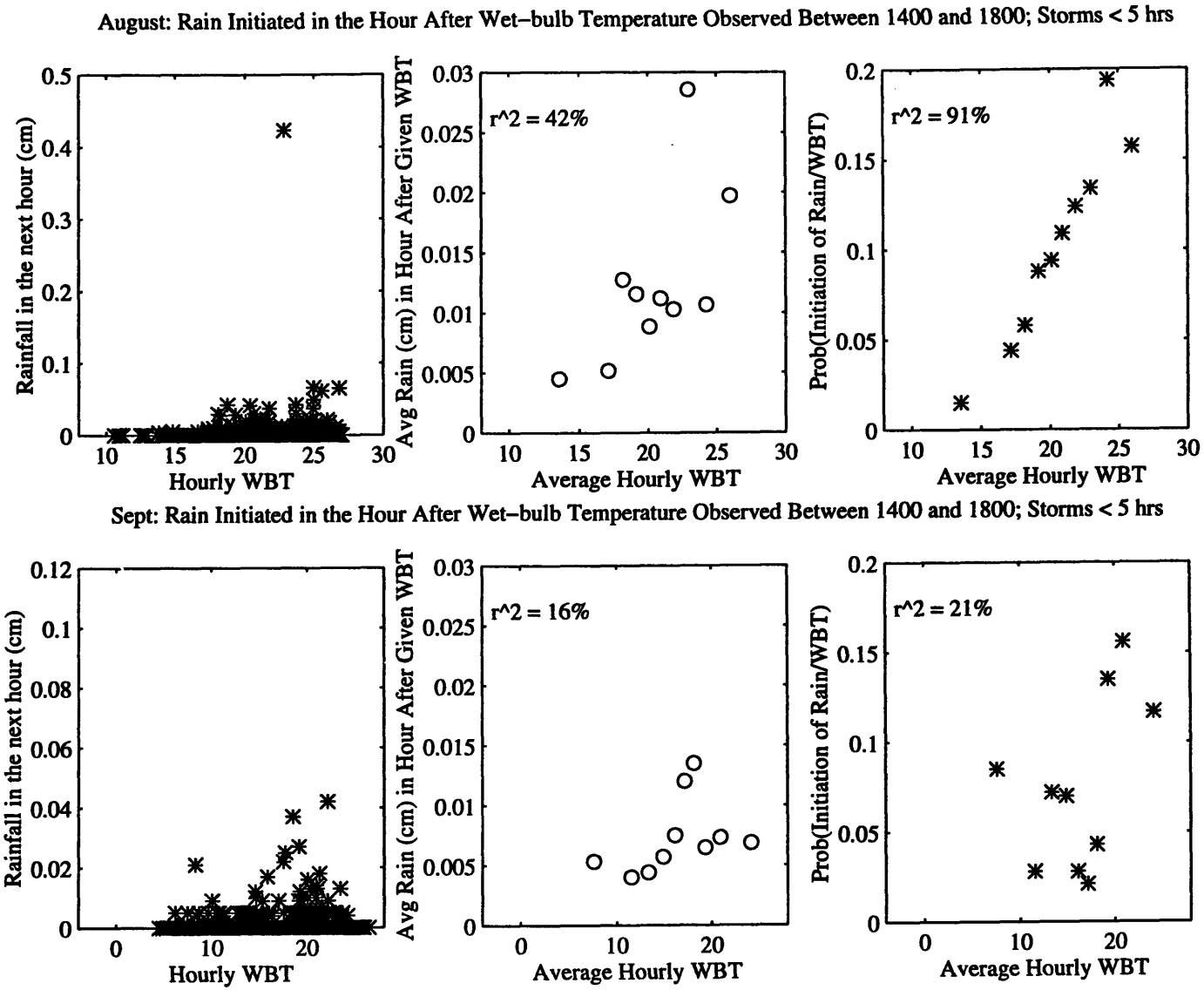

Figure 5.6 (cont.): Correlations between hourly wet-bulb temperature (T_w) and rainfall during August and September.

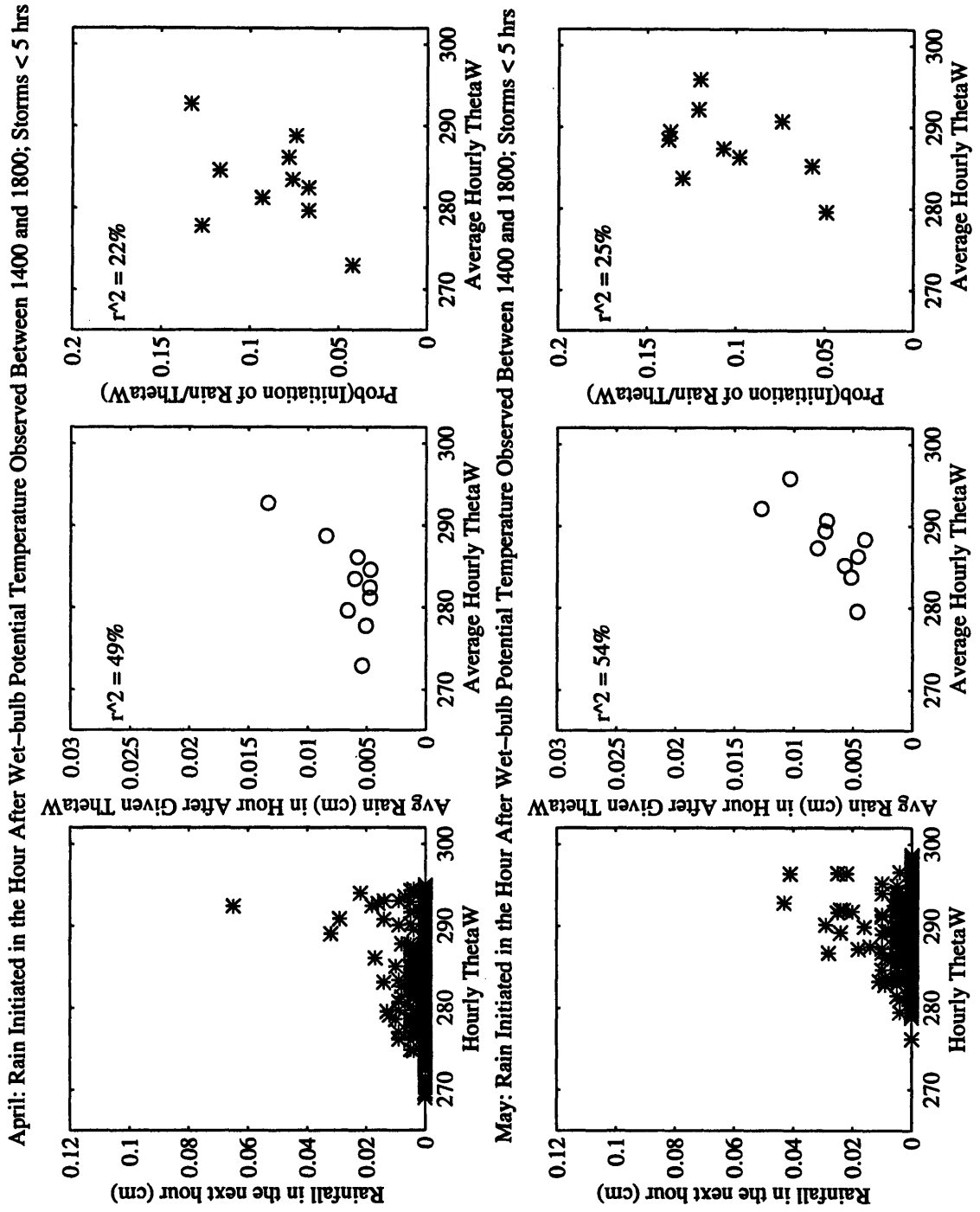

Figure 5.7: Correlations between hourly wet-bulb potential temperature (θ_w) and subsequent rainfall during April and May.

Figure 5.7 (cont.): Correlations between hourly wet-bulb potential temperature (θ_w) and rainfall during June and July.

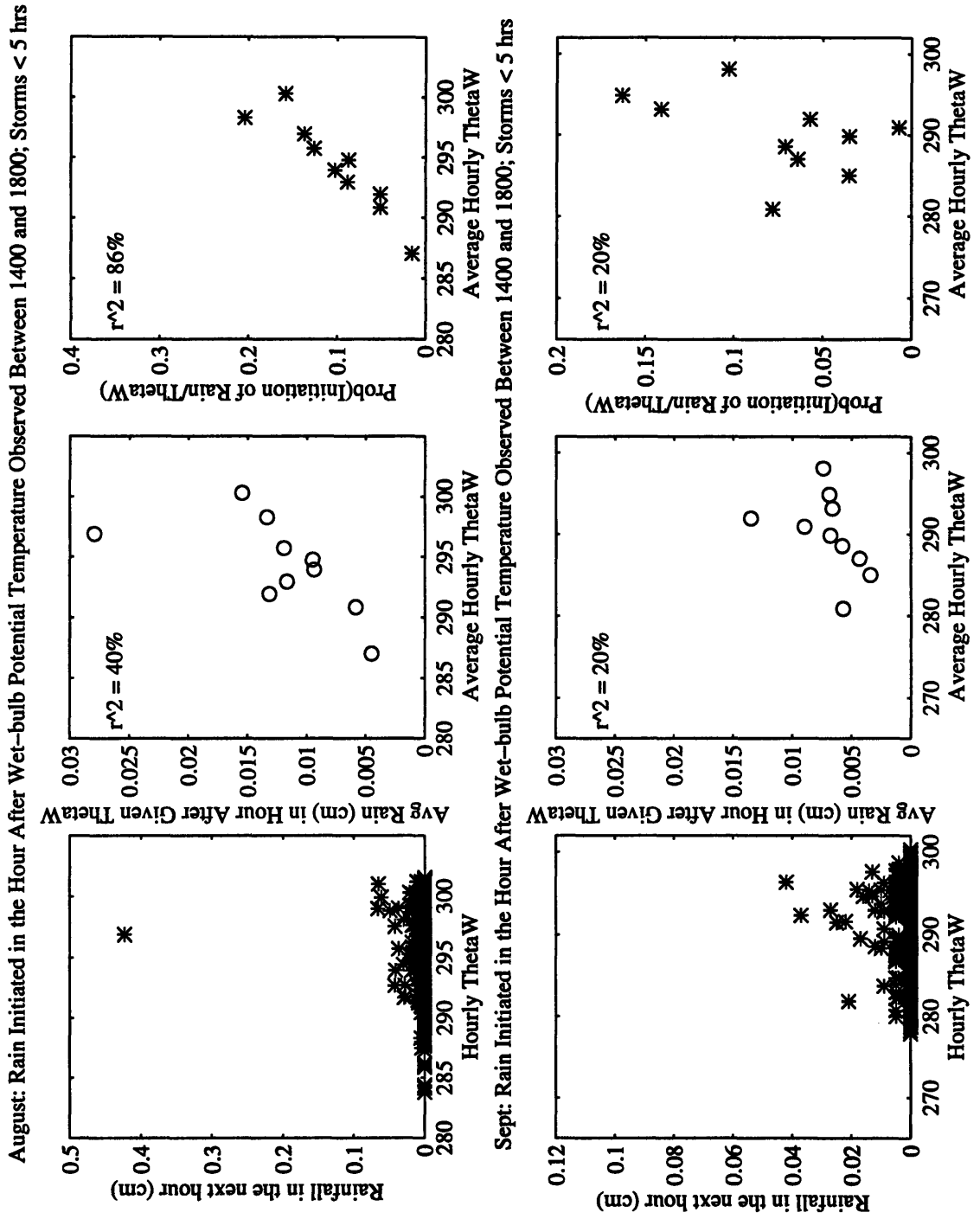

Figure 5.7 (cont.): Correlations between hourly wet-bulb potential temperature (θ_w) and rainfall during August and September.

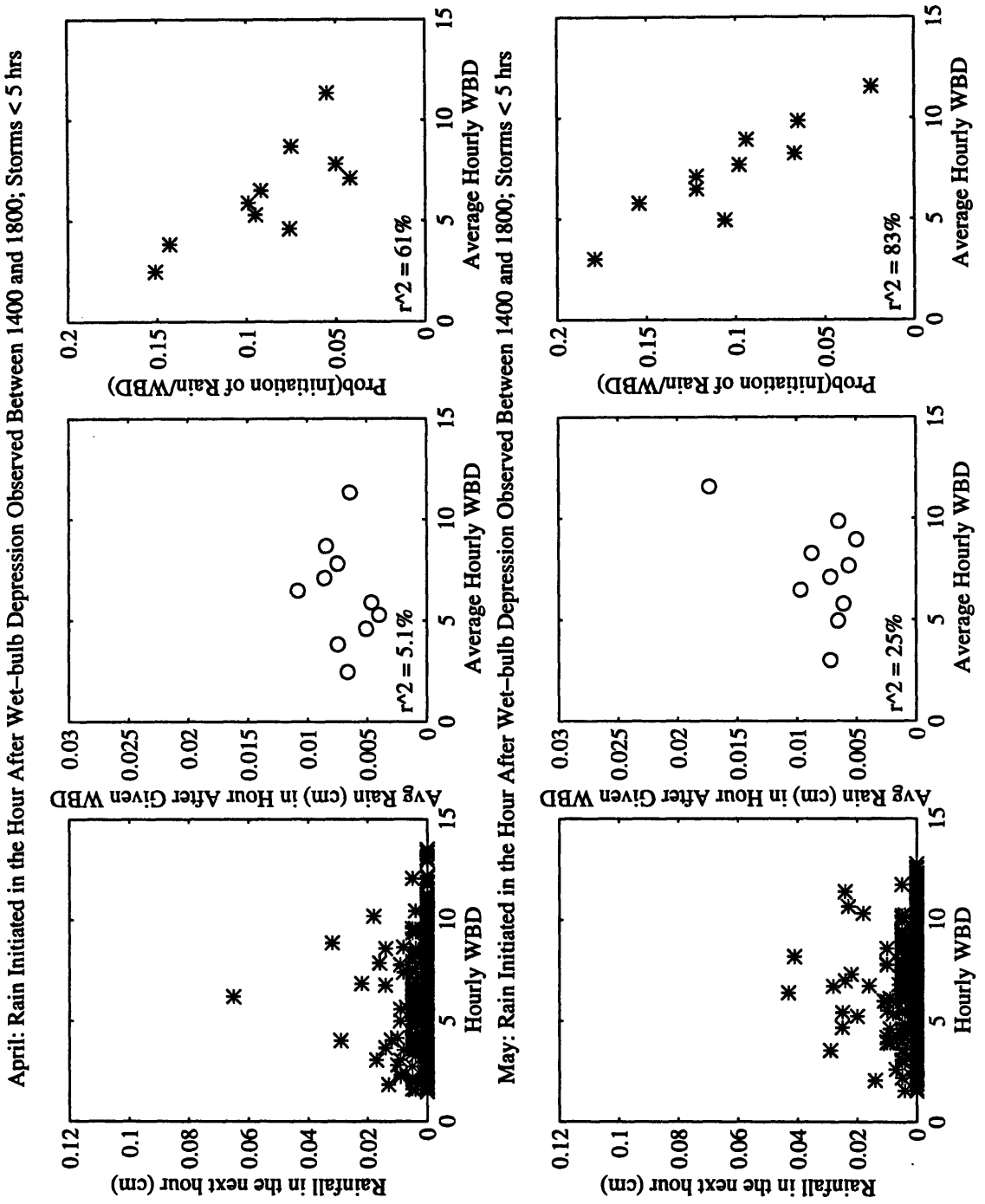

Figure 5.8: Correlations between hourly wet-bulb depression (T_{dpr}) and subsequent rainfall during April and May.

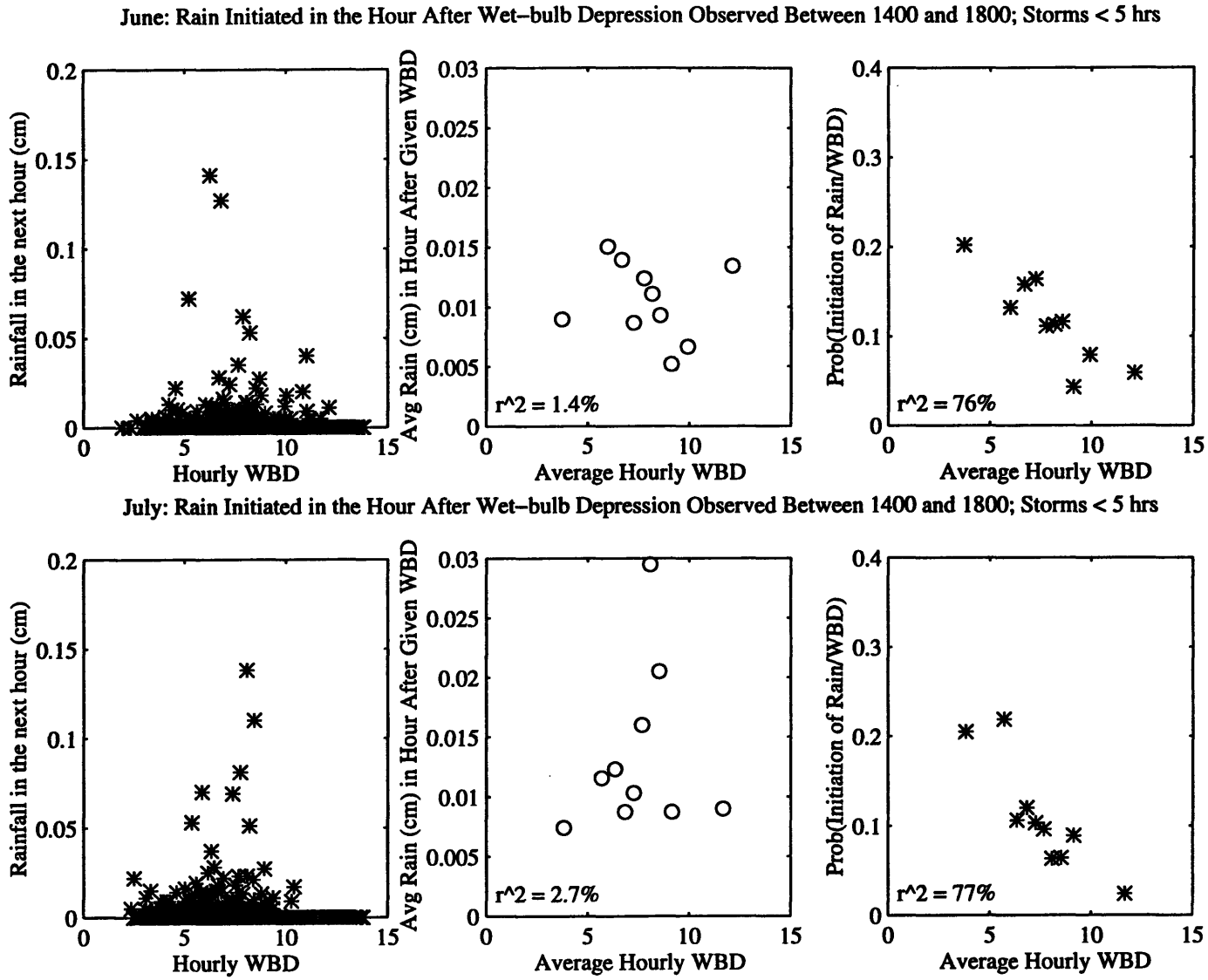

Figure 5.8 (cont.): Correlations between hourly wet-bulb depression (T_{dep}) and rainfall during June and July.

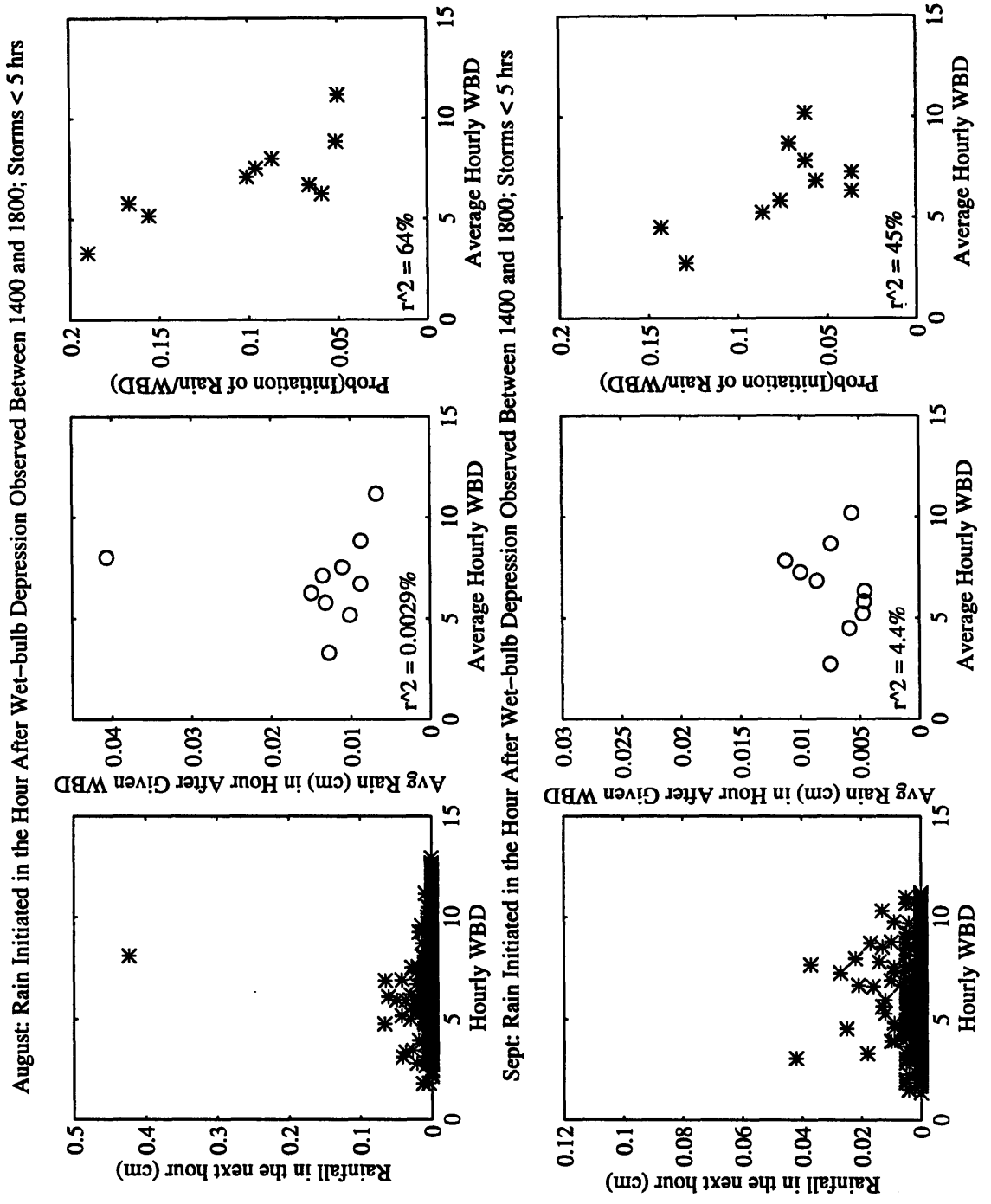

Figure 5.8 (cont.): Correlations between hourly wet-bulb depression (T_{dpr}) and rainfall during August and September.

Figure 5.9: Correlations between hourly temperature of the lifting condensation level (T_{LCL}) and subsequent rainfall during April and May.

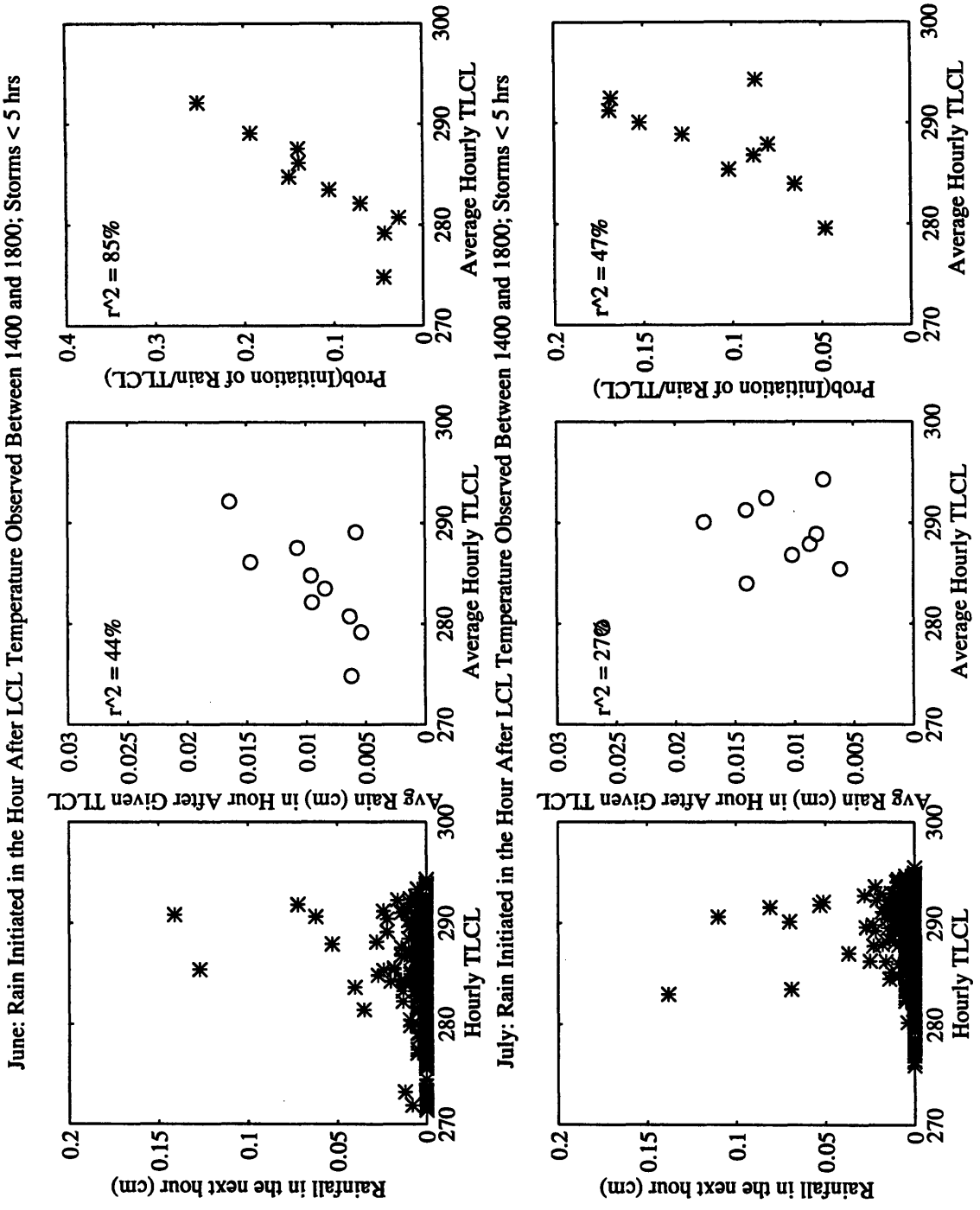

Figure 5.9 (cont.): Correlations between hourly temperature of the LCL (T_{LCL}) and rainfall during June and July.

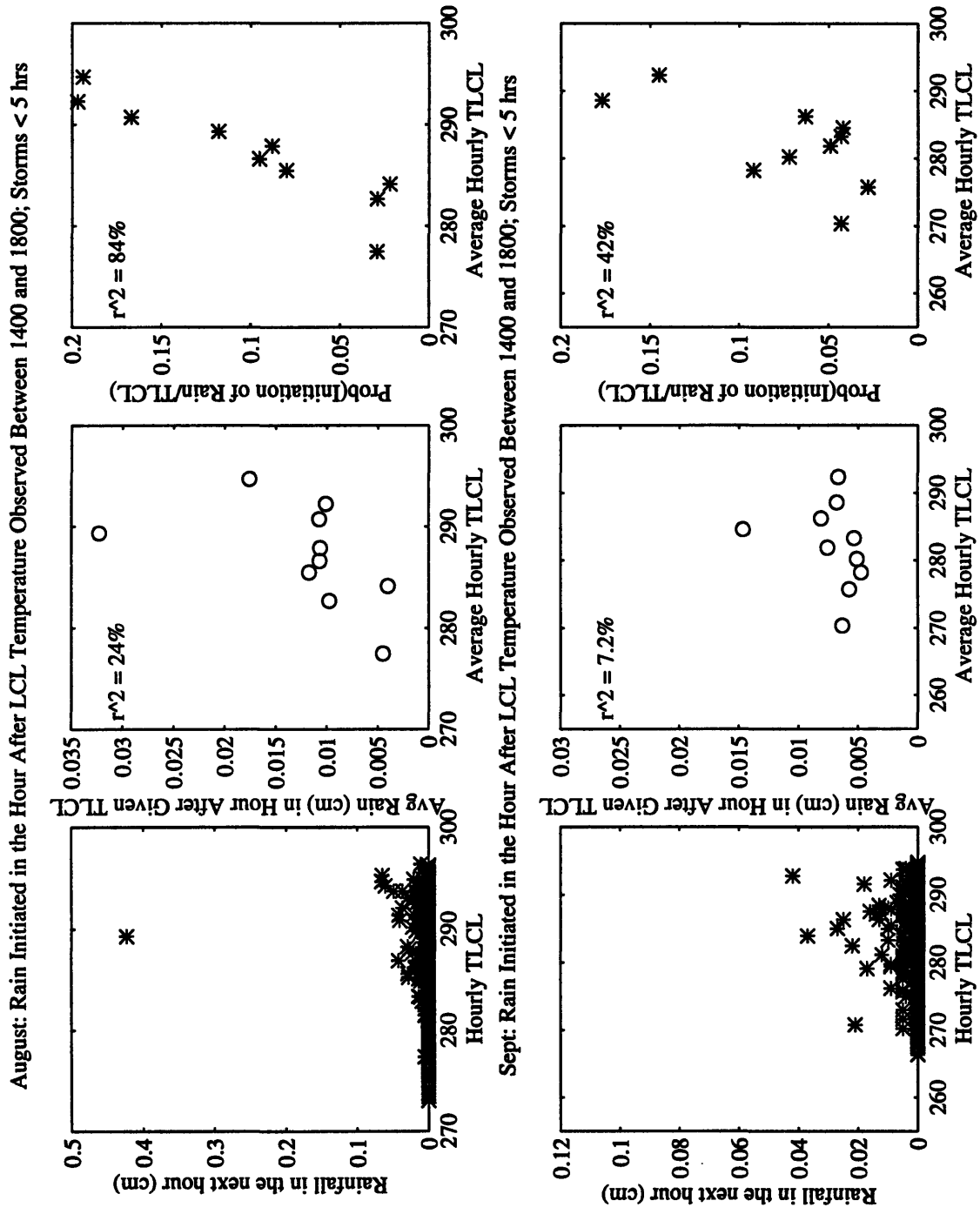

Figure 5.9 (cont.): Correlations between hourly temperature of the LCL (T_{LCL}) and rainfall during August and September.

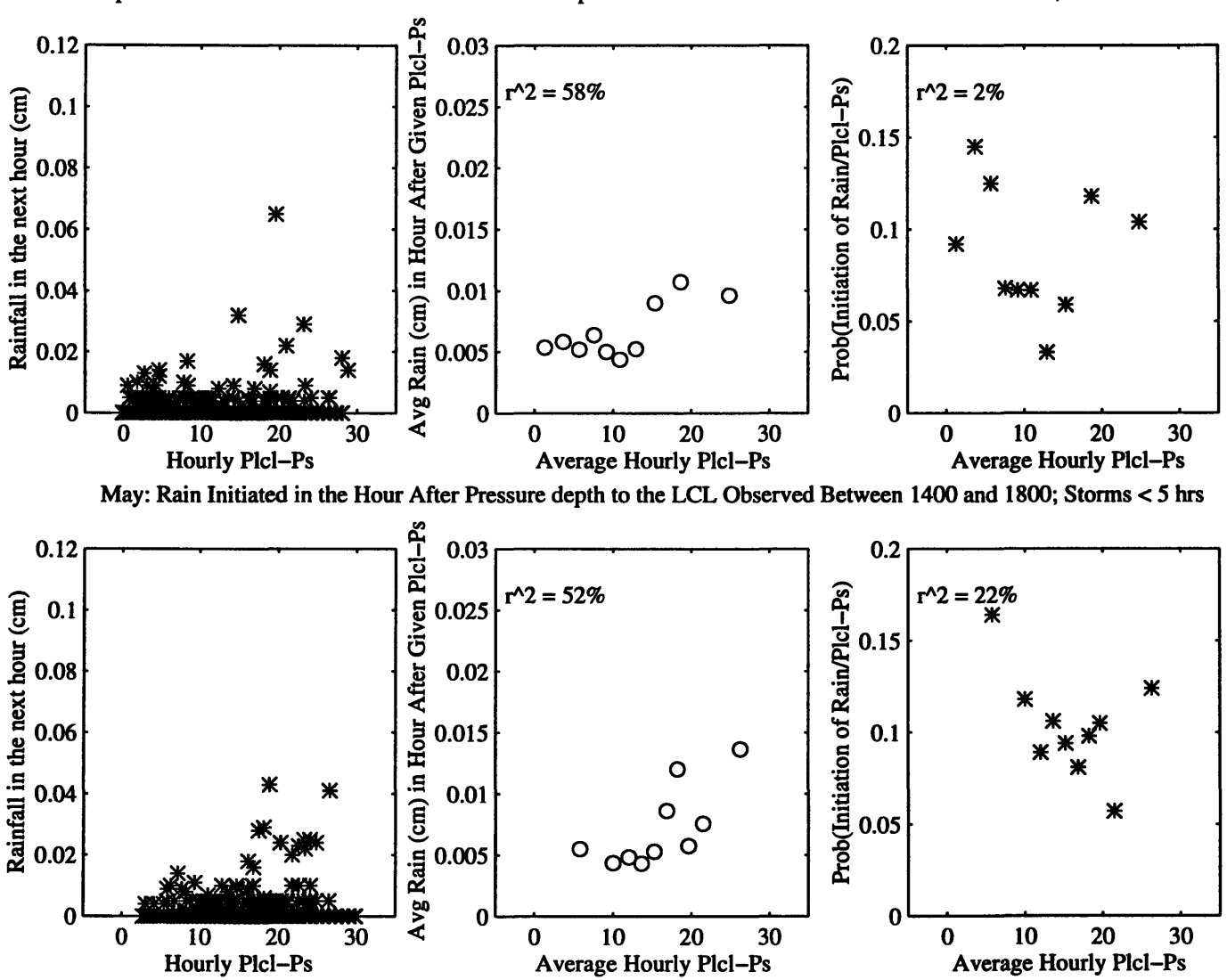

Figure 5.10: Correlations between hourly pressure depth to the LCL (P_{LCL} - P_s) and rainfall during April and May.

Figure 5.10 (cont.): Correlations between hourly pressure depth to the LCL (P_{LCL} - P_s) and rainfall during June and July.

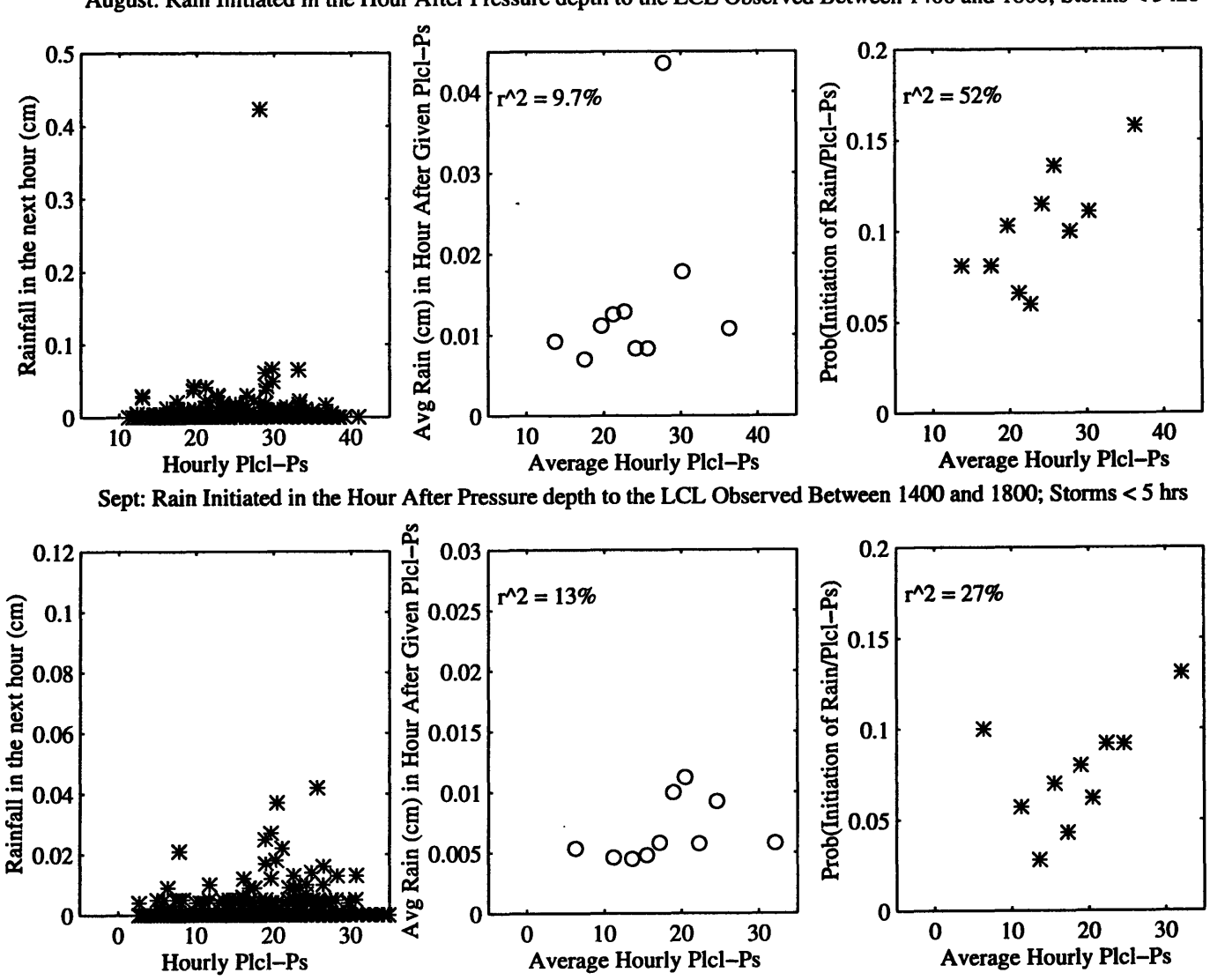

Figure 5.10 (cont.): Correlations between hourly pressure depth to the LCL (P_{LCL} - P_t) and rainfall during August and September.

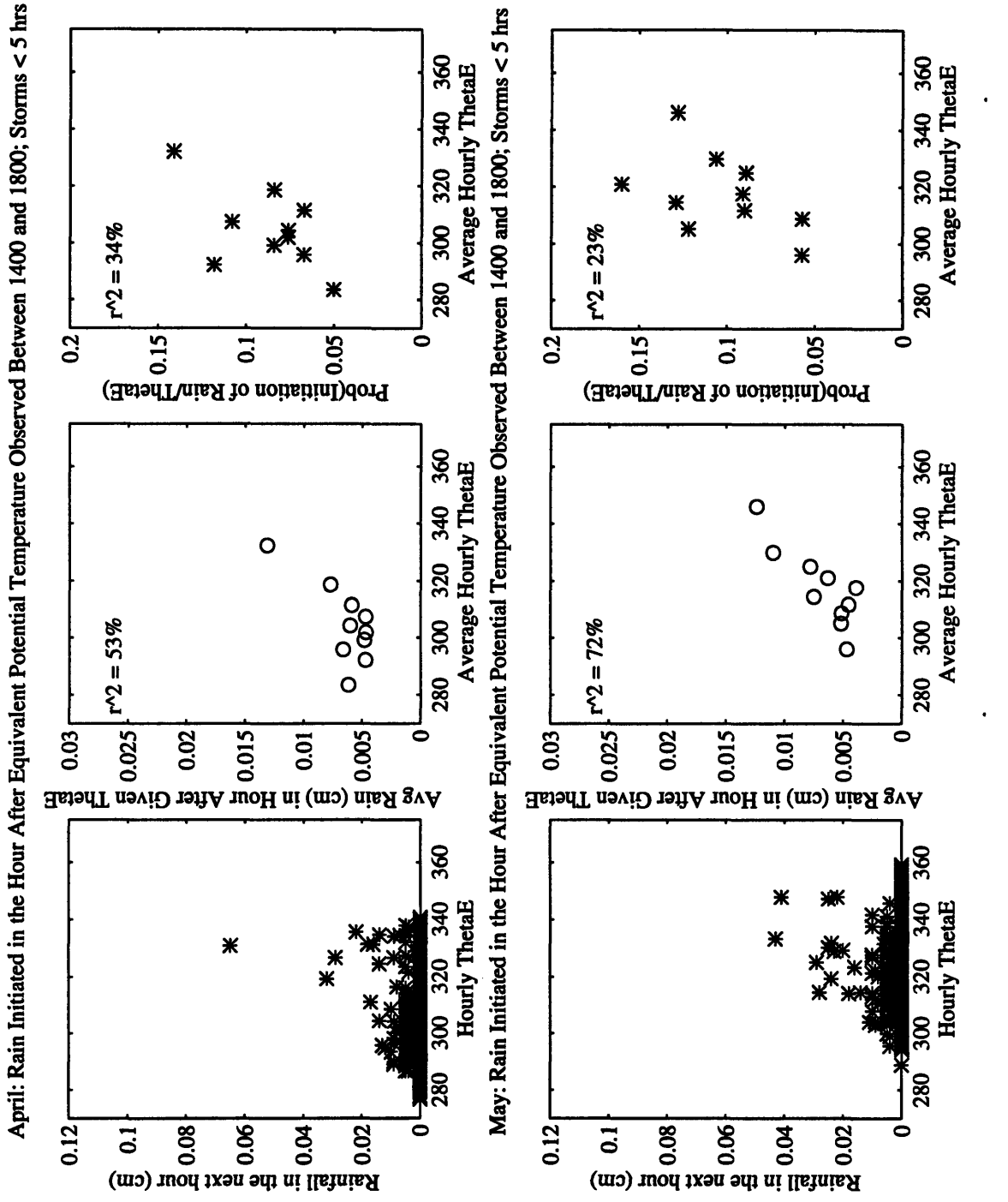

Figure 5.11: Correlations between hourly equivalent potential temperature (θ_E) and rainfall during April and May.

Figure 5.11 (cont.): Correlations between hourly equivalent potential temperature (θ_E) and rainfall during June and July.

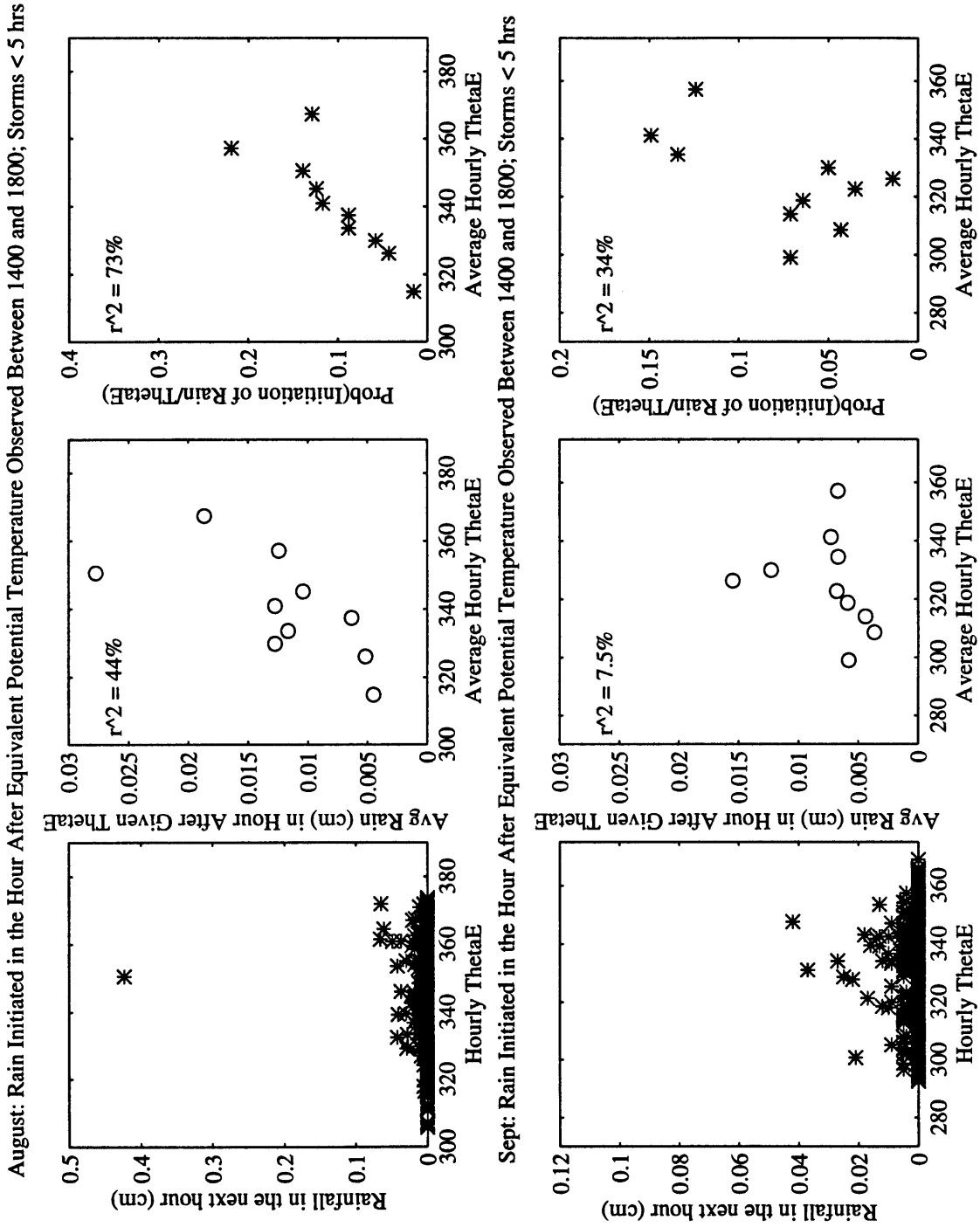

Figure 5.11 (cont.): Correlations between hourly equivalent potential temperature (θ_E) and rainfall during August and September.

Figure 5.12: Correlations between hourly air temperature (*T*) and subsequent rainfall during April and May.

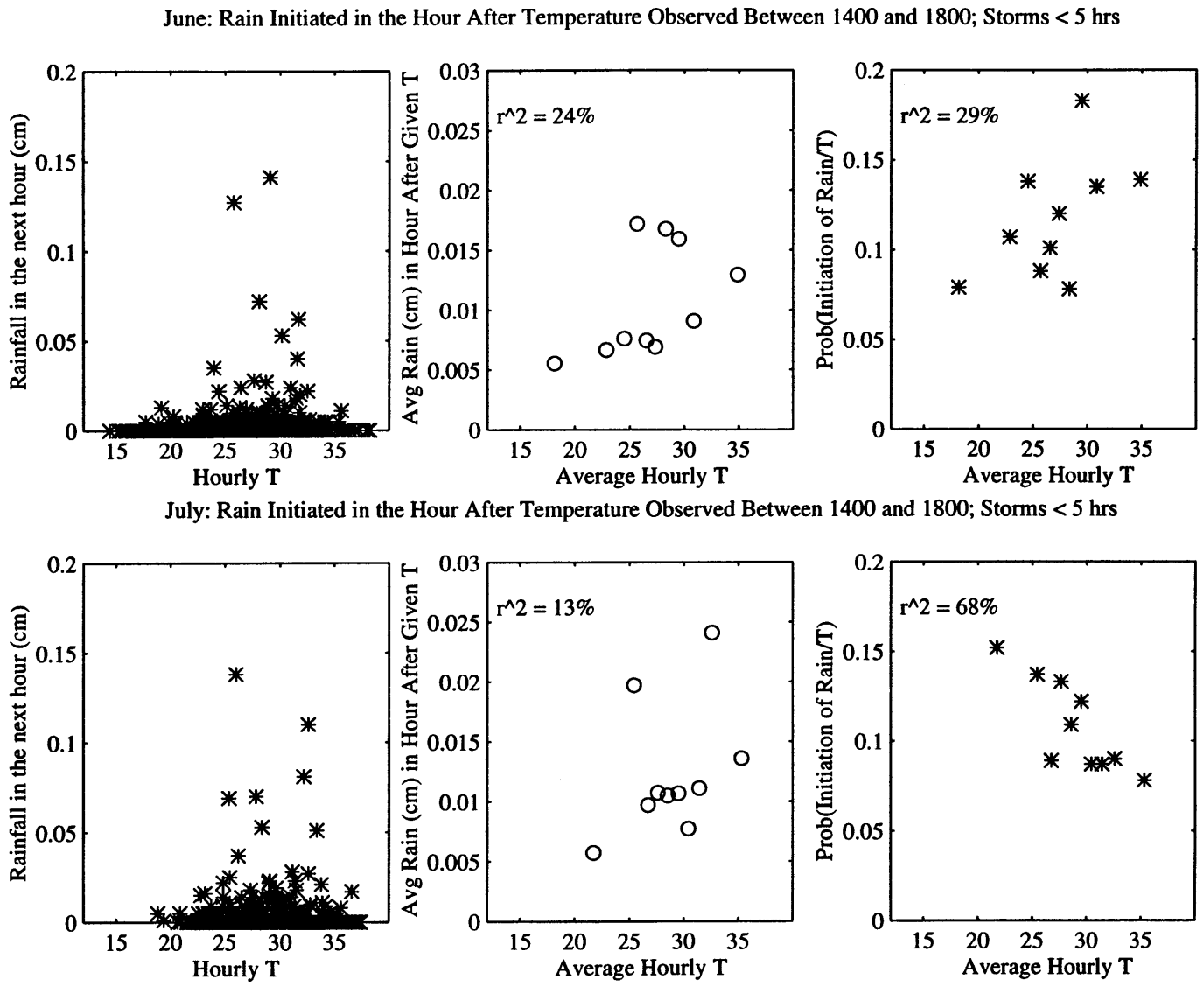

Figure 5.12 (cont.): Correlations between hourly air temperature (*T*) and rainfall during June and July.

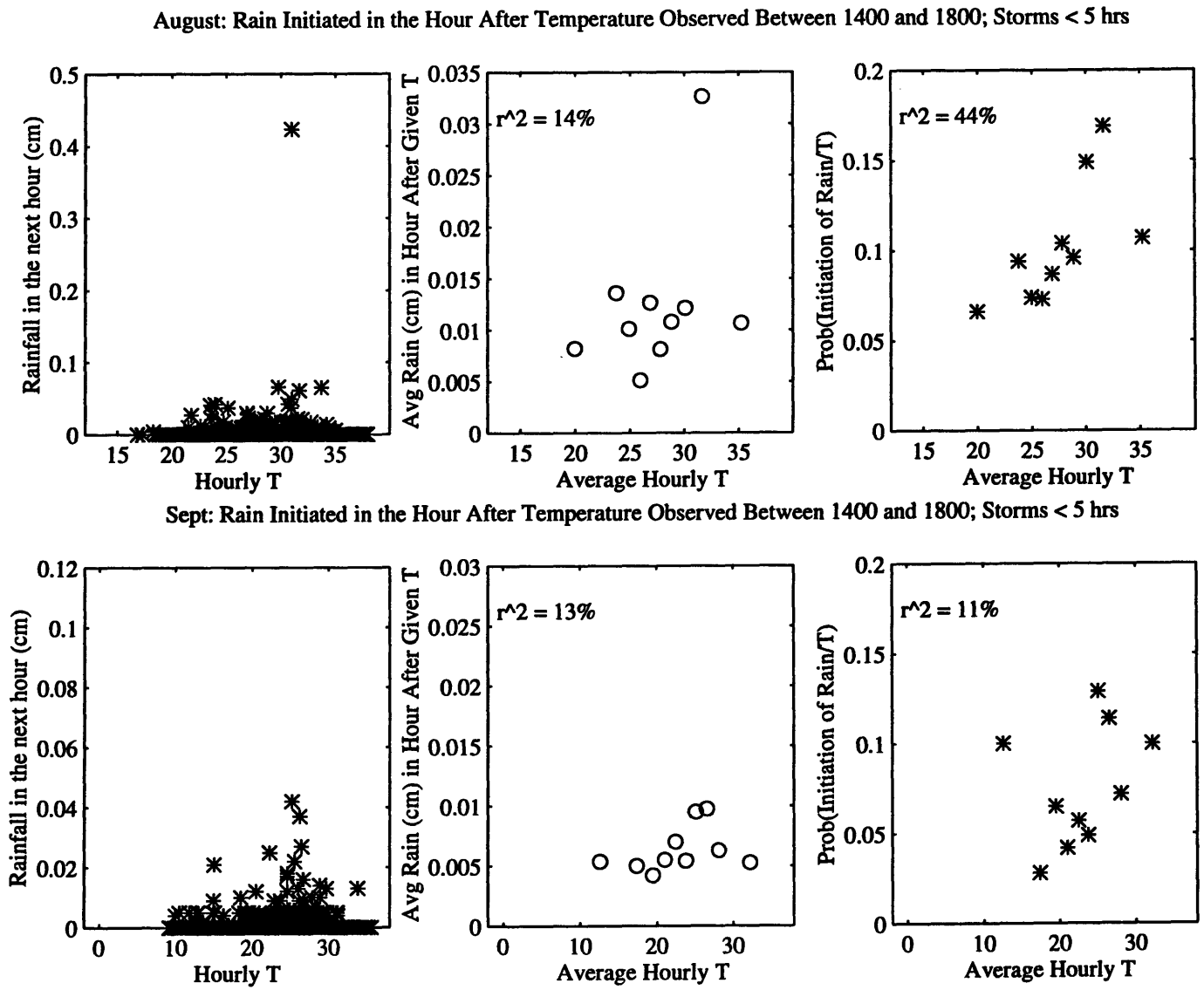

Figure 5.12 (cont.): Correlations between hourly temperature (*T*) and rainfall during August and September.

D. Discussion of Results

This chapter focused on the relationship between hourly observations of boundary layer conditions, as measured by hourly observations at 13 stations in the NCDC Surface Airways Hourly Database, and rainfall in the subsequent hour. Variables used to describe boundary layer conditions are the same as those used in Chapter 4. Hourly rainfall data at 82 stations within Illinois was obtained through EarthInfo, Inc., and is a subset of the NCDC Hourly Rainfall Database TD-3240. The analyses were performed on hourly state-wide averages of each of the boundary layer variables and of rainfall in the subsequent hour.

Wet-bulb depression, T_{dpr}, relative humidity, f, mixing ratio, w, and the temperature of the lifting condensation level (LCL), T_{LCL}, consistently showed strong correlations with the probability of initiation of a rainfall event. T_{LCL} showed some correlation with average depth of rainfall in the hour after the surface observation, given that rainfall occurs, but the others showed weak to no correlation with this quantity.

The strong negative correlation between wet-bulb depression and rainfall initiation (low wet-bulb depression is associated with higher probability of a storm beginning) is an important result, in light of the results of the soil moisture–boundary layer study of Chapter 4. The analyses of Chapter 4 revealed a negative correlation between soil moisture and subsequent wet-bulb depression, particularly during summer. These two results combined, then, suggest that wet-bulb depression may act as the carrier of information from the soil to rainfall. This will be discussed more thoroughly in the conclusions.

Wet-bulb depression and the other three variables mentioned above (f, w, and T_{LCL}) showed strong association with initiation of rainfall in all months between May and September,

but practical experience of Illinois weather indicates that climatic behavior is different during the summer months than during the spring and fall. We expect the data to reflect this difference. The positive linear trends seen in June, July, and August (strong association in June and August, weaker in July) between rainfall and the moist static energy of the boundary layer over a large portion of its range (between approximately 15 and 25 °C for T_w, 288 and 298 K for θ_w, and 320 and 362 K for θ_E) are perhaps a manifestation of this difference. They are indicative of the land-surface controls on convection which we expect to be important during the summer in mid-latitudes, as discussed in Chapter 2. More moist static energy in the lower levels of the boundary layer should be associated with a higher likelihood of overturning and initiation of convection. This is consistent with the results of Eltahir and Pal (1996), Williams and Renno (1993), and Betts et al. (1996). At low levels of moist static energy, the probability of initiation of rainfall is nearly constant, suggesting the likelihood of a threshold moist static energy necessary for convection. This, too, is consistent with many previous studies (e.g., Carlson and Ludlam, 1966; Williams and Renno, 1993; Eltahir and Pal, 1996) and is a reasonable result, given that convective rainfall results from the release of energy temporarily locked in a conditionally unstable vertical profile of temperature and humidity. The drop in both rainfall depth and occurrence at high T_w, θ_w, and θ_E, on the other hand, is not an easily explained phenomenon.

Buoyancy variables (T, θ, θ_v, and P_{LCL} - P_s) showed inconsistent connections with subsequent rainfall. In June, August and September (except for at low values of each variable in September), there was a scattered positive trend between buoyancy and the probability of rainfall occurrence. In July, however, there was a weak negative trend, and in April and May there was only scatter. These spring months were the only ones to show any association between buoyancy and average rainfall depth in the next hour.

This lack of association between surface buoyancy measures and rainfall may be an indication of the complexity of the interactions between boundary layer growth and triggering of moist convection. As discussed in Chapter 2, increased sensible heating of the air (associated with higher temperatures) increases the depth of the boundary layer, such that the contribution of moist static energy (MSE) from the ground, which is proportional to the sum of sensible and latent heat fluxes, is spread over a greater depth. The increase of MSE per unit depth, then, is smaller in high temperature conditions than in low temperature conditions. According to our previously mentioned theory and to results connecting higher MSE to higher likelihood of rainfall (except at very high MSE), this suggests that, given similar early-morning MSE, days with higher temperature should have a lower afternoon MSE and therefore a lower likelihood of rainfall than days with lower temperature. This is complicated by the fact that a necessary condition for the triggering of convection is a lifting agent to pull low level air up beyond its level of free convection (LFC). Turbulence generated by sensible heat flux often is this mechanism. Higher temperatures lead to greater boundary layer growth and a higher likelihood of the boundary layer breaking through the LFC associated with surface air. These competing factors may explain the lack of a consistent relationship between buoyancy of near-surface air and subsequent precipitation.

In summary, the results in this chapter indicate that there are connections between near-surface measurements of atmospheric quantities and subsequent rainfall in the state of Illinois. Wet-bulb depression is a good indicator of the likelihood of the initiation of afternoon rain storms in all of the months analyzed (April through September). Boundary layer entropy, or moist static energy, as quantified by T_w, θ_w, and θ_E, shows a positive linear association with rainfall occurrence through a limited range of observations. Below this range of moist static energy, the probability

of rainfall is nearly constant and very small, while above this range, the probability drops back down to a low level. Buoyancy, as measured by T, θ, θ_v, and P_{LCL} - P_s, on the other hand, shows little clear association with subsequent rainfall.

Chapter 6: Conclusions and Future Research

This study of the soil moisture—rainfall feedback was focused on the state of Illinois, an area of approximately 300 by 650 km centered around 40°N and 89°W. The Illinois State Water Survey's (ISWS's) extensive dataset of bi-weekly neutron probe measurements of soil moisture at up to 19 stations, beginning in 1981, motivated the study. Most previous investigations of this feedback mechanism have used inferred or modeled soil moisture time series, rather than directly observed data. Though these data are not of ideal spatial or temporal resolution, this is the largest long-term record of directly observed soil moisture currently available, and can provide much-needed validation of modeling results which often use simulated or non-realistic soil moisture conditions.

Results of a linear correlation analysis between initial soil moisture and rainfall in the subsequent three weeks showed that a positive correlation between these two variables is present from early June through mid-August. This correlation is more significant than the serial correlation within precipitation time series, suggesting the likelihood of a physical mechanism linking soil moisture to subsequent rainfall.

This result prompted further investigation into the nature of such a physical pathway linking soil moisture to subsequent rainfall. Theory and previous studies indicated the likelihood of a positive impact of soil moisture on the moist static energy (MSE) of the boundary layer, and a positive impact of MSE on rainfall. To explore these possibilities, hourly data of surface air

conditions and precipitation since 1981 (corresponding to the soil moisture dataset) were obtained for 13 and 82 stations, respectively. Near-surface hourly observations of pressure, P, temperature, T, wet-bulb temperature, T_w, and relative humidity, f, were obtained from the National Climatic Data Center (NCDC) Surface Airways Hourly Dataset TD-3280. Data from 13 such stations in and close to Illinois were used in the analyses. From each hourly set of direct observations of P, T, T_w, and f, many other variables were calculated and used in the analyses. These included wet-bulb depression, T_{dpr}, temperature of the lifting condensation level (LCL), T_{LCL}, pressure depth to the LCL, P_{LCL}-P_s, mixing ratio, w, potential temperature, θ, virtual potential temperature, θ_v, wet-bulb potential temperature, θ_w, and equivalent potential temperature, θ_E. Time series of the spatial average of each of these quantities were then calculated by averaging data from the 13 stations at each hour. These time series were used as a representation of the average near-surface conditions over the whole state of Illinois. These conditions were assumed to be an indication of conditions in the whole boundary layer. This assumption could be relaxed by including data from soundings in subsequent analyses.

An analysis of the connections between an average soil saturation time series for the whole state of Illinois with these state-wide average boundary layer conditions did not yield the expected result of a positive correlation between soil moisture and moist static energy, as quantified by T_w, θ_w, or θ_E. This result is at odds with previous research on this topic (Betts and Ball, 1995). It is not clear if this is due to limitations of the data or of the theory. The impact of variable incoming solar radiation was not accounted for in these analyses, and may be relevant to this result, but two other possible factors may also be playing a role; the observations from the surface may not truly be representative of conditions in the boundary layer, or data used in this study may not robust enough to describe either the surface air conditions or the soil conditions over the entire state of

Illinois at a daily time scale. Though one of the important aspects of this study is the use of directly observed soil moisture data, these data are still quite limited in both space and time and may not accurately represent conditions in the state as a whole. When more extensive datasets are available, particularly data on incoming solar radiation, it may be instructive to revisit this analysis.

Though the anticipated soil moisture–boundary layer entropy link was not observed, there was evidence that moisture availability (or lack thereof) at the surface has a very strong impact on the wet-bulb depression of near-surface air, particularly from mid-May through the end of August, showing good correspondence to the period of significant soil moisture–rainfall association.

The final set of analyses performed included an investigation of the hourly boundary layer and rainfall data. The latter dataset was also NCDC hourly data, purchased through EarthInfo, Inc. Data from the 82 hourly rainfall stations were averaged to compare state-wide hourly rainfall to state-wide hourly boundary layer conditions. A link between high MSE and high rainfall was noted for much of the range of MSE during the summer months, and a link between low T_{dpr} and high rainfall was evident for all of the months analyzed (April through September). These analyses, then, suggest that the significant but weak correlation between soil moisture and rainfall during Illinois summers is due not to soil moisture controls on the boundary layer entropy, but rather to soil moisture controls on the wet-bulb depression of near-surface air.

In addition to the complete pathway by wet-bulb depression between soil moisture and subsequent rainfall, some other interesting results were seen in the two phases of this interaction. In the first phase of this physical connection, i.e., the interaction between the soil and the mixed layer of the atmosphere, a negative feedback on buoyancy of near surface air was seen at low to

normal soil moisture conditions. In July, this effect of lower soil moisture leading to higher buoyancy is also seen in the jump from normal to wet soils, though this is not seen in June and August. One possible reason that this effect is not present between normal and wet soils during the other summer months is the decreased sensitivity of evapotranspiration to soil moisture in wet or very wet conditions. This is due to that fact that above a certain level of soil moisture, water availability is no longer the limiting factor on the rate of evapotranspiration (Betts and Ball, 1995). This behavior could be investigated in more detail by accounting for differences in incoming radiation. As discussed by Eltahir (1997), the role of soil moisture on atmospheric processes is not as significant as other factors such as incoming solar radiation. On days with equivalent inputs of solar energy, different soil moisture conditions may account for differences in boundary layer conditions. We see some evidence of the role of soil moisture in affecting the boundary layer, but research which accounts for the solar conditions should be performed.

The second phase of the link between soil conditions and rainfall is between the boundary layer and rainfall. Results of this work show that the saturation of near surface air is positively associated with rainfall in the subsequent hour. The buoyancy measures T, θ, and θ_v, however, show poor association with rainfall. This may be due to the competing factors of increased soil moisture leading to increased moist static energy in the boundary layer–which is expected to lead to more convective rainfall, and decreased sensible heat flux–which decreases the likelihood of boundary layer growth overtaking the level of free convection and initiating convection.

As mentioned above, measures of the moist static energy (MSE) of the boundary layer did show reasonable connections with rainfall during the summer months. Over most of the range of MSE observations, there was a strong positive correlation with rainfall. At the very top of the

MSE range, however, the likelihood and the depth of rainfall dropped well below that in the next-to-highest MSE bin. At the bottom of the range, there is a nearly constant probability of initiation of rainfall until the MSE surpasses some threshold. This is understandable, given the threshold nature of convection in general, but the suppression of rain at high MSE is not as easily explained.

The spatial and temporal limitations of the soil moisture dataset, the spatial limitations of the surface conditions dataset, and the lack of both radiation data and vertical profiles of temperature and humidity throughout the boundary layer restrict the potential for more detailed investigations of the energetics of the different environments corresponding to dry, normal, and wet soil moisture conditions. Despite these limitations, these analyses show that during the summer in Illiois, soil moisture significantly impacts subsequent rainfall through its impact on the wet-bulb depression of the boundary layer. Future work intended to refine our understanding of the role of soil moisture in the energy balance of the mixed layer will include vertical soundings and radiation data.

References

Atlas, R., N. Wolfson, and J. Terry: The Effect of SST and Soil Moisture Anomalies on GLA Model Simulations of the 1988 U.S. Summer Drought. Journal of Climate, Vol. 6, No. 11, Pages 2034-2048, 1993.

Betts, Alan K. and J.H. Ball: Budget Analysis of FIFE 1987 Sonde Data. Journal of Geophysical Research, Vol. 99, No. D2, Pages 3655-3666, 1994.

Betts, Alan K. and J.H. Ball: The FIFE Surface Diurnal Cycle Climate. Journal of Geophysical Research, Vol. 100, No. D12, Pages 25,679-25,693, 1995.

Betts, Alan K., John H. Ball, Anton C.M. Beljaars, Martin J. Miller, and Pedro A. Viterbo: The Land Surface-Atmosphere Interaction: A Review based on Observational and Global Modeling Perspectives. Journal of Geophysical Research, Vol. 101, No. D3, Pages 7209-7225, 1996.

Bolton, David: The Computation of Equivalent Potential Temperature. Monthly Weather Review, Vol. 108, Pages 1046-1053, 1980.

Carlson, T.N. and F.H. Ludlam: Conditions for the Occurrence of Severe Local Storms. Tellus XX, Vol. 2, Pages 203-226, 1968.

Chang, Jy-Tai and Peter J. Wetzel: Effects of Spatial Variations of Soil Moisture and Vegetation on the Evolution of a Prestorm Environment: A Numerical Case Study. Monthly Weather Review, Vol. 119, Pages 1368-1390, 1991.

Dessens, Jean: Severe Convective Weather in the Context of a Nighttime Global Warming. Geophysical Research Letters, Vol. 22, No. 10, Pages 1241-1244, 1995.

Eagleson, Peter S.: Climate, Soil, and Vegetation; 3. A Simplified Model of Soil Moisture Movement in the Liquid Phase. Water Resources Research, Vol. 14, No. 5, pp. 722-730, 1978.

EarthInfo CD^2 Reference Manual; EarthInfo, Inc., 1996.

Eltahir, Elfatih A.B. and Jeremy S. Pal: The Relationship Between Surface Conditions and Subsequent Rainfall in Convective Storms. Journal of Geophysical Research, Vol. 101, No. D21, 1996.

Eltahir, Elfatih A.B.: On the Soil Moisture-Rainfall Feedback. Submitted to Water Resources Research, April 1997.

Emanuel, Kerry A.: Atmospheric Convection. Oxford University Press, 1994.

Entekhabi, Dara, Ignacio Rodriguez-Iturbe, and Fabio Castelli: Mutual Interaction of Soil Moisture State and Atmospheric Processes. Journal of Hydrology, Vol. 184, pp. 3-17, 1996.

Fennessy, Michael J. and J. Shukla: Impact of Initial Soil Wetness on Seasonal Atmospheric Prediction. Center for Ocean-Land-Atmospheric Studies, Report No. 34, 1996.

Georgakakos, Konstantine P., Deg-Hyo Bae, and Daniel R. Cayan: Hydroclimatology of Continental Watersheds, 1. Temporal Analyses. Water Resources Research, Vol. 31, No. 3, pp. 655-675, 1995.

Giorgi, Filippo, Linda O. Mearns, Christine Shields, and Leslie Mayer: A Regional Model Study of the Importance of Local Versus Remote Controls of the 1988 Drought and the 1993 Flood Over the Central United States. Journal of Climate, Vol. 9, Pages 1150-1162, 1996.

Hollinger, S.E. and S.A. Isard: A Soil Moisture Climatology of Illinois. Journal of Climate, Vol. 7, No. 5, Pages 822-833, 1994.

Huang, Jin, Huug M. van den Dool, and Konstantine P. Georgakakos: Analysis of Model-Calculated Soil Moisture over the United States (1931-1993) and Applications to Long-Range Temperature Forecasts. Journal of Climate, Vol. 9, No. 6, Pages 1350-1362, 1996.

Johnston, John: Econometric Methods, McGraw-Hill, 1984.

Karl, T.R.: The Relationship of Soil Moisture Parameterizations to Subsequent Seasonal and Monthly Mean Temperature in the United States. Monthly Weather Review, Vol. 114, Pages 675-686, 1986.

Kunkel, Kenneth E., Stanley A. Changnon, Carl G. Lonnquist, and James R. Angel: A Real-Time Climate Information System for the Midwestern United States. Bulletin of the American Meteorological Society, Vol. 71, No. 11, Pages 1601-1609, 1990.

Ludlam, F.H.: Clouds and Storms: The Behavior and Effect of Water in the Atmosphere. The Pennsylvania State University Press, 1980.

McCorcle, Michael D.: Simulation of Surface-Moisture Effects on the Great Plains Low-Level Jet. Monthly Weather Review, Vol. 116, Pages 1705-1719, 1988.

Namias, J.: The Annual Course of Month-to-Month Persistence in Climatic Anomalies. Bulletin of the American Meteorological Society, Vol. 33, No. 7, Pages 279-285, 1952.

Namias, J.: Factors in the Initiation, Perpetuation and Termination of Drought. International Association of Scientific Hydrology Commission on Surface Waters, Publication 51, Pages 81-94, 1960.

Namias, J.: Influences of Abnormal Surface Heat Sources and Sinks on Atmospheric Behavior. Proceedings of the International Symposium on Numerical Weather Prediction, Tokyo, November 7-13, 1960.

Oglesby, Robert J. and David J. Erickson III: Soil Moisture and the Persistence of North American Drought. Journal of Climate, Vol. 2, Pages 1362-1380, 1989.

Oglesby, R.J.: Springtime Soil Moisture, Natural Climatic Variability, and North American Drought as Simulated by the NCAR Community Climate Model 1. Journal of Climate, Vol. 4, Pages 890-897, 1991.

Owe, Manfred and Alfred Chang: Estimating Surface Soil Moisture from Satellite Microwave Measurements and a Satellite Derived Vegetation Index. Remote Sensing of Environment, Vol. 24, Pages 331-345, 1988.

Pal, Jeremy S. and Elfatih A.B. Eltahir: On the Relationship between Spring and Summer Soil Moisture and Summer Precipitation over the Midwest. Proceedings of the 13th Conference on Hydrology, Long Beach, California, February 2-7, 1997.

Pan, Z., M. Segal, R. Turner, and E. Takle: Model Simulation of Impacts of Transient Surface Wetness on Summer Rainfall in the United States Midwest during Drought and Flood Years. Monthly Weather Review, Notes and Correspondence, Vol. 123, Pages 1575-1581, 1995.

Peppler, Randy A. and Peter J. Lamb: Tropospheric Static Stability and Central North American Growing Season Rainfall. Monthly Weather Review, Vol. 117, Pages 1156-1180, 1989.

Rind, D.: The Influence of Ground Moisture Conditions in North America on Summer Climate as Modeled in the GISS GCM. Monthly Weather Review, Vol. 110, Pages 1487-1494, 1982.

Rogers, R.R. and M.K. Yau: A Short Course in Cloud Physics. Third Edition. Pergamon, 1989.

Rowntree, P.R. and J.A. Bolton: Simulation of the Atmospheric Response to Soil Moisture Anomalies over Europe. Quart. Journal of the Royal Meteorological Society, Vol. 109, Pages 501-526, 1983.

Shukla, J. and Y. Mintz: Influence of Land-Surface Evapotranspiration on the Earth's Climate. Science, Vol. 215, Pages 1498-1500, 1982.

Surface Airways Hourly TD-3280. National Climatic Data Center, 1994.

Trenberth, K.E., G.W. Branstator, and P.A. Arkin: Origins of the 1988 North American Drought. Science, Vol. 24, Pages 1640-1645, 1988.

Wallace, John M. and Peter V. Hobbs: Atmospheric Science, An Introductory Survey. Academic Press, Inc., 1977.

Wallis, J.R., D.P. Lettenmaier, and E.F. Wood: A Daily Hydroclimatological Data Set for the Continental United States. Water Resources Research, Vol. 24, No. 7, Pages 1657-1663, 1991.

Williams, Earle and Nilton Renno: An Analysis of the Conditional Stability of the Tropical Atmosphere. Monthly Weather Review, Vol. 121, Pages 21-36, 1993.

Yeh, T.-C., R.T. Wetherald and S. Manabe: The Effect of Soil Moisture on the Short-Term Climate and Hydrology Change-A Numerical Experiment. Monthly Weather Review, Vol. 112, Pages 474-490, 1984.

Zawadzki, I.I. and C.U. Ro: Correlations between Maximum Rates of Precipitation and Mesoscale Parameters. Journal of Applied Meteorology, Vol. 17, No. 9, Pages 1327-1331, 1978.

Zawadski, I., E. Torlaschi, and R. Sauvageau: The Relationship between Mesoscale Thermodynamic Variables and Convective Precipitation. Journal of The Atmospheric Sciences, Vol. 38, No. 8, Pages 1535-1540, 1981.